231
1-16-79

DR. 2457

SAN-1202-77/3

THIN FILMS OF GALLIUM ARSENIDE ON LOW-COST SUBSTRATES

Final Report, July 5, 1976—July 2, 1977

By
R. P. Ruth
P. D. Dapkus
R. D. Dupuis
A. G. Campbell
R. E. Johnson
H. M. Manasevit
L. A. Moudy
J. J. Yang
R. D. Yingling

August 1977

Work Performed Under Contract No. EY-76-C-03-1202

Rockwell International Corporation
Electronics Research Center
Electronic Devices Division
Anaheim, California

U.S. Department of Energy

Solar Energy

DISCLAIMER

NOTICE

C76-1168/501

SAN-1202-77/3
Distribution Category UC-63

THIN FILMS OF GALLIUM ARSENIDE ON LOW-COST SUBSTRATES

Final Report

for the period
July 5, 1976 - July 2, 1977

R. P. Ruth, P. D. Dapkus, R. D. Dupuis, A. G. Campbell,
R. E. Johnson, H. M. Manasevit, L. A. Moudy, J. J. Yang, and R. D. Yingling

ROCKWELL INTERNATIONAL

Electronic Devices Division
Electronics Research Center
3370 Miraloma Avenue
Anaheim, CA 92803

August 1977

PREPARED FOR THE DIVISION OF SOLAR ENERGY, UNITED STATES
ENERGY RESEARCH AND DEVELOPMENT ADMINISTRATION,
UNDER CONTRACT NO. E(04-3)-1202

ABSTRACT

The first year or work on the contract is summarized, with emphasis on details of the fourth quarter activities. The metalorganic chemical vapor deposition (MO-CVD) technique has been applied to the growth of thin films of GaAs and GaAlAs on inexpensive polycrystalline or amorphous substrate materials (glasses, glass-ceramics, alumina ceramics, and metals) for use in fabrication of large-area low-cost photovoltaic device structures. Trimethylgallium (TMG), arsine (AsH_3), and trimethylaluminum (TMAl) are mixed in appropriate concentrations at room temperature in the gaseous state and pyrolyzed at the substrate, which is heated in a vertical reactor chamber to temperatures in the range 600-800°C, to produce the desired film composition and properties.

The early stages of the program emphasized experiments to test the compability of various low-cost substrates with the deposition process, and evaluation of the structural and electrical properties of films deposited on these substrates, utilizing a variety of characterization techniques. Of ten candidate low-cost substrates initially identified for investigation, Corning Code 0317 glass and composites of CVD Ge/glass and sputtered Mo/glass were found to be the most satisfactory, the latter eventually serving as a reference substrate against which to compare the performance of other substrates. In addition, the MO-CVD process was further developed to achieve controlled n- and p-type doping of single-crystal materials and abrupt heterojunctions of GaAlAs/GaAs, employing the automated reactor system designed and constructed specifically for this work.

Resistivities of doped (n- or p-type) polycrystalline GaAs films were found to be 2 to 3 orders of magnitude larger than those of single-crystal films similarly doped. Such films on low-cost substrates were found to have apparent grain sizes in the 2-10 μm range – predominantly ≤5 μm in films ~5 μm thick. Orientations tend to be preferentially {111}, although this varies with deposition temperature and substrate species. Methods for determination of grain size (by etching techniques and by SEM-EBIC examination) have been explored and developed, and a procedure for determining Al content in GaAlAs films by electron microprobe analysis combined with x-ray lattice parameter measurement has been established.

Single-crystal window-type solar cells, polycrystalline Schottky-barrier cells, and deposited-junction polycrystalline cells have been grown, fabricated, and characterized. Epitaxial GaAlAs/GaAs p-n junction cells with thin (~500Å) $Ga_{0.2}Al_{0.8}As$ windows and GaAs:Zn – GaAs:Se junctions were made with AM0 efficiencies as high as 12.8 percent with no AR coating, indicating the high quality of the films grown by the MO-CVD process. Schottky barrier cells with efficiencies of 2.25 percent AM0 (no AR coating) have been made on n/n^+ polycrystalline GaAs structures on Mo/glass composite substrates, with short-circuit current densities up to 12.5 mA/cm^2. The GaAs-Mo interface has been found to be ohmic when the GaAs donor doping concentration exceeds ~10^{18} cm^{-3}. Deposited junction cells in polycrystalline structures have been generally leaky, although better for n/p than for p/n configurations; Zn diffusion along grain boundaries is believed to be responsible for some of the observed problems. Details of these experimental studies are presented.

Also, results of analyses of material and processing costs associated with fabrication of thin-film GaAlAs/GaAs solar cells by the MO-CVD process are discussed. Available data on present and future supplies of Ga metal are reviewed relative to the prospect of meeting future ERDA production goals for low-cost solar arrays with GaAs cells made by this technique, and relatively optimistic conclusions are reached.

Suggestions for continued work are outlined.

CONTENTS

CONTENTS (Cont)

ILLUSTRATIONS

ILLUSTRATIONS (Cont)

TABLES

1. INTRODUCTION

The long-range objective of the National Photovoltaic Conversion Program is to develop low-cost reliable photovoltaic systems and to stimulate the creation of a viable industrial and commercial capability to produce and distribute these systems for widespread use in residential and commercial applications.

Two of ERDA's specific technical objectives that relate directly to this contract are (1) to conduct research, development, and demonstrations to show a factor of 10 reduction in solar array prices and to establish the viability of this technology in the latter half of this decade (i.e., by 1980), and (2) to conduct a focused research and development effort on advanced technologies for photovoltaic devices that show a potential reduction in solar array prices of one hundred or greater.

Specific goals of the National Photovoltaic Conversion Program include establishment of total solar array production capacities of (1) 500 peak Mw/year of solar array modules at a market price of less than $500 per peak Kw by FY 1985 and (2) 5×10^4 peak Mw/year of solar array modules at a market price of $100 to $300 per peak Kw by FY 2000.

The work of this contract was directed toward those goals. The overall objective of the contract was the performance of intensive studies that constitute an initial step in ERDA's program to overcome current problems and deficiencies in design and fabrication of arrays of extremely low-cost thin-film photovoltaic cells of relatively high efficiency and long life. Acquisition of further important knowledge of thin-film deposition methods and thin-film technology for polycrystalline GaAs on various substrates was also expected.

In addition, it was expected that any proposed device configuration should lead, within a period of one or two years at most, to the ability to produce solar photovoltaic cell configurations having 10 percent AM1 efficiency. This technical goal was not achieved during the performance period of the 12-month contract, but it provided a continuous guideline for conduct of the program.

Specific studies and/or tasks required by ERDA included (1) selection of appropriate low-cost substrates; (2) deposition of thin films of GaAs, which might be polycrystalline, on the selected substrate(s); (3) conduct of a deposition parameter investigation to optimize the process; (4) determination of film properties in terms of quantitative physical parameters; (5) alteration of the physical parameters of the films in a manner directed toward production and deployment of high-efficiency photovoltaic solar cells capable of scale-up to an annual production rate of 5×10^4 peak Mw by the year 2000, with a selling price of $100 to $300 per peak Kw, "without creating inordinate technical and economic problems;" (6) the delivery of thin-film samples (minimum 4 cm^2 per month) to ERDA; and (7) the analysis and projection of cell costs for large-scale production in the future.

1.1 ADVANTAGES OF GaAs FOR THIN-FILM SOLAR CELLS

In the years since the modern era of photovoltaic cell development began in the early 1950's, considerable research and engineering have gone into achieving improvements in the single-crystal Si solar cell and into developing experimental cells of

single-crystal GaAs and other compound semiconductors. The Si cell has become the industry standard and has received by far the greatest amount of engineering and production effort. Arrays of Si cells have supplied reliable auxiliary power for most of the space vehicles and satellites launched throughout the world in various space programs over the past 16 years.

However, theoretical considerations (see, e.g., Ref 1) have shown that various compound semiconductors - especially GaAs and its related alloys - should provide significantly higher conversion efficiencies than are available with Si cells. Although pilot-line quantities of GaAs cells were fabricated several years ago, the performance of experimental arrays in actual space missions was generally disappointing (Ref 2).

Relatively recent work with composite cells involving GaAs and a front layer of another material as a "window" has, however, been very encouraging (Ref 3) and has renewed interest in the significant advantages of GaAs as a solar cell material; these advantages include the following characteristics:

1. The bandgap (~1.4 eV) is a better match to the solar spectrum; higher theoretical efficiencies (in excess of 20 percent) than for Si are thus to be expected.

2. The decrease of power output with increasing temperature for GaAs is about half of that for Si cells, because of the larger bandgap that allows higher temperature operation of the junction.

3. GaAs cells typically have lower minority carrier lifetimes and diffusion lengths than Si cells, and so are less susceptible to radiation damage.

4. The larger bandgap of GaAs results in higher output voltage per cell than for Si, although the current per unit area is smaller.

5. The optical absorption edge in GaAs is steep (it is a direct-bandgap semiconductor), so most solar radiation is absorbed very near the surface, eliminating the need for thick cells to capture most of the incident energy.

There are some disadvantages of GaAs relative to Si, not the least of which is related to Item 5 above. Because of the absorption and generation of charge pairs so close to the surface, the high surface recombination velocity that is also characteristic of GaAs (10 to 100 times that found in Si) results in reduced minority carrier collection efficiencies in junction-type devices, due to surface recombination losses. Additionally, since the minority carrier diffusion lengths in GaAs are typically small compared with those found in single-crystal Si, very thin (~0.5μm) layers with extensive electroding (grids) are typically required on the illuminated side of the junction to reduce cell series resistance as much as possible. Even with these measures the losses at the front of the cell have been found to be too high for acceptable cell operation under normal conditions.

This problem was the principal motivation for development of the window-type cell, in which a layer of another semiconductor is applied to the illuminated surface of the GaAs to remove the active junction region sufficiently far from the incident-light surface to reduce recombination losses, and at the same time add conductive material that reduces the series resistance of the cell. The window material must provide an

interface with the GaAs that is sufficiently good structurally that the interface does not itself become a source of recombination losses. Additionally, the bandgap of the window material must be large enough that there are no significant losses of the incident solar radiation due to absorption in the window material (unless other aspects of the design allow the carriers generated by such absorption to be collected by the active junction).

It should also be noted that the costs of GaAs and Si differ by about an order of magnitude for comparable quality (i.e., "solar grade" single-crystal) material, with GaAs the more expensive. The costs of both of these materials - especially after they are processed into solar cells - are major factors in the increased interest in thin-film solar cells, as addressed in this contract.

The large absorption coefficient of GaAs in the wavelength region to the high-energy side of its fundamental absorption edge is such that most (i.e., 90 percent or more) of the available radiation in the solar spectrum is absorbed within a thickness of 2 μm or less. A Si thickness in excess of 100 μm is required for similar absorption. The fact that GaAs is a direct-bandgap material and Si an indirect-bandgap semiconductor means that the transition from non-absorbing to absorbing is much more abrupt for GaAs than for Si in progressing from long wavelengths to shorter wavelengths, past the band edge.

The difference in bandgap energy for these two semiconductors means that GaAs responds only to that portion of the total solar spectrum that is to the short-wavelength side of ~0.9 μm, while Si reponds to all photons to the short-wavelength side of ~1.1 μm. There is a significant amount of solar energy in the band between these two wavelengths, but the net result of all factors that bear on photovoltaic conversion efficiency is that the theoretical values for GaAs are significantly higher than for Si (Ref 1).

The small thickness of GaAs required for adequate absorption of solar radiation strongly suggests the use of deposited films of the material instead of bulk single-crystal wafers. This would clearly help in reducing the cost of the cell, simply by using less of the expensive active material; it would also assist in the continuing effort to reduce the weight of photovoltaic cell arrays, irrespective of whether they are intended for space or terrestrial applications. Whether or not the hoped-for reductions in cost and weight are realized depends upon the extent of other complications that arise because of the thin-film configuration.

Ideally, single-crystal thin films would be most desirable, but the known methods for producing single-crystal (i.e., epitaxial) deposited films of the III-V compounds all require single-crystal substrates (Ref 4), and this does not allow the needed extensive reductions in materials costs. Furthermore, if only single-crystal substrate materials are considered then there are serious limitations on the maximum area that can be achieved for the basic cell module to be fabricated by thin-film growth procedures. This reasoning leads directly to consideration of less expensive substrate materials that are available in relatively large areas. It also leads to the realization that the resulting thin-film cells will almost certainly be polycrystalline, because of the absence of any strong ordering forces associated with the surface of such a substrate material.

Several important factors are introduced when thin-film polycrystalline solar cells are considered. The first has long been recognized as one of the principal deterrents to the use of polycrystalline thin films for solar cell fabrication, and relates to the nature of the crystal structure in the deposited film. If the individual crystal grains are randomly oriented on the substrate, as shown in Figure 1-1a, then - on the average - only those grains that intersect the illuminated surface of the cell will contribute to the collected photocurrent. Carriers generated in other grains, farther from the junction, will tend to be lost by recombination at the grain boundaries that intercept the path between the region of generation and the junction.

A more desirable growth configuration is shown in Figure 1-1b, in which the grain boundaries are depicted as being oriented predominantly normal to the film surface (and thus also normal to the junction). In this film structure the carriers generated in the individual grains are far more likely to be collected across the junction, except for those lost due to a lateral diffusion component that still allows them to encounter a grain boundary. The long-standing rule-of-thumb that suggests that average grain sizes must be at least of the same magnitude as the film thickness for reasonable thin-film solar cell performance has its origin in such considerations.

The fact that GaAs thicknesses of only 1 to 2 μm are required to absorb up to 90 percent of the useful solar radiation (in the proper energy range) indicates that polycrystalline films with average grain sizes of 1 to 2 μm could be expected to exhibit respectable solar efficiencies, whereas for Si polycrystalline film cells the same criterion dictates that average grain sizes approaching 100 μm are required.

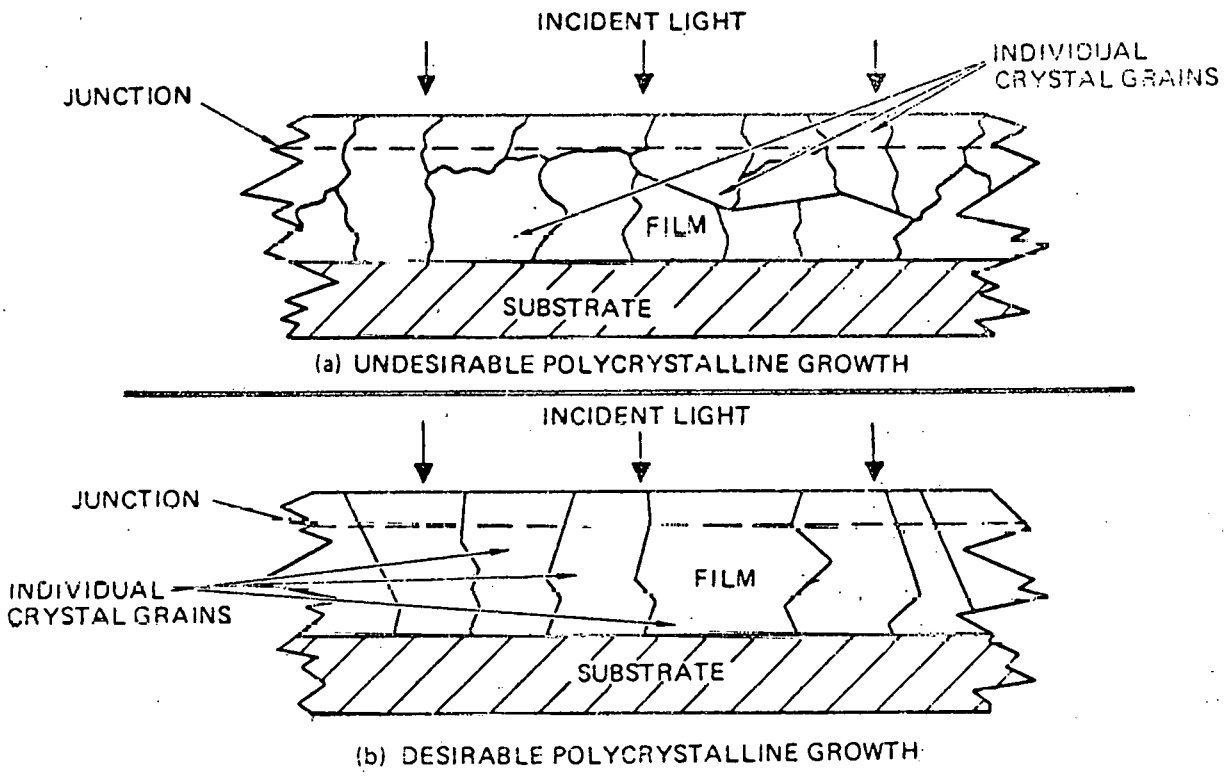

Figure 1-1. Two Possible Crystallite Configurations in Polycrystalline Film Solar Cells Grown on Foreign Substrates

Calculations of the expected performance of polycrystalline GaAs solar cells have been described by Woodall and Hovel (Ref 5). For a 1μm GaAs layer and a 10 μm Si layer, and assuming that 1μm average grain sizes could be obtained in both cases, it was found that a 21 percent theoretical efficiency resulted for GaAs and only 6 percent for Si. Using a more conservative analysis carried out by Soclof and Iles (Ref 6) for polycrystalline Si solar cells as the basis, Woodall and Hovel found a theoretical efficiency of 11 percent and 1.5 percent for GaAs and Si, respectively, for the same dimensional configurations mentioned above.

Although such predictions must be viewed with caution, there is enough validity in the analyses to suggest that significantly higher efficiencies should be expected for polycrystalline cells in thin-film GaAs than in thin-film Si, if average grain sizes the order of only 1 μm are obtainable in both cases. Such dimensions seemed well within the realm of achievement for GaAs films deposited on non-crystalline substrates by the chemical vapor deposition technique, so there appeared to be good prospect for fabricating thin-film solar cells that could meet the 10 percent AM1 efficiency goal mentioned earlier. If grain sizes significantly larger than 1 μm were to be achieved, then the chances for success would be even better.

1.2 GENERAL TECHNICAL APPROACH USED IN PROGRAM

The general technical approach of this program has involved the use of the metalorganic chemical vapor deposition (MO-CVD) technique for the growth of thin films of GaAs and GaAℓAs on inexpensive polycrystalline or amorphous substrate materials in configurations permitting fabrication of photovoltaic devices. The parameters of the CVD process have been chosen so that the required properties of the deposited films could be achieved and the efficiency goal of the photovoltaic device (10 percent AM1) could be realized, subject to the constraints imposed by the properties of the selected substrate material(s).

The CVD method is believed to be potentially the best method for achieving large areas of solar cells of reasonable efficiency at low cost and thus meet both the production capacity goal and the cost-per-watt goal of the National Photovoltaic Conversion Program. Some of the technical problems that remain to be solved before those goals can be reached are among those specifically addressed in this program.

As it has been applied in this program, the MO-CVD process involves the mixing of a metalorganic compound of a Group III element with a hydride or metalorganic compound of a Group V element, and pyrolysis of this mixture or its reaction product under appropriate conditions to produce the Group III-Group V semiconductor. Thus, trimethylgallium (TMG) and AsH_3 are mixed at room temperature in the gaseous state and pyrolyzed at established temperatures in a cold-wall reactor to form GaAs according to the following simplified equation:

$$(CH_3)_3\,Ga + AsH_3 \rightarrow GaAs + 3CH_4.$$

By mixing TMG in the gas phase with trimethylaluminum (TMAℓ) and AsH_3, GaAℓAs is obtained upon pyrolysis at appropriate temperatures; the composition of the alloy is controlled by the ratio of the reactants. The organic byproduct, methane (CH_4), is stable at film growth temperatures. In similar fashion, AℓAs can be prepared from TMAℓ and AsH_3, if desired. Many such compounds and alloys have been prepared by the MO-CVD process (Ref 7).

The MO-CVD process has several attributes that are important to the application involved in this program:

1. The process is completely free of halides, thus eliminating competing etching reactions, reducing generation of unwanted impurities by reactions with the low-cost substrate materials, and minimizing complication of the heterogeneous film-growth process involved

2. Only a single high-temperature zone is required, greatly simplifying the apparatus and the necessary control systems, and allowing the deposition chamber walls to remain relatively cool because only the pedestal and the samples are heated

3. The reactants used are either liquid or gaseous at room temperature, facilitating their handling and introduction into the reactor system carrier gas upstream from the deposition chamber, and allowing control of composition of the deposited film by means of flowmeter adjustments

4. Impurity doping of the deposited films can be achieved by introduction of appropriate dopant compounds (liquid metalorganic and/or gaseous hydride sources) into the primary reactant gas stream, again with doping levels controllable by means of flowmeter adjustments

5. The growth process can be observed directly by the operator, since the reactor walls are transparent and unobstructed, thus allowing changes in growth conditions to be made during an experiment if it is desired or necessary

6. Large-area, uniform surface coverage can be achieved in a single growth sequence, using the same type of commercially available apparatus that is used for epitaxial growth of elemental semiconductors (e.g., Si)

7. The process requires neither single-crystal GaAs material nor semiconductor-grade (ultrahigh-purity) polycrystalline GaAs for its application, since only compounds of Ga and of As are used in the reaction, thus eliminating the expensive and energy-wasteful processes of producing melt-grown GaAs source material that is required for other crystal growth and/or film deposition techniques.

The availability of high-purity reactants is a primary requisite for the ultimate success of the MO-CVD process in the application involved in this contract. This is a matter that still needs considerable attention; it requires cooperation of the relatively small number of manufacturers now engaged in supplying the various compounds used in this work to assure that materials of increasing purity and improved control of quality will become available.

Additional principal technical problems to be solved are (1) identifying suitable substrate materials that will survive the environment of the MO-CVD process and be potentially inexpensive and available in large areas, yet be as favorable as possible to GaAs and GaAlAs grain growth; (2) establishing preferred CVD process parameters (temperature, reactant concentrations, carrier gas composition, doping impurities, growth rate) for optimized intragrain properties of the films grown on various substrate

materials; and (3) achieving adequate grain size in the films to provide satisfactory solar cell properties.

To pursue these technical problems and to meet the objectives of the program, the contract work was organized into five main technical tasks, as follows:

Task 1. Substrate Material Selection, Evaluation, and Development

Task 2. CVD Experiments and Parameter Studies

Task 3. Evaluation of Film Properties

Task 4. Experimental Photovoltaic Device Fabrication and Evaluation

Task 5. Analysis and Projection of Cell Fabrication Costs

In addition, the Program Management Task defined in the Statement of Work of the contract has been carried on in parallel with the above technical tasks.

This is the Final Report for the first year of this contract and covers the period 5 July 1976 through 2 July 1977. The contract activities during that period are described by task in the following section.

THIS PAGE

WAS INTENTIONALLY

LEFT BLANK

2. TECHNICAL PROGRESS

The work of the 12-month experimental performance period is described by task in this section. Considerable detail is given for the final quarter of the program, although this report is intended to provide an overall summary of the entire contract activity. The three individual quarterly project reports (Refs 8, 9, 10) should be consulted for any specific details that are not included in this report.

2.1 TASK 1. SUBSTRATE MATERIAL SELECTION, EVALUATION AND DEVELOPMENT

The summary of the work of this task, as given in the original proposal, is as follows:

> Selected samples of both commercially available and specially prepared materials--including high-purity polycrystalline aluminas, special glass-ceramics, some high-temperature glasses, and certain metal foils and deposited layers--will be evaluated for suitability of physical properties and chemical stability in the MO-CVD environment. Special substrate preparation procedures--including chemical cleaning and processing, mechanical polishing, surface texturing, and high-temperature annealing--will be investigated and developed to improve surfaces for film growth. Substrate materials will be carefully characterized to provide correlation with film properties.

During the first quarter a variety of candidate substrate materials was considered for use. Only a relatively small number of materials commercially available--including amorphous glasses, glass-ceramics, polycrystalline ceramics, and certain metals and alloys--can meet the stringent requirements of physical and chemical properties, cost, and eventual availability in large areas required for application to low-cost terrestrial solar arrays.

Selection criteria were developed to serve as the basis for identifying those candidate materials to be evaluated. Ten such materials were selected: (1) Corning Code 0317 glass; (2) Corning Code 7059 glass; (3) Corning Code 1723 glass; (4) Corning Code 0211 glass; (5) Corning Code 9606 glass-ceramic; (6) ASM805 polycrystalline alumina ceramic (3M Co.); (7) Vistal polycrystalline alumina ceramic (Coors Porcelain Co.); (8) thin-film Ge on glass; (9) thin-film Ge on Kovar-type alloy sheet; and (10) thin-film Mo on glass.

Several of these materials were evaluated in the first quarter by a standard GaAs film growth procedure using the MO-CVD process. Analysis of the properties of the polycrystalline GaAs films grown on these substrates in the first quarter showed only minor differences among the films. All of the candidate insulating substrate materials tested appeared to be non-reactive with the GaAs film or the reactants used to produce it, under the particular growth conditions investigated. However, it was found that bare Kovar was attacked by AsH_3 at temperatures above 500°C. The resulting compound formation and the high incidence of Ni-rich inclusions found in the deposited GaAs films make these Ni alloys unsuitable as substrates for direct growth of GaAs films by the MO-CVD method. The use of an intermediate layer of another material on the alloy might still permit its successful use as an inexpensive supporting

underlayer, and the achievement of large-grain (10-20 μm) growth of Ge films on this alloy by GeH_4 pyrolysis in the first quarter indicated some promise for this configuration as a composite substrate.

Mo substrates were also used for GaAs film growth and, contrary to the case for the Fe-Ni-Co alloys, no attack of the Mo substrates by AsH_3 was observed. Growth of GaAs on Corning Code 0317 and Code 1723 glasses did not result in any detectable bowing of the substrate-film composite. These glasses appeared to be stable in H_2 up to ~730°C. The high-purity polycrystalline aluminas ASM805 (99.9 percent) and ASM838 (99.5 percent) also appeared to be completely stable, physically and chemically, in the GaAs CVD environment.

During the second quarter contacts were maintained with various manufacturers of the substrate material types selected for use in the program, to ensure that samples would be available as needed for the CVD experiments (Task 2) and to encourage continuing efforts to identify other materials that might be even more satisfactory than those selected. As a result, additional supplies of the candidate substrate materials were obtained. Although several new sources of polycrystalline aluminas were found, none of the material received from such sources appeared any better in surface characteristics than ASM805 alumina (3M Co.), one of the 10 selected materials.

Predeposition characterization of candidate substrate materials continued, with GaAs film growth by the MO-CVD method under a set of standard conditions still used as the critical test of a substrate's suitability. Composite substrates consisting of films of Mo 1-2 μm thick deposited by sputtering onto Kovar and several glasses and polycrystalline aluminas were prepared and tested by GaAs film growth. The effects of H_2 and AsH_3 atmospheres at two different temperatures (625 and 725°C) on the surfaces of the candidate glass substrates were examined, with only one glass (Corning Code 0211) adversely affected. Several substrate surface cleaning procedures were also evaluated. The most effective procedure tested included etching the substrate in Caro's acid (1:1 H_2SO_4:30 percent H_2O_2) as one of the steps.

During the third quarter, additional samples of materials were obtained from various suppliers. A number of samples of Mo, Mo alloys, specially annealed Mo sheet having different grain sizes, and W sheet were obtained. However, emphasis in the program was then shifted to thin Mo films applied to glass substrates (see details below) and, consequently, these samples were not evaluated as substrates.

In the third quarter, based on the experimental results obtained for GaAs growth on the various substrate materials under investigation, it became possible to narrow further the list of 10 candidate substrate materials selected at the end of the second month of the program for experimental evaluation. Because of the high resistivities consistently obtained in polycrystalline films of GaAs or GaAlAs grown on substrates of the various candidate glasses--irrespective of the conductivity type or the concentration of added dopant--it was clear that a conducting metal layer or grid of large area coverage would be required for adequate contact to the base layer of a polycrystalline solar cell structure.

Consequently, totally bare glasses (Corning Codes 0317, 7059, 1723, and 0211) and totally bare Corning Code 9606 glass-ceramic were no longer considered candidate substrates. However, Codes 0317, 7059, 1723, and 9606 when accompanied by an appropriate open conducting grid on the growth surface were retained as candidates.

Corning Code 0211 glass was eliminated from further extensive use because of its excessive Zn impurity content. The required conducting layer on these insulating substrates was expected to be sputtered Mo.

ASM805 polycrystalline alumina ceramic from the 3M Co. was also eliminated from further experimental use, primarily because polycrystalline films grown on it exhibited high resistivities that would require extensive contact gridding at the film-substrate interface, and its relatively higher cost compared with that of the glasses renders it non-competitive with them for the present application. One of the original reasons for conducting growth experiments with a large-grained polycrystalline alumina substrate was that it provided a useful intermediate crystal structure between single-crystal and fine-grained polycrystalline or amorphous substrates, and permitted the study of various aspects of film nucleation and early-stage growth. However, the large-grained Vistal polycrystalline alumina ceramics from Coors filled this need more satisfactorily than did ASM805; the former was thus retained as an experimentally useful candidate substrate material, despite its relatively high cost.

During the fourth quarter, it was learned that Corning intended to phase out production of Code 0317 glass. Since this glass was the one in the candidate list found to be most compatible with thin-film Mo intermediate layers, a relatively large quantity of the glass was purchased from the Corning Advanced Products Group to assure availability of substrates for continued experimental use.

Because the use of carbon as a substrate was found to compatible with the MO-CVD process, it was added to the list of candidate substrates, and some GaAs deposition experiments were carried out with this material. However, owing to a continued delay in the shipment of polished graphite substrates ordered from Poco Graphite, Inc. (Decatur, TX), high-purity substrates were not used in this program.

Much of the work of the fourth quarter utilized composite substrates consisting of 2000 Å-thick Mo films that had been sputtered onto Corning Code 0317 glass substrates. These sputtered Mo films were deposited in two different Rockwell laboratories, one a device group in the Electronics Research Center and the other a thin-film microcircuits group in another division at the Rockwell Anaheim site.

In addition, Mo grid contacts were fabricated on some of the composite Mo/glass substrates (those with Mo films 2000Å thick) by photolithographic techniques. This grid pattern involved line spacings of 1.00mm and line widths of 50 μm, with a net coverage factor of ~10 percent. These substrates were used in GaAs deposition experiments to determine if such a contact grid would be adequate for contacting the GaAs base layer of solar cell structures on glass. Results of the experiments are described in later sections of this report.

2.2 TASK 2. CVD EXPERIMENTS AND PARAMETER STUDIES

This task was summarized in the original program proposal as follows:

> The MO-CVD process will be used to grow films of GaAs, GaAℓAs, and possibly AℓAs (and/or AℓAsP) on the polycrystalline and amorphous substrates identified in Task 1. The effects of deposition conditions on the properties of candidate substrate materials and of the resulting films will be determined. Experiments to establish the effects of growth conditions on film grain size will be carried out, and optimum film doping methods and conditions will be established for specific desired film properties and photovoltaic device configurations. Special processing methods --such as in situ gas-phase etching and/or annealing and the growth of intermediate nucleating layers--will be investigated, to improve film properties. Early in the program a second CVD reactor system will be assembled to supplement the one initially used for this task.

During the course of this program, the MO-CVD process has been applied to the growth of thin films on numerous polycrystalline and amorphous substrate materials as well as various single-crystal substrates. The deposition experiments can be grouped into eight major divisions: (1) growth of doped and undoped single-crystal films of GaAs and GaAℓAs alloys on single-crystal GaAs substrates; (2) studies of the effects of H_2 and AsH_3 on low-cost substrates at the growth temperature; (3) studies of the deposition of polycrystalline GaAs films on various insulating and conducting low-cost substrates; (4) growth of Ge films for use as intermediate layers for the deposition of GaAs on low-cost substrates; (5) deposition of GaAs films on composite substrates; (6) deposition of thin (500Å) undoped films of $Ga_{(1-x)}A\ell_xAs$ ($x = 0.8$) on single-crystal large-diameter (3.8 cm) sapphire (α-$A\ell_2O_3$) substrates; (7) growth of multilayer polycrystalline solar cell structures on low-cost substrates; and (8) growth of multilayer single-crystal solar cell structures on single-crystal substrates.

In addition, a second MO-CVD reactor was designed, built, and made operational during the first half of the program. Also investigated was the problem of inadequate SiC coatings on graphite susceptors supplied by numerous manufacturers.

The work of this task can be summarized as follows; additional details are given subsequently.

In the first quarter, experimental investigation of the MO-CVD process began early in the first month, and employed an existing CVD reactor system that had been used for previous company-sponsored investigations in the GaAs-GaAℓAs materials system. A second MO-CVD reactor system was designed and fabrication was begun, but delays in delivery of some of the essential components prevented its completion before the end of the quarter.

The existing reactor system was used in the first quarter for 101 MO-CVD experiments. The majority of these were in two groups: (1) those designed to give data on the doping of GaAs and $Ga_{(1-x)}A\ell_xAs$ ($x = 0.9$) single-crystal films grown on single-crystal GaAs substrates, and (2) those designed to give information on the growth of polycrystalline GaAs films on a variety of potentially low-cost substrates. Early in the quarter single-crystal films of Se-doped GaAs, Zn-doped GaAs, Se-doped $Ga_{1-x}A\ell_xAs$ ($x = 0.9$), and Zn-doped $Ga_{1-x}A\ell_xAs$ ($x = 0.9$) were grown on single-crystal Cr-doped

GaAs substrates. The dependence of doping concentration upon the flow rate (i.e., concentration) of the doping gas was investigated, and study of the first three doping systems was completed. Polycrystalline GaAs films with apparent grain sizes in the 2 to 5 μm range and high electrical resistivities in the undoped condition were grown by MO-CVD on several of the candidate low-cost substrate materials in the first quarter.

During the second quarter of the contract, 59 MO-CVD experiments were performed in the original reactor (Reactor A) and 26 MO-CVD experiments were done in the new dedicated CVD reactor (Reactor B), which was completed in the second quarter. The experiments done in Reactor A included (1) growth of GaAℓAs on single-crystal substrates; (2) growth of polycrystalline GaAs on candidate low-cost substrates; (3) studies of the nucleation of GaAs on low-cost substrates; (4) studies of the effects of H_2 and AsH_3 on the candidate glasses; (5) studies of the effect of surface texturing on the growth of GaAs on a selected glass substrate (Corning Code 0211); and (6) studies of the growth of GaAs on Mo films deposited on various low-cost substrates.

In addition, 45 other MO-CVD runs were made in Reactor A to study the problem of faulty SiC-coated graphite susceptors. The fact that adequatly sealed susceptors were not available from the usual suppliers prevented continuation of the study of doping of GaAℓAs films at that time, and prompted an extensive parallel investigation of various alternative solutions to this problem.* This also delayed the planned fabrication of thin-film GaAℓAs/GaAs heterostructure solar cells by the MO-CVD technique.

The experiments done in the new Reactor B were principally the growth of undoped GaAs films on single-crystal substrates and Se-doped GaAs films on single-crystal substrates. The undoped GaAs films were grown to check out the reactor performance, while the doped films were grown to determine the n-type Se-doping characteristics of this new reactor.

During the second quarter polycrystalline undoped and Se-doped films of GaAs were grown on Corning Codes 0211, 0317, 1723, and 7059 glasses and on the polycrystalline aluminas ASM805 (3M Co.) and Vistal (Coors), the latter two in various refired conditions which result in increased grain sizes. All of these substrates except 0211 glass appeared stable in H_2 at 725°C. Grain sizes in films on the glasses were typically in the 1-2 μm range, although some larger grains were found intermixed under certain conditions -- e.g., in films grown on 7059 glass at 675°C and on Corning Code 9606 glass-ceramic at 725°C. Grain sizes in polycrystalline GaAs films on the aluminas were found to be directly related to the grain sizes in the substrates, and were quite large in some cases (up to ~100 μm or more).

It was also found that at temperatures above ~600°C the Corning Code 0211 glass begins to discolor and soften in H_2, and at higher temperatures (those used for deposition of GaAs) additional changes occur that result in film properties quite different from those found with other glasses. Relatively large grains (5-10 μm) and p-type carrier concentrations were found in the GaAs films; the apparent acceptor doping was attributed to Zn impurity in the glass, and the larger grain size was probably associated

*Because of the nature of the problem and the fact that solution was important to several other programs in progress at Rockwell, these investigations were supported largely by company (i.e., not contract) funding.

with a tendency of this glass to induce relatively widely-spaced nucleation of the growing GaAs film -- a tendency also shared, to a much smaller degree, by Corning Code 1723 glass.

Some similarities were also observed in the post-nucleation early-stage growth behavior at 725°C of GaAs films on Corning Code 9606 glass-ceramic and polished ASM805 polycrystalline alumina substrates, presumably due to the regions in the surface of the former in which recrystallization occurred during formation of the glass-ceramic material. Polycrystalline GaAs films grown by the MO-CVD method were found to show a slightly preferred {111} crystallographic orientation on the metals and the aluminas investigated. The films deposited on the various glasses, however, exhibit a marked tendency for completely random crystallographic orientation.

During the third quarter 69 MO-CVD experiments were carried out using Reactor A and 61 MO-CVD experiments were performed in Reactor B. In addition, 55 separate experiments were done to examine further the problem of faulty susceptors; as before, the latter studies were supported largely by separate company funds.

The 130 contract-related MO-CVD experiments performed during the third quarter were in nine categories: (1) growth of polycrystalline GaAs layers on uncoated low-cost substrates (from the candidate list); (2) growth of polycrystalline GaAs layers on low-cost composite substrates of sputtered Mo films that had been deposited on glasses, polycrystalline aluminas and Kovar metal; (3) growth of polycrystalline Ge films on uncoated low-cost substrates; (4) growth of GaAs films on low-cost composite substrates consisting of Ge films on glasses, aluminas, and Kovar metal; (5) growth of polycrystalline GaAs n/n^+, p/p^+, and p-n junction structures on low-cost substrates; (6) growth of polycrystalline p-type $Ga_{(1-x)}Al_xAs$:Zn ($x \approx 0.8$) films on low-cost substrates; (7) growth of doped and undoped single-crystal GaAs and $Ga_{(1-x)}Al_xAs$ ($x \approx 0.8$) films on GaAs:Cr single-crystal substrates; (8) growth of single-crystal AlAs films on single-crystal substrates; and (9) growth of single-crystal GaAlAs/GaAs heterostructure solar cells.

By the end of the third quarter polycrystalline GaAs films had been grown on all of the potentially low-cost materials in the candidate list. All of the MO-CVD experiments involving the growth of polycrystalline GaAs films were carried out in Reactor A, while most of the single-crystal films were grown in Reactor B; however, some single-crystal films were grown in Reactor A, also.

Single-crystal films of GaAs and $Ga_{(1-x)}Al_xAs$ ($x \approx 0.8$) were grown to study the Zn and Se doping of these materials and to provide the doping data needed to grow p-n junctions and heterostructure solar cell configurations. Two-layer single-crystal structures, consisting of p-GaAlAs/p-GaAs on an n-type single-crystal GaAs substrate, and three-layer epitaxial structures, consisting of p-GaAlAs:Zn/p-GaAs:Zn/n-GaAs:Se on an n-type single-crystal Si-doped GaAs substrate, with very thin (~500Å) GaAlAs window layers, were prepared for fabrication of solar cells. Polycrystalline n/n^+, p/p^+, and p-n junction structures were also grown on the low-cost substrates.

The experimental CVD investigations in the fourth quarter were largely devoted to the growth of various structures for use in fabricating experimental polycrystalline solar cells. These experiments were in three main categories: 1) growth of polycrystalline n/n^+ structures; 2) growth of polycrystalline p-n juntion structures; and 3) growth of single-layer polycrystalline films for doping studies.

The polycrystalline GaAs n/n^+ structures were grown on substrates of 1) small-grained polycrystalline bulk GaAs; 2) W metal; 3) Mo films deposited on Corning Code 0317 glass substrates; 4) Ge films on patterned Mo layers on 0317 glass; 5) Ge films on patterned Mo layers on Vistal 5* polycrystalline alumina; 6) patterned Mo layers on single-crystal (0001)-oriented sapphire; 7) Pt films deposited on patterned Mo layers on single-crystal (0001) sapphire; and 8) Pt films on patterned Mo on 0317 glass. Many of these polycrystalline GaAs composite structures were subsequently used for fabrication of Schottky-barrier devices, using Au as the barrier-forming metal, for subsequent measurement of photovoltaic properties. In addition, some of the same composite substrates were used for growth of polycrystalline p-n junction devices which subsequently were characterized. (See Sections 2.3 and 2.4.)

In addition, during the final quarter CVD experiments were performed in several other areas of importance to the program. For example, both doped and undoped polycrystalline GaAs single-layer and multilayer films were grown on Mo-coated Corning Code 0317 glass substrates. In some cases, the Mo films were photolithographically processed into a square grid structure, leaving square areas of the glass substrate surface exposed. The Mo metal is required for the large-area distributed back contact to the GaAs film for solar cell structures. Single-layer polycrystalline GaAs:Se and GaAs:Zn doped films were prepared on composite substrates of Mo/0317 glass to study further the doping characteristics of such films.

As indicated above, GaAs n/n^+ structures were also grown on these Mo/0317 composite substrates. The thickness and doping levels of the n and n^+ layers were varied to determine the effect these parameters would have on Schottky-barrier solar cell device performance. GaAs p-n junction structures were also grown on the Mo/0317 composite substrates to study the properties of polycrystalline p-n junctions grown under various experimental conditions.

In an attempt to grow an inverted polycrystalline Schottky-barrier solar cell using the glass substrate itself as a window, a n^+/n GaAs film was grown on a Mo-grid-patterned Code 0317 glass substrate that had been coated with a thin (~50Å) Pt film prior to growth of the GaAs. The structure showed some photocurrent generation under preliminary testing, but further analysis is required to determine if a Schottky barrier is actually formed at the Pt-GaAs interface.

Polycrystalline Ge films have been grown on Mo/0317 composite substrates having both full-coverage and grid-patterned Mo films. These Ge films exhibited relatively small grain size, as evidenced by SEM examination of surface features as described in a later section. A GaAs film was grown on such a Ge intermediate layer that had been deposited on a Mo/0317 composite substrate earlier in the same CVD run. The result of SEM examination of its surface is described in Section 2.3.

Ge films were also deposited on Corning Code 9606 glass-ceramic at temperatures of 725, 775, and 825°C to study the dependence of the morphology of the deposited film upon the deposition temperature. At 725°C a relatively smooth and small-grained film resulted, while at 775 and 825°C large projections occurred in the surface and the film was quite rough.

*Vistal 5 is Vistal polycrystalline alumina refired five separate times beyond the normal commercial processing, to produce enlarged grains.

In an attempt to enhance the grain size of Ge films deposited at 725°C, post-deposition in situ annealing of Ge films deposited on 9606 glass-ceramic was carried out at 925 and 950°C (the melting point of Ge is 947°C) for 1-5 min. The films appeared to be smoother than unannealed films, but SEM examination of the film surfaces did not indicate that any significant enhancement of grain size had occurred.

Undoped GaAs films were also grown on composite substrates of Ge/9606 glass-ceramic, to investigate the apparent autodoping of GaAs films grown on Ge intermediate layers. (No solution to this autodoping problem has yet been found.) GaAs films grown on the Ge/9606 composite substrates had relatively large (5-10μm) grains. Annealing of the Ge film at 925 and at 950°C immediately prior to the growth of the GaAs film also did not appear to lead to larger grains in the GaAs layer, consistent with the absence of grain growth in the Ge layer itself, mentioned above. The results of SEM examination of these films are described in the Task 3 discussion (Section 2.3).

A two-layer n/n^+ GaAs film was grown on a sample of Poco graphite at 725°C. The film had relatively small grains. An attempt to fabricate a Schottky-barrier solar cell in this material was not successful, as described in the discussion of Task 4 activities (Section 2.4).

In addition to the experiments with polycrystalline films on various substrates, a number of undoped and Zn- and Se-doped single-crystal GaAs and $Ga_{(1-x)}Al_xAs$ ($x = 0.8$) films were grown on single-crystal GaAs:Cr substrates to evaluate recently installed trimethylgallium (TMG) sources on both Reactor A and Reactor B. The measured values of carrier mobilities and the dependence of the net carrier concentration upon the dopant flow rate in these films were in good agreement with values obtained for the previous TMG sources used in this program, indicating the new sources were satisfactory.

Undoped GaAlAs films with various alloy compositions were also grown in Reactor B to determine the dependence of the Al mole fraction in the film upon the Ga and the Al source flow rates. The lattice parameters of these films were measured by x-ray diffraction so that the alloy compositions could be determined by a method described in Section 2.3.

Finally, single-crystal three-layer p-GaAlAs/p-GaAs/n-GaAs heterostructure solar cell structures were grown on (100)-oriented GaAs:Si single-crystal substrates. These structures were similar to those described in Quarterly Project Report No. 3 (Ref 10). Solar cell structures of this type have now been grown totally covering substrate areas as large as 8 cm^2.

The principal results of the CVD growth experiments and parameter studies carried out during the 12-month program are described in further detail in the following sections.

2.2.1 Growth of Single-crystal Films on GaAs Substrates

Early in the program, a series of undoped and doped films of GaAs and $Ga_{0.2}Al_{0.8}As$ were grown on (100)-oriented high-resistivity single-crystal GaAs:Cr substrates in the original reactor (Reactor A) employed in this program. These experiments were designed to provide data relating the measured room-temperature

carrier concentration for n-type and p-type epitaxial layers to the flow rates of the corresponding H_2Se and diethylzinc (DEZn) dopant sources.

During the initial studies of the p-type doping of $Ga_{0.2}Al_{0.8}As$ films, it was discovered that even undoped films were heavily doped p type. Concurrently, it was noticed that after a run the deposit on the susceptor had dark spots near some surface irregularities. These were apparently unsealed pinholes in the coating, through which the graphite absorbed the liquids used during the susceptor cleaning process. This resulted in outgassing during heating and adversely affected the growth.* Since these problems seemed to be most severe for the growth of GaAlAs alloys, emphasis during the first and second quarters was shifted to the growth of polycrystalline GaAs films on low-cost substrates and to the evaluation of various potentially low-cost substrate materials.

During the second and third quarters additional single-crystal GaAs and $Ga_{0.2}Al_{0.8}As$ films were grown to determine the doping parameters of the second MO-CVD reactor (Reactor B) that was built expressly for this program in the first two quarters. These depositions were carried out after a supplier of adequately sealed susceptors had been found.** In these experiments Se-doped n-type GaAs films and Zn-doped p-type GaAs and $Ga_{(1-x)}Al_xAs$ ($x \approx 0.8$) films were grown on (100)-oriented GaAs:Cr high-resistivity substrates. Some earlier data for the Se doping of GaAs films grown in this reactor were given in Quarterly Report No. 2 (Ref 9). Both the older data and data obtained in the third quarter are shown in Figure 2-1.

It can be seen that the Se doping of GaAs films grown at temperatures of 700 and 750°C follows very nearly the same function of the H_2Se flow rate employed. The line drawn through the data of Figure 2-1 has a slope of unity, showing a linear relationship between the dopant gas flow rate and the measured net donor concentration, as is expected.

Single-crystal GaAs:Zn and GaAlAs:Zn films were also grown on GaAs:Cr substrates, to determine the dependence of the Zn doping upon the effective flow rate of the DEZn carrier gas (H_2) into the reactor chamber. Figure 2-2 shows the results obtained by van der Pauw measurements made on the GaAs:Zn films. The line in this figure is also drawn with a slope of unity. The measured values of the net acceptor concentration are seen to follow a linear dependence upon the effective H_2 carrier gas flow rate through the DEZn, as would be expected.

Single-crystal p-type $Ga_{(1-x)}Al_xAs$:Zn ($x \approx 0.8$) films were also grown on GaAs:Cr substrates, to determine the experimental conditions required for the growth of heavily doped p-type GaAlAs films as are needed for the window layers for GaAlAs/GaAs heterostructure solar cells. $Ga_{0.2}Al_{0.8}As$:Zn films were grown with a doping of $\sim 10^{18}$ cm^{-3}, as required for this window layer.

Because AlAs has a higher bandgap energy than either GaAs or GaAlAs alloys, it might be the best material for the window layer of a heterostructure GaAs solar cell. Single-crystal films of AlAs were grown at 750°C on single-crystal (0001) sapphire and (100) GaAs substrates early in the program. Some of the AlAs/GaAs

*See Refs 8, 9, and 10 and Section 2.2.10 for additional details.
**See Ref 10 for detailed discussion.

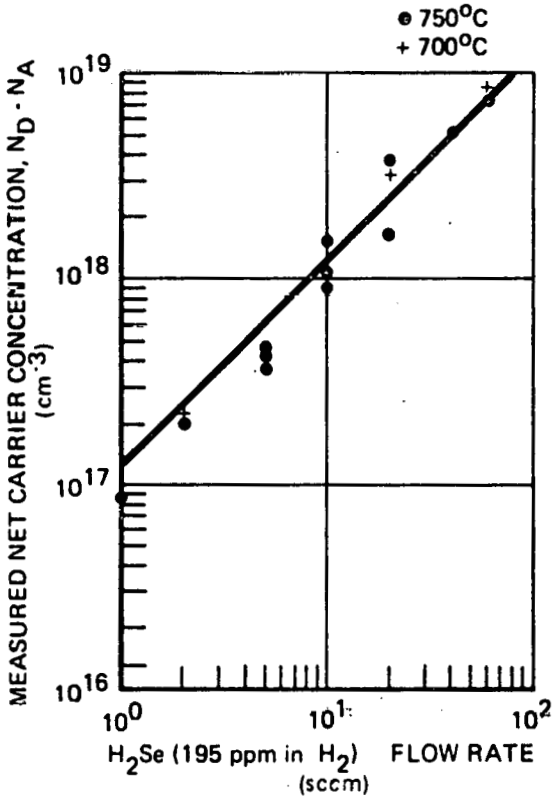

Figure 2-1. Measured Carrier Concentration for Se-doped GaAs Films Grown at 700 and 750°C, as Function of H_2Se Flow Rate

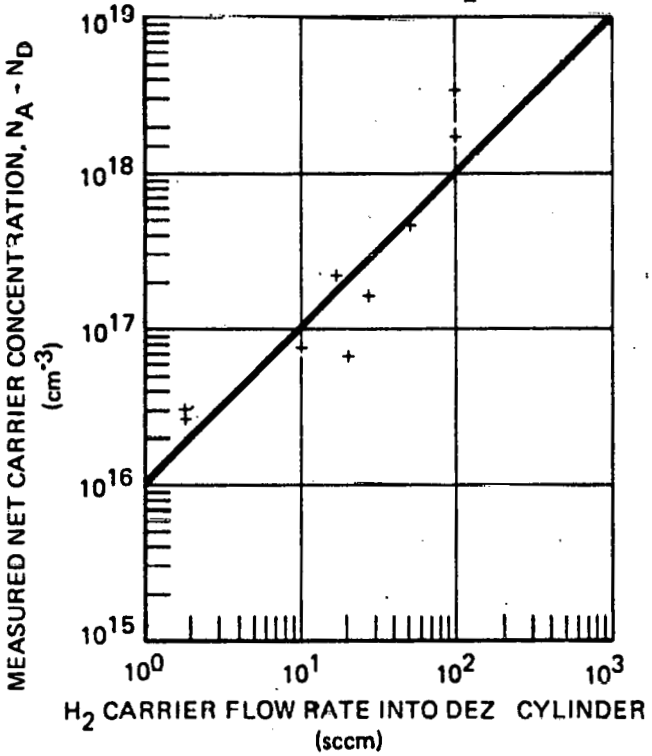

Figure 2-2. Measured Carrier Concentration of Zn-doped GaAs Films as Function of Carrier Gas Flow Rate through DEZn Source

films were stored in a dry N_2 atmosphere to prevent any oxidation of the epitaxial film. These were subsequently used in x-ray diffraction measurements of the AℓAs lattice parameter. AℓAs films that were exposed to air gradually oxidized over a period of 1-2 weeks.

During the fourth quarter of this program, single-crystal GaAs, GaAℓAs, and AℓAs films were grown on (100) GaAs:Cr and GaAs:Si substrates to be used in x-ray diffractometer, x-ray double-crystal, and electron-microprobe studies of the dependence of $Ga_{(1-x)}Al_xAs$ alloy composition upon the relative flow rates of TMG and trimethylaluminum (TMAℓ) employed during the growth. Alloy films were grown at two temperatures and for two different times. Films of GaAs and AℓAs were prepared to establish the composition end-point values for these measurements. The results of these measurements are discussed in Section 2.3.4.

2.2.2 Effects of H_2 and AsH_3 Atmosphere on Low-cost Substrate Materials

To aid in the evaluation and selection of potentially useful low-cost substrates, a number of these materials were heated to the growth temperature in a H_2 and/or $H_2 + AsH_3$ atmosphere. Two of the potentially useful materials that were tested showed obvious macroscopic effects during these tests, namely, Kovar (Fe-Ni-Co alloy) and its related alloy metals and Corning Code 0211 glass. Both of these materials changed color upon being heated in a $H_2 + AsH_3$ mixture. GaAs films grown on Kovar were found (by energy-dispersive x-ray analysis) to contain large quantities of Ni. GaAs films deposited upon Code 0211 glass substrates were found to be heavily Zn-doped, by similar analyses.

The results of these experiments were used in conjunction with other data on the physical properties and estimated costs of prospective substrate materials to form a list of candidate materials (see Task 1 discussion, Section 2.1) that would be employed as substrates in subsequent portions of this program (Ref 8). These materials were the following:

1. Glass: Corning Codes 0317, 7059, 1723, and 0211
2. Glass-ceramic: Corning Code 9606
3. Polycrystalline alumina: ASM805 (3M Co.) and Vistal (Coors)
4. Composite structure: Ge/glass, Ge/Kovar-type alloys, Mo/glass

Based on the early experience gained in the growth of polycrystalline films of GaAs on a number of different substrates--including metals, glasses, and polycrystalline aluminas--a standard MO-CVD evaluation procedure was established for use in evaluating these candidate low-cost substrate materials. This procedure consisted of a standard MO-CVD run to grow an undoped GaAs film ~5 μm thick on the substrate material to be evaluated.

The following standard conditions were employed in this procedure:

1. H_2 atmosphere (carrier gas)
2. H_2 flow rate during growth: 3500 sccm
3. Total gas flow rate in reactor during growth: 4000 sccm
4. Temperature of substrate for deposition: 725°C
5. Predeposition processing time: 3 min
6. AsH_3 flow rate during predeposition process: 75 sccm
7. AsH_3 flow rate during growth: 200 sccm
8. TMG carrier gas H_2 flow: 20 sccm
9. TMG "push" H_2 flow: 500 sccm
10. TMG source temperature: 0°C
11. 2-in. diameter SiC-coated graphite susceptor.

In general, this test run included two or more separate pieces of the candidate substrate material cleaned by different procedures. A piece of (0001)-oriented single-crystal sapphire was also included as a monitor of the progress of the CVD growth run and of the quality of the resulting deposits.

2.2.3 Deposition of Polycrystalline Films of CVD GaAs on Low-cost Substrates

Doped and undoped films of polycrystalline GaAs were grown on numerous low-cost insulating substrates as well as certain conducting materials.

The growth of p-type and n-type polycrystalline GaAs on all of the insulating substrates resulted in films that exhibited resistivities that were much greater (by a factor of 100 to 1000) than the single-crystal GaAs films grown simultaneously on (0001)-oriented sapphire control wafers. As expected, the films with the lowest resistivity were those grown on the largest-grained refired Vistal 5 polycrystalline alumina substrates.

These results indicate that polycrystalline GaAs films grown on such insulating substrates will not be useful in photovoltaic applications without a full- or partial-coverage back contact in the form of an intermediate conducting layer between the GaAs film and the substrates. As a consequence, the primary emphasis in this program was shifted to the investigation of possible composite substrates that consist of a deposited conducting thin film on a low-cost insulator. Experiments with such composites are described more fully below.

The conducting bulk (i.e., not thin-film) materials employed in this program are the metals Kovar, W, and Mo. In addition, a few experiments were carried out with graphite substrates, as noted earlier. Because the Kovar was found to react with

AsH_3, as already mentioned, and to result in the incorporation of large quantities of Ni into the GaAs film, presumably by some alloy formation with As, the studies of Kovar substrates were suspended.

Because Mo has a thermal expansion coefficient that is close to that of GaAs and is relatively low in cost (compared with some other materials used as substrates) it was the principal conducting substrate investigated in this work. However, since bulk Mo is probably too expensive to be compatible with ERDA program goals, it was used primarily to evaluate its compatibility with the MO-CVD process and to determine its suitability as a possible thin-film conducting intermediate layer for use on glass substrates under deposited GaAs films.

The grain sizes observed in GaAs films grown on glass substrates in this program have typically been in the 2-10 μm range. The grain structure of GaAs films grown on polycrystalline aluminas reproduces the grain structure of the substrate. Studies were made to determine if the grain size in polycrystalline films deposited on glasses was influenced by the growth temperature in the range 650°C to 750°C, but no strong influence was observed.

The grain sizes observed in GaAs films grown on Corning Code 0317, 1723, and 7059 glass substrates were typically in the 2-5 μm range. GaAs films grown on Code 0211 glass exhibited much larger grain sizes - the order of 10-20 μm. This is a result of the much lower nucleation-site density that was observed to occur for GaAs deposits on Code 0211 glass. Unfortunately, this glass contains Zn as a significant impurity, and undoped GaAs films grown on this material are heavily doped p type. In fact, the addition of H_2Se to the gas stream during growth failed to produce n-type films. Because of this, Code 0211 glass was dropped from the candidate list.

The grain size of GaAs films deposited upon polycrystalline aluminas was found to be identical to that of the substrate. This is a result of the fact that the GaAs grows epitaxially on the individual single-crystal $A\ell_2O_3$ grains. Thus, the largest grains occur for films grown on the largest-grained alumina substrate, namely Coors Vistal 5.

2.2.4 Growth of Ge Intermediate Layers on Low-cost Substrates

As mentioned earlier, the studies of the electrical properties of GaAs films grown on bare insulating substrates indicated that a conducting intermediate layer (or grid structure) between the GaAs film and the substrate would be required to provide a low-resistance back contact to any device utilizing this structure. One potentially useful material for such a layer is a thin film of Ge, owing to the close match of its lattice constant and thermal expansion coefficient of those of GaAs.

To investigate this possibility and to study the effects such a layer might have on grain size in the GaAs layer, the deposition of Ge films upon various low-cost substrates was undertaken. In these studies Ge films were deposited by the pyrolysis of germane (GeH_4) at 725°C upon Corning Code 0211, 0317, 1723, and 7059 glasses; the polycrystalline aluminas ASM805, ASM805-1,* and Vistal 5; and polished metal substrates.

*This designation is used for ASM805 polycrystalline alumina that has been refired once beyond the normal commercial processing, to produce enlarged grains.

It was determined that polycrystalline Ge films deposited upon glasses exhibited somewhat larger grain size than did GaAs films grown on the same substrate material. This appears to be principally a result of lower nucleation site density occurring for Ge films than for GaAs films on these materials.

2.2.5 Growth of GaAs Films on Composite Substrates

To develop a method for providing a distributed ohmic contact to the substrate side of a Ga As film grown on an insulator, the growth of doped GaAs films on a number of composite substrates was studied. This work was mainly concerned with full-coverage Ge and Mo films and grid-patterned Mo films on glass substrates, although Pt/Mo-grid/glass composites were also employed as substrates for GaAs growth.

Both Ge and Mo intermediate layers provided an ohmic contact to the over-grown GaAs film. The GaAs/Ge/glass composite structures had somewhat rougher surface topography than the GaAs/Mo/glass structures. This is a direct result of the relatively rough surface of the Ge/glass composite. It was discovered that undoped GaAs films deposited upon Ge intermediate layers were highly conductive, apparently due to auto-doping of the GaAs film by the Ge film. As a result of this undesirable effect the principal composite substrate studied was the Mo/glass structure.

The grid-patterned Mo intermediate layers resulted in higher resistance devices than did the full-coverage Mo films, as a consequence of the relatively high resistance of the polycrystalline GaAs film itself.

2.2.6 Growth of Thin GaAℓAs Films on Large-area Sapphire Substrates

An important part of a GaAℓAs/GaAs heterostructure solar cell is the GaAℓAs window itself. To determine the capabilities of the MO-CVD process for the reproducible formation of the desired uniform, thin, large-area $Ga_{(1-x)}Al_xAs$ window layer, $Ga_{0.2}Al_{0.8}As$ films were grown on large-area (3.8 cm diameter) single-crystal sapphire substrates. Films as thin as 350Å were grown with excellent thickness uniformity, control, and reproducibility. The area of these films (>11 cm^2) is larger by at least a factor of 3 than the largest films of this type yet grown by liquid-phase epitaxy (LPE), and the MO-CVD films are much more uniform in thicknesses. Thicker films (~1μm) were measured to have ±3 percent thickness uniformity across a substrate 3.8 cm in diameter.

2.2.7 Growth of Polycrystalline Solar Cell Structures on Low-cost Substrates

A number of different types of polycrystalline GaAs solar cell structures were grown in this program. Much of the emphasis was placed upon n/n+ structures for the fabrication of polycrystalline Schottky-barrier solar cells. These structures were prepared by growing first a heavily-doped n+ layer of GaAs:Se and then an undoped n-type layer of GaAs on the low-cost substrate. The n+ layer allows good contact to the Mo or Ge/Mo intermediate layer, to provide a distributed back contact to the device. The undoped n-type layer allows a good Schottky barrier to be made. The performance of these devices is discussed in Section 2.4.2.

In addition, p/p+, p/n, n/p, and p/n/n+ polycrystalline GaAs multilayer films were grown, as well as p-GaAℓAs/p-GaAs/n-GaAs/n+GaAs polycrystalline heterstructure cell configurations.

In general, the n/n+ Schottky barrier cells exhibited the best performance. The p-n junction cells had poor I-V characteristics and in many cases were shorts. The results are discussed further in Section 2.4.3.

In most cases, these structures were grown on Mo/Code 0317 glass composite substrates, although Ge/Mo/0317 glass, Mo/Code 9606 glass-ceramic, and polycrystalline bulk GaAs substrates were also employed. As might be expected, the best device performance occurred for devices on the polycrystalline bulk GaAs substrate.

The performance of these polycrystalline solar cells under air-mass-zero (AM0) illumination is reviewed in the Task 4 discussion (Section 2.4).

2.2.8 Single-crystal Solar Cell Structures Grown by MO-CVD

Two types of single-crystal solar cell structures have been grown in this program: (1) three-layer p-GaAℓAs/p-GaAs/n-GaAs heterostructure solar cells, and (2) two-layer p-GaAs/n-GaAs cells employing a thin (~3000Å) p layer. Both types of structure were grown on single-crystal (100)GaAs and (0001)sapphire substrates, although primary emphasis was placed upon heterstructure cells grown on GaAs substrates.

These heteroface cells were typically grown with the following structure: GaAℓAs:Zn (~ 500Å)/GaAs:Zn(1-2μm)/GaAs Se(3-4μm), grown on n-type GaAs:Si substrates. Au/Zn/Au grid-patterned contacts were applied to the p-type top layer and Au-12 percent Ge contacts to the substrate (n-type) side.

A number of these structures were cleaved and chemically stained to define the interfaces between layers. Both stained and unstained cleaved cross-sections were examined in the SEM to determine layer thicknesses. Figure 2-3 shows an SEM photograph of an unstained cleaved cross-section of one of the three-layer epitaxial structures. The location of the p-n junction is easily seen. The location of the interface between the n-type epitaxial layer and the n-type substrate, however, is not easily seen on unstained cross-sections because the n-type doping concentrations in the two regions are nearly equal (~10^{18} cm^{-3}). The location of this interface was determined for this device by SEM examination of a stained portion of the cleaved piece shown in Figure 2-3.

The 500Å-thick GaAℓAs window layer is not visible in the figure because of secondary electron reflection at the top sample edge. The thickness of this layer was estimated from the results of studies of heteroepitaxial GaAℓAs films grown under the same deposition conditions on single-crystal (0001) sapphire substrates. Surface profilometer measurements of the thicknesses of the GaAℓAs heteroepitaxial films on sapphire were made after a portion of the deposited layer was completely removed from the sapphire substrate. These measurements have shown that good film thickness reproducibility and control have been realized in the reactors used in these studies.

Simulated AM0 efficiencies of 12.8 percent (uncorrected for contact area) have been measured for cells without anti-reflection (AR) coatings. These results are described further in Section 2.4. Cells are large as 8 cm^2 in area have been fabricated, as indicated earlier; these are believed to be the largest GaAs solar cells that have been fabricated to date.

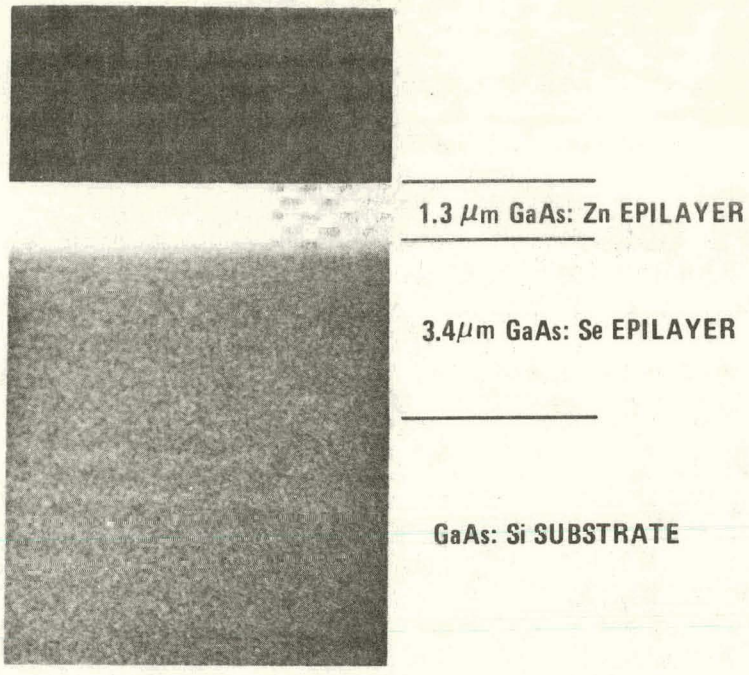

Figure 2-3. SEM Photograph of Unstained Cleaved Cross-section of 3-layer Epitaxial Solar Cell Structure. Thin (~500Å) GaAℓAs Window Layer Masked by Secondary Electron Reflection at Upper Edge of Sample

Single-crystal p-n junction solar cell structures were also grown with very thin (0.3μm) p-type GaAs layers to form shallow-junction devices. In these devices the majority of the carriers are generated in the n-type region of the device, below the junction, eliminating the adverse effects of the high surface recombination velocity at a bare GaAs surface.

As mentioned previously, these two types of solar cell structures (heteroface and shallow-junction) were also grown on (0001)-oriented sapphire substrates. Some of the heteroface structures were grown with the GaAℓAs window layer directly on the sapphire, to use the sapphire as a window and protective cover for the cell as well as for a substrate. This is the so-called inverted cell structure that is one of the thin-film cell designs suggested in the original program proposal and one of the two conceptual designs described in Section 2.5 (Task 5 discussion). However, the devices on sapphire substrates had not yet been evaluated at the conclusion of the experimental performance period covered by this report.

2.2.9 Design and Construction of MO-CVD Reactor System

A second MO-CVD reactor system, to be used exclusively for the work of this contract, was designed at the start of the program, and its construction was completed during the second quarter. It was made operational and tested in the fifth month.

The flow rates of all of the gas constituents in this reactor are controlled by electronic mass-flow controllers (Tylan Corp) having a ±1 percent accuracy and ±0.02 percent full-scale repeatability. The readout unit for these controllers has a 3-1/2 digit display reading directly in standard cc per min (sccm) or standard liters per min (slm) of the corresponding gas. During a growth run the reactant gas flow paths are controlled by air-operated bellows-sealed valves which are in turn controlled by a card-programmable electronic sequencer. The metallorganic constituents are injected into the main reactor manifold by special three-port, low-dead-volume bellows-sealed valves. This allows abrupt changes in doping and film composition to be made.

The liquid source materials are held in stainless-steel cylinders with dip tubes. The metallorganic source material is carried to the reaction zone by H_2 gas which is bubbled through the corresponding liquid source. The gaseous sources are stored in high-pressure cylinders equipped with stainless-steel two-stage pressure regulators. Flow control is provided by mass-flow controllers, as previously indicated.

The reactor chamber is made of quartz, and the SiC-coated graphite susceptor is supported in the rf field by a quartz rod that is rotated during a deposition experiment. The susceptor temperature is monitored by an infrared thermometer. The deposition sequence is controlled by the card-programmable electronic sequencing timer, which controls the air-operated valves and thus the reactant gas flow paths. The quartz reactor chamber is designed with a quartz baffle which aids in the production of a homogeneous gas mixture and improves the thickness uniformity of the film grown on the substrate, which rests on the horizontal susceptor in the vertical deposition chamber.

The reactor system also has a vacuum system using a direct-drive chemical-resistant vacuum pump. This vacuum capability is used to evacuate the quartz reactor chamber prior to each growth run and to aid in leak-checking the reactor gas lines.

The reactor system is shown schematically in Figure 2-4 and in the photograph in Figure 2-5.

2.2.10 Evaluation of SiC-coated Graphite Susceptors

As discussed in Section 2.2.1 and in Quarterly Report No. 1 (Ref 8), early in the program it was discovered that the SiC-coated graphite susceptors that had been received from a supplier were defective and were unusable for the growth of high-quality GaAlAs films. The defective susceptors were returned to the manufacturer for recoating with SiC. However, the recoated susceptors were still not adequate to permit achieving good GaAlAs films. Apparently it is not possible to recoat used susceptors with satisfactory results.

A number of alternate suppliers were then contacted and additional susceptors were ordered. Only one supplier was able to provide a SiC coating that adequately sealed the graphite susceptors. In each case the susceptor was evaluated by the growth of a $Ga_{(1-x)}Al_xAs$ ($x \approx 0.8$) alloy film on a sapphire substrate placed on the susceptor. Fifteen different susceptors were tested, but only those of one manufacturer were acceptable; these have been used for all of the alloy film growth work since that time.

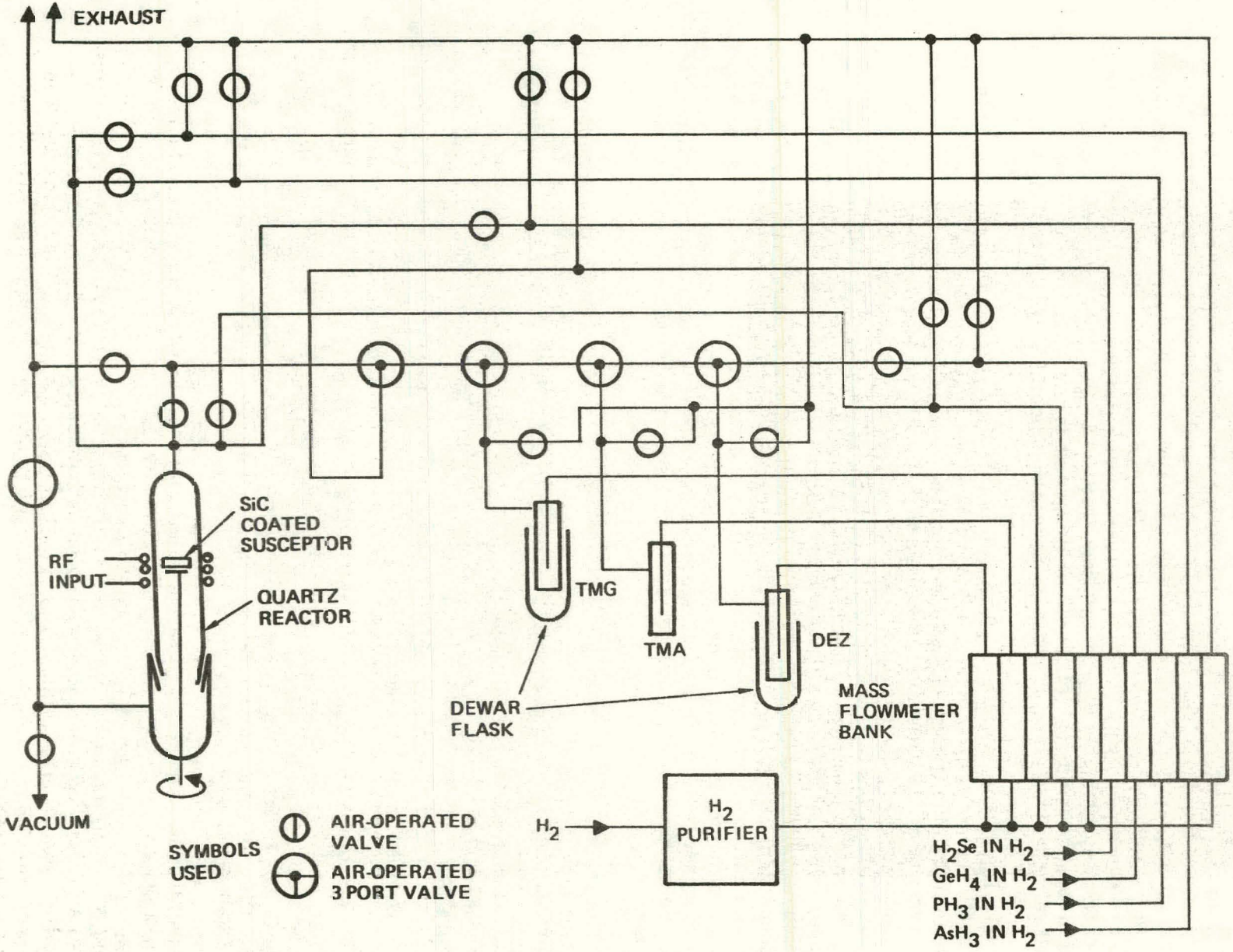

Figure 2-4. Schematic Diagram of MO-CVD Reactor System for Deposition of GaAs and GaAlAs Films

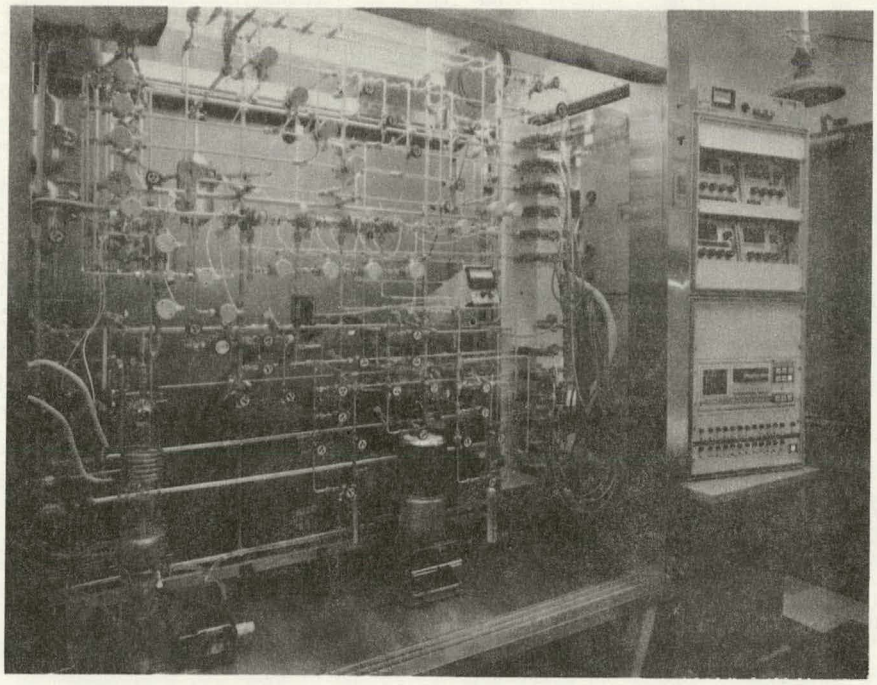

Figure 2-5. MO-CVD Reactor System B (see text)

During the period in which the various SiC-coated graphite susceptors were being prepared and shipped by the suppliers contacted, a number of alternate susceptor materials were evaluated experimentally. For example, an uncoated high-purity graphite susceptor was tested. This susceptor was baked out at 1200°C for 30 min prior to being first used in a GaAℓAs CVD experiment. The susceptor exhibited a somewhat lower thermal conductivity than the SiC-coated susceptors normally used, as evidenced by greater nonuniformity in the radial temperature distribution. This susceptor was used for eight successive CVD experiments without being cleaned. While the early runs showed promise, later runs again resulted in films with poor morphology.

This uncoated susceptor was then cleaned by vapor-phase etching with HCℓ gas at ~725°C. After this cleaning, it was again used in a GaAℓAs deposition. The deposited film had poor morphology, as in the runs prior to the cleaning. Thus, this cleaning procedure was apparently not adequate.

Several other possible alternative solutions to the problem were also studied: (1) a fused-quartz shroud was fabricated to fit over the graphite susceptor, to minimize reaction of the Aℓ species with the outgassing products; (2) a susceptor of thin (500 μm) Mo metal was used; (3) a SiC-coated susceptor was coated with undoped polycrystalline GaAs; (4) a SiC-coated susceptor was coated on both sides with ~100 μm of high-purity silicon nitride; (5) a high-purity (99.97 percent) Mo disk 0.4 in. thick and 2 in. in diameter was used; and (6) a disk of high-purity (and thus high-resistivity) Si was tested as a susceptor.

All of these possibilities were evaluated by the growth of undoped $Ga_{(1-x)}Al_xAs$ ($x \approx 0.8$) films on sapphire substrates resting on the susceptor configuration under test. The quartz shroud and the Mo sheet susceptor showed poor temperature uniformity across the substrate. The susceptors coated with silicon nitride and with GaAs did not result in improved GaAlAs films. The Mo disk was used as the susceptor for growth of a $Ga_{(1-x)}Al_xAs$ ($x \approx 0.8$) film on (0001) sapphire at ~775°C, but that film also had poor morphology so this alternative was not pursued further.

The Si disk was placed on a SiC-coated graphite susceptor to aid in the coupling of the rf field into the low-conductivity (~158 ohm-cm) Si. Even with this arrangement, it was difficult to attain measured susceptor temperatures greater than 760°C, despite the fact that the full output of the rf generator was used. The GaAlAs film deposited in this run had poor morphology, but this may have been a result of the presence of the SiC-coated susceptor support used for the Si disk. This susceptor was known to be incompletely sealed, and it was used simply to determine if the use of the Si disk on top would permit the growth of high-quality GaAlAs films.

2.3 TASK 3. EVALUATION OF FILM PROPERTIES

The activities planned for this task were summarized at the start of the contract as follows:

> A variety of materials characterization methods will be used to evaluate the films grown on various substrates in Task 2. Early in the program, emphasis will be placed on determination of film-substrate interactions, preferred orientation tendencies in the films, grain size, and film surface topography. Surface profilometry, x-ray diffraction analyses, scanning electron microscope examination, reflection electron diffraction analyses, and replica electron microscopy will be used for structural characterization; Auger electron spectroscopy, electron microprobe analysis, and ion-microprobe mass analysis will be employed where appropriate. Electrical properties of the films will be determined by Hall-effect measurements of transport properties, C-V analyses with Schottky barriers, spreading resistance measurements, and other techniques as required. Optical transmission spectra, reflectance spectra, and surface photovoltage measurements will also be used to supply additional information about film properties.

The task of characterizing the wide variety of films grown during the first 12 months of contract activity followed the above general outline, with various evaluation methods and procedures being applied where and as appropriate. Those techniques that were already well developed were applied to both single-crystal and polycrystalline films. Included were physical and structural characterization by scanning electron microscopy and x-ray diffraction analysis, and electrical characterization by van der Pauw techniques and C-V analysis. In all cases the validity of the technique was verified before it was applied to polycrystalline materials.

In some instances it was necessary to adapt or further develop a characterization technique in order to use it with polycrystalline or even – in one or two cases – with single-crystal materials. Examples of this are techniques for determining grain size and preferred orientation of polycrystalline films and methods for the determination of the Al concentration in GaAlAs alloys.

The activities of this task are discussed in detail in the sections that follow, with emphasis on the work that was done during the fourth quarter of the contract. First, however, the principal activities of the entire four quarters are briefly summarized.

The first-quarter activity was dominated by two main areas of investigation - the electrical characterization of single-crystal GaAs and GaAlAs films, and the electrical and structural evaluation of polycrystalline GaAs grown on a variety of dissimilar substrates. In addition, some characterization technique development was begun.

The majority of the effort during the second quarter was devoted to characterizing the physical and electrical properties of polycrystalline films of GaAs grown on various potentially low-cost substrate materials - mainly insulators - from the list of candidate substrate materials identified in the first quarter (see Section 2.1). The rationale for emphasizing the low-cost substrates earlier in the program than

originally planned was provided by early measurements of polycrystalline films grown on insulators, which indicated high electrical resistivity for most polycrystalline GaAs films examined. Because of the importance of these electrical properties to eventual cell design, fabrication, and utilization, this part of the planned program was undertaken early in the second quarter.

Unfortunately, all undoped and Se-doped polycrystalline GaAs films on the candidate insulator substrates (other than 0211 glass) were found to have resistivities greater than is desirable for the fabrication of solar cells on these low-cost materials. The lowest resistivity obtained in any Se-doped polycrystalline GaAs film on glass (excluding Corning Code 0211) was about 10 ohm-cm. The lowest resistivity obtained in any Se-doped polycrystalline film on the aluminas was about 2 ohm-cm; in these films the resistivities were found to have an inverse relationship to grain size in the substrate, at all doping levels.

Whereas good correlations were obtained for carrier concentration measurements by C-V analysis and the van der Pauw method for polycrystalline GaAs films on Mo, carrier concentrations in polycrystalline films on aluminas as determined by C-V analysis were at times two to three orders of magnitude lower than that found for the companion epitaxial film on sapphire as determined by van der Pauw measurements. It was suggested that these discrepancies might be caused by excessive series resistance of the polycrystalline samples, giving erroneous results by the C-V method. The use of thin intermediate layers of Mo on some of the other substrate materials was proposed as a means of improving the base region sheet conductivity in polycrystalline GaAs thin-film cell structures prepared by the MO-CVD process.

During the third quarter the film evaluation activities were expanded to include determination of the structural and physical properties of GaAs films deposited on conducting and composite substrates and the electrical properties of p-type polycrystalline GaAs films. The composite substrates considered to be the best "first attempt" substrates were (1) Mo films on glass, (2) Ge films on glass, and (3) Ge films on Kovar. SEM examination showed that GaAs grown on Mo/glass composite substrates exhibited surface features similar to those found on many other materials, including bulk Mo metal sheet, with surface features 2-5 μm across and height variations of 1-2 μm. Similar properties were seen on GaAs films grown on Mo/alumina composites. The electrical properties of GaAs:Zn p-type material grown on the insulating substrates were also evaluated. This was considered to be of great importance, since the behavior of n-type polycrystalline GaAs was shown to be dominated by grain boundary effects which limited the resistivity of the material to very high values, even at high doping levels. The electrical resistivity of doped p-type polycrystalline GaAs films, determined by van der Pauw measurements, was found to vary with doping in a manner similar to that of Se-doped n-type films; that is, $\rho \propto p^{-3/2}$, where p is the net hole concentration. Resistivities were generally two orders of magnitude greater than that of comparably doped single-crystal material, with the minimum observed resistivity being ~0.07 ohm-cm.

The physical properties of GaAs films grown on Ge layers deposited on all of the candidate insulator materials were also studied. In most cases the presence of the Ge intermediate layer resulted in more planar growth and, in some cases, in larger grain sizes than obtained for GaAs growth directly on the low-cost substrate material. However, Ge nucleation and growth on all of the glasses was found to be at relatively widely separated sites, with the result that incomplete coverage of the substrate

was obtained in most instances. This caused the GaAs overgrowth to be similarly discontinuous.

Also during the third quarter the development of characterization techniques for polycrystalline materials continued with some success. However, the very high resistivity of the polycrystalline GaAs frustrated some of the planned activity, particularly in the area of grain size determination, where suitable Schottky barrier samples for EBIC-mode examination of films on insulators were not achieved. The reference x-ray standard sample for polycrystalline GaAs was prepared and techniques for establishing preferred orientation were specified. Efforts continued on development of rapid and unambiguous methods for determining grain size. Experiments to determine the Aℓ concentrations in GaAℓAs alloys also continued, with a comparison of electron microprobe measurements of composition and x-ray determination of lattice parameters being made in an attempt to establish standards of $\Delta a/a_o$ to be used for composition determination.

The work of this task in the fourth quarter continued in the areas of (1) determination of electrical properties of polycrystalline solar cell structures, (2) determination of grain size, and (3) determination of Aℓ concentration in GaAℓAs films, in addition to routine characterization of electrical and structural properties of various individual films. Carrier concentration profiles were determined in polycrystalline and single-crystal n/n^+ composite GaAs films by C-V analysis using Au Schottky barriers, although some variations in results with the area of the Schottky barrier were observed for the polycrystalline films. It was found that films doped to $\leq 10^{16}$ cm^{-3} and grown on a conducting substrate could be successfully characterized by this technique to depths up to ~ 4 μm. GaAs n/n^+ films on Mo/glass substrates appeared well suited to this type of analysis. Considerable progress was made in the attempts to determine grain size in polycrystalline films by etching and/or EBIC techniques, principally as a result of development of a successful polishing etch for polycrystalline GaAs films.

Details of these investigations follow.

2.3.1 Physical Characteristics of Polycrystalline GaAs Films on Various Substrates

During the course of this program GaAs was deposited by the MO-CVD technique on a wide variety of potentially low-cost substrate materials. Other materials, although not particularly low in cost, were also used in deposition experiments when it was expected that the properties of films grown on them would represent in some way an intermediate between those obtained on single-crystal substrates and those on low-cost substrates. A good example of this is bulk Mo sheet, which was used to test the feasibility of growing GaAs on Mo prior to growth on thin-film Mo/glass composites.

The physical properties of GaAs films were found to be quite similar on a wide variety of substrates. Only in cases where the substrate imposed crystalline growth patterns was there any marked difference. The surface of a typical film grown 5-8 μm thick showed crystalline surface features 2-10 μm in diameter with typical surface height variations of 1-2 μm. The physical characteristics were most often determined in the SEM, although on occasion surface profilometry using a Dektak was also employed.

2.3.1.1 Films on Polycrystalline Substrates

A variety of polycrystalline materials were employed to provide properties intermediate between those of single-crystal material and amorphous substrates. Included were several kinds of polycrystalline aluminas, ranging in grain size from 2 to 1000 μm, and polycrystalline GaAs. In general, GaAs grew epitaxially on the grains of polycrystalline GaAs and to a lesser extent on those of Al_2O_3. The polycrystalline GaAs substrates were used primarily as a means to study the effects of grain boundaries on the electrical behavior of photovoltaic devices; that work will be described in a later section.

Figure 2-6 shows SEM photographs of GaAs films grown on four different polycrystalline alumina substrates: ASM838, ASM805, refired ASM805, and refired Vistal. All of these substrates were found to be stable at growth temperatures up to 840°C, with no reactions occurring in the pre-growth gas stream. The films on ASM838 and ASM805 are seen (Figure 2-6a and b) to be quite similar in appearance. Crystallites 2-5 μm across with 1-2 μm height variations occurred in both films, though there was a tendency for larger grains in the film on ASM838. By contrast, the films grown on the refired substrates (Figures 2-6c and d) had considerably larger grains. For example, the film on refired ASM805 (Figure 2-6c) shows crystallites as large as 30 μm sparsely distributed and embedded in a field of other crystallites smaller than those seen in the film grown on the as-manufactured substrate (Figure 2-6b). The larger crystallites resulted from the epitaxial growth of GaAs on large individual grains in the substrate. This is shown graphically in Figure 2-6d; large grains (1mm) in the substrate served as seeds for epitaxial growth of single-crystal GaAs of comparable size. The majority of the grains in Vistal are larger than some of the epitaxial regions observed in the film, suggesting that some orientations of the Al_2O_3 grains did not promote single-crystal growth.

Thus, the progress from fine- to coarse-grained polycrystalline alumina in these substrates provided a similar progression in crystallite size in the GaAs films. This feature was of interest in determining the effects of grain size on the electrical properties of GaAs polycrystalline films, as discussed in Section 2.3.3

2.3.1.2 Films on Amorphous Substrates

Most of the low-cost substrate materials considered for growth of thin-film GaAs solar cells in this program are amorphous rather than crystalline in their structure. Because of the absence of a regular crystal structure such materials do not typically induce any significant grain sizes or grain orientations in the GaAs films deposited on them. Rather, the film characteristics are determined more by the net effect of various random nucleation, island growth, and island coalescence processes. The substrates selected which fall into this category are glasses, metals (Kovar, molybdenum, tungsten), carbon (graphite), and — to a lesser extent — glass-ceramics, which are partially crystallized glasses.

Because early nucleation behavior is so important to the final film properties on these substrates, studies of transient early-growth phenomena were undertaken. Figure 2-7 shows examples of early island growth of GaAs on two glasses, Mo and a glass-ceramic. Note that except in some areas of the glass-ceramic (Figure 2-7d) the early island growth is quite sparse and random for these substrates, with typical island (and therefore probably also nucleation-site) separation of 1-5 μm. Corning

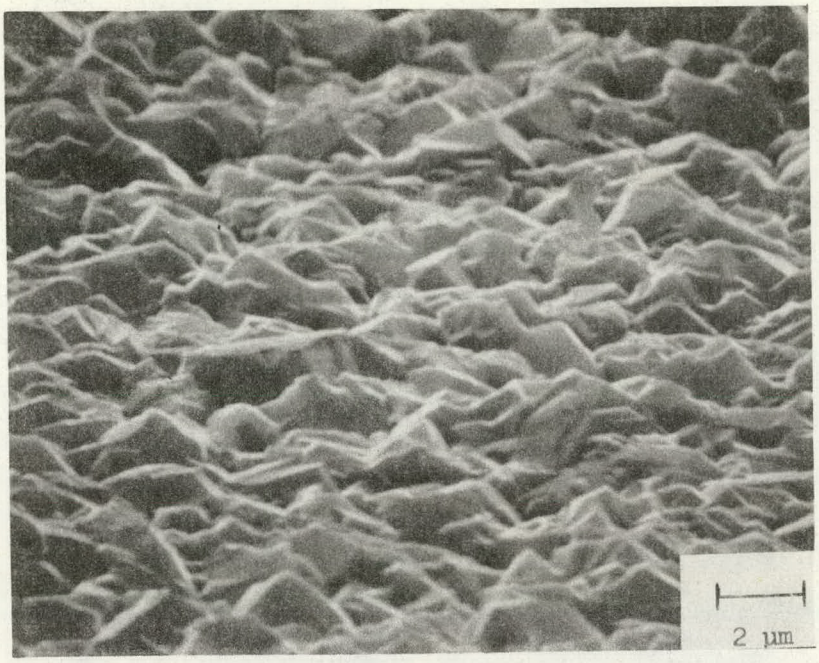

(a)

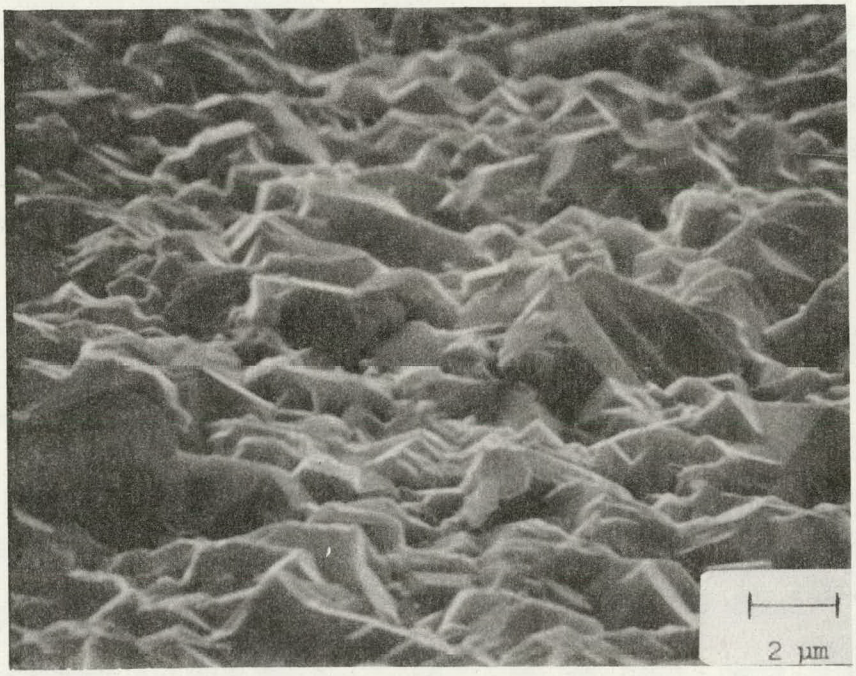

(b)

Figure 2-6. SEM Photographs of GaAs Films Deposited by MO-CVD at 725-735°C on Substrates of (a) ASM805 Alumina; (b) ASM838 Alumina; (c) Refired ASM805 Alumina; (d) Refired Vistal Alumina

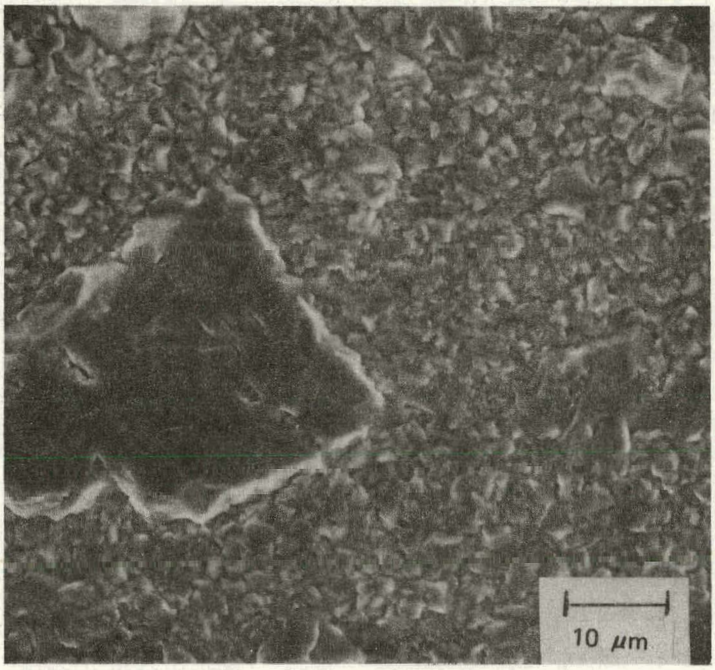

(c)

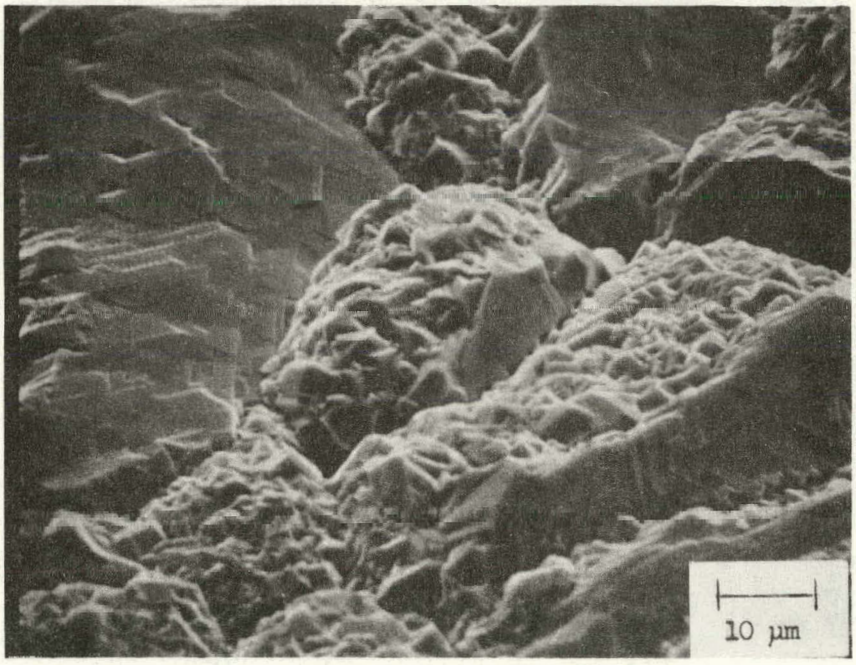

(d)

Figure 2-6. (Continued)

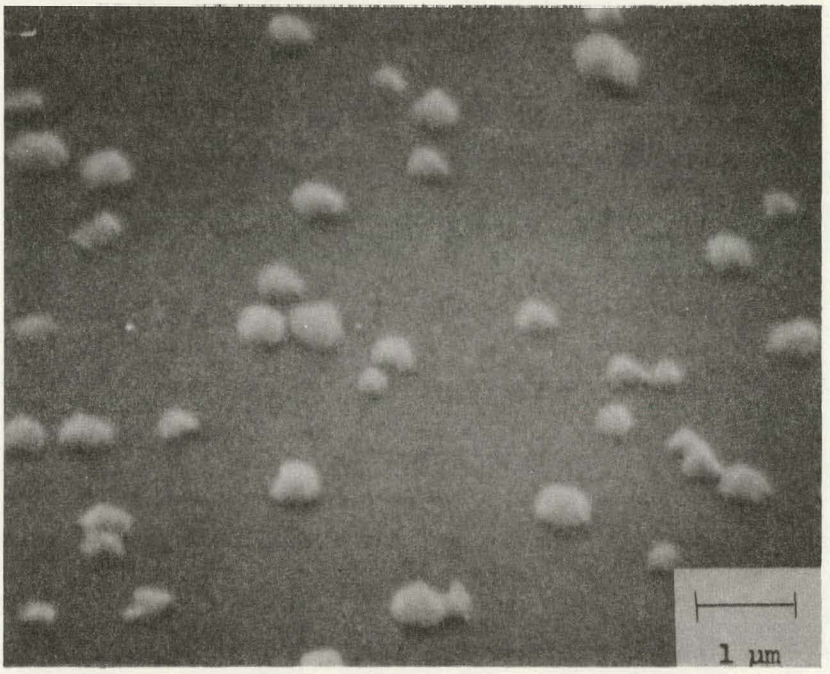

(a)

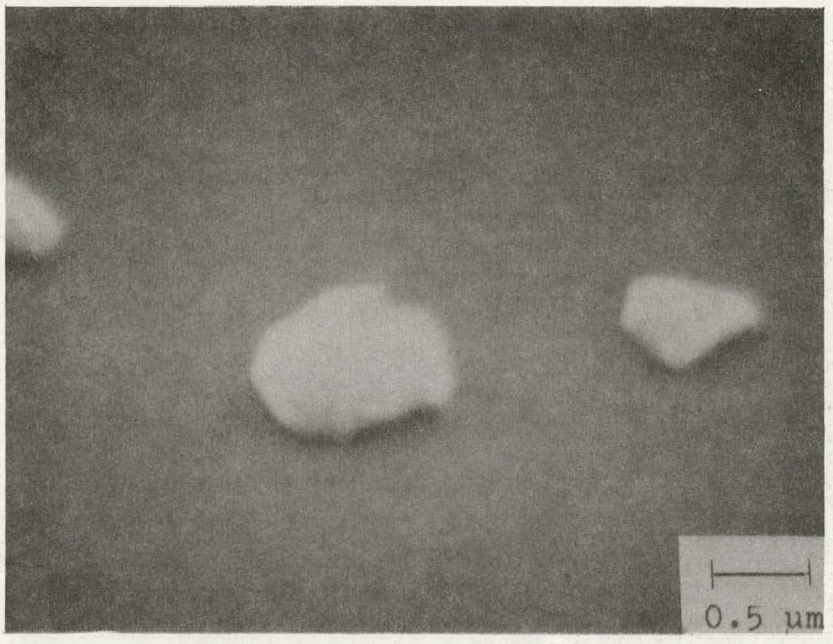

(b)

Figure 2-7. SEM Photographs of Early-stage Growth of Deposits of GaAs on Substrates of (a) Corning Code 0317 Glass, (b) Corning Code 0211 Glass, (c) Mo Sheet, (d) Corning Code 9606 Glass-ceramic

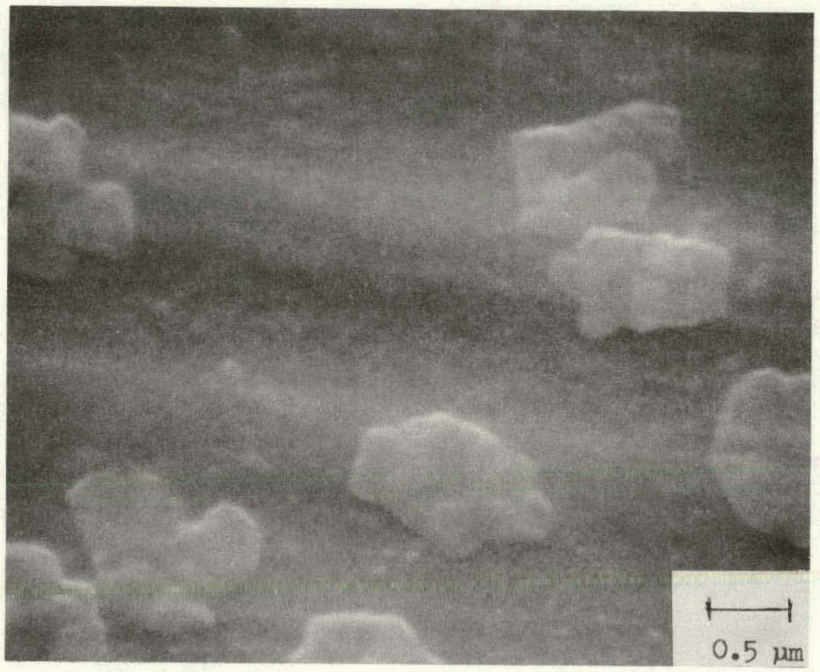

(c)

(d)

Figure 2-7. (Continued)

Code 0211 glass showed a marked tendency to sparse nucleation of GaAs and to incomplete coverage, even for longer growth times. Experiments to induce nucleation by treating the surface were successfully performed with this substrate. Note also that on portions of the Code 9606 glass-ceramic very dense nucleation and island growth occurred. This dense nucleation is reminiscent of that which occurs on single-crystal sapphire substrates and suggests that these regions of the glass-ceramic are recrystallized portions that tend to encourage ordered film growth.

Upon further growth (to 5 μm thickness) these films had the appearance shown in Figure 2-8. The film on 0317 glass is similar to that observed on many amorphous and fine-grained substrates, with 2-5 μm grain size and 1-2 μm surface roughness. For example, the film on Mo shows similar, although somewhat larger, features. The GaAs film on 0211 glass (Figure 2-8b) is incomplete at this growth stage and temperature but shows large (10-20 μm) crystallites. This is believed to be an extension of the sparse initial nucleation and indicates subsequent growth of islands on these same nucleation sites. The film grown on 9606 glass-ceramic (Figure 2-8d) shows similar features to the glasses but with the occurrence of large crystallites. These, too, are the product of the early dense island growth on recrystallized parts of the glass-ceramic.

Films grown on tungsten, carbon (graphite), and Rodar* substrates are shown in Figure 2-9. The average crystallite size was found to be ~2μm for films on tungsten, 2-5μm for films on carbon (graphite), and 5-10μm for films on Rodar. The polycrystalline films readily peeled away from the tungsten substrates. The films on the alloy (Rodar) substrates showed prominent evidence of a second Ni-rich phase, seen as the lacy structure in Figure 2-9c. This rendered this material (and similar Fe-Ni-Co alloys) useless as a growth substrate for GaAs.

2.3.1.3 Films on Composite Substrates

A few composite substrates were chosen for experimental evaluation because they either provided a conducting back plane or potentially might induce larger grain growth in the GaAs. For example, a composite consisting of a Mo film on glass could provide a conducting, low-cost substrate for solar cell fabrication. Similarly, composites consisting of Ge films on glasses or glass-ceramics not only could provide a conducting substrate but also could result in some enlargement of the grain size of GaAs films grown subsequently on the Ge.

During the course of the program summarized in this report the Mo/glass composite substrate yielded the most reproducible and uniform GaAs films. In addition, the Mo/GaAs interface was found to be ohmic and to have relatively low resistance when the GaAs film was doped to $\sim 10^{18}$ cm^{-3}. Both of these characteristics are important for large-area solar cells.

By contrast, Ge deposits on a variety of materials were not as reproducible or conducive to the growth of GaAs of solar cell quality. As will be seen below, it has been difficult to achieve continuous Ge films on many of the glasses, and Ge coatings on Kovar failed to prevent interaction of the Kovar with the GaAs reactants. In

*Rodar is an alloy of Fe, Ni, and Co similar in composition to Kovar.

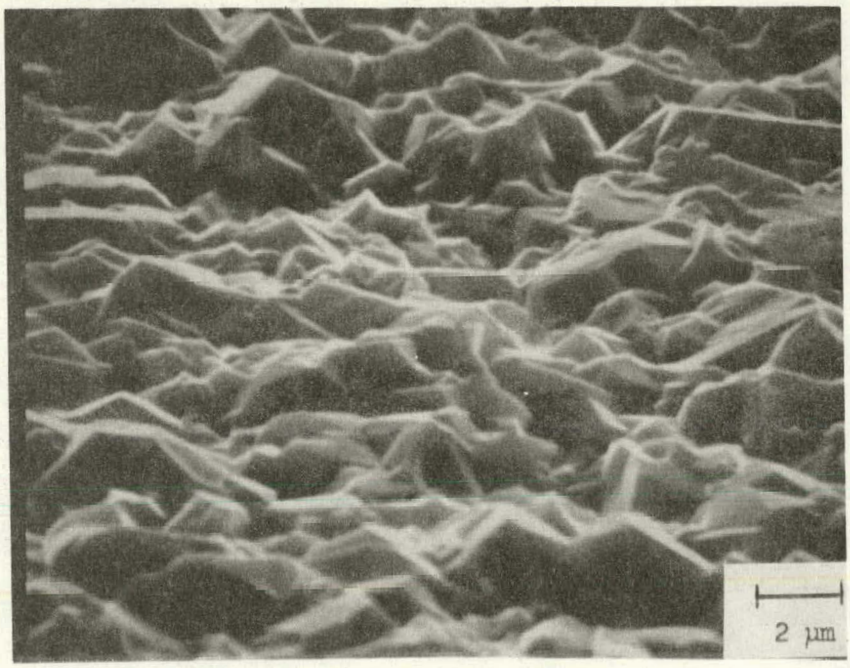

(a)

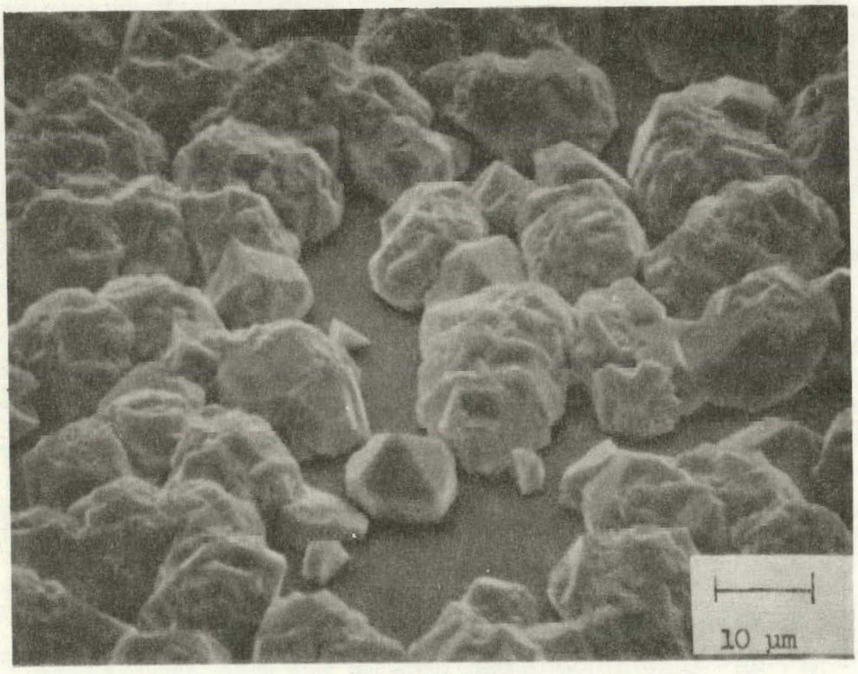

(b)

Figure 2-8. SEM Photographs of MO-CVD GaAs Films Grown on Various Substrate Materials to Nominal 5μm Thickness. (a) Corning Code 0317 Glass, (b) Corning Code 0211 Glass, (c) Mo Sheet, (d) Corning Code 9606 Glass-ceramic

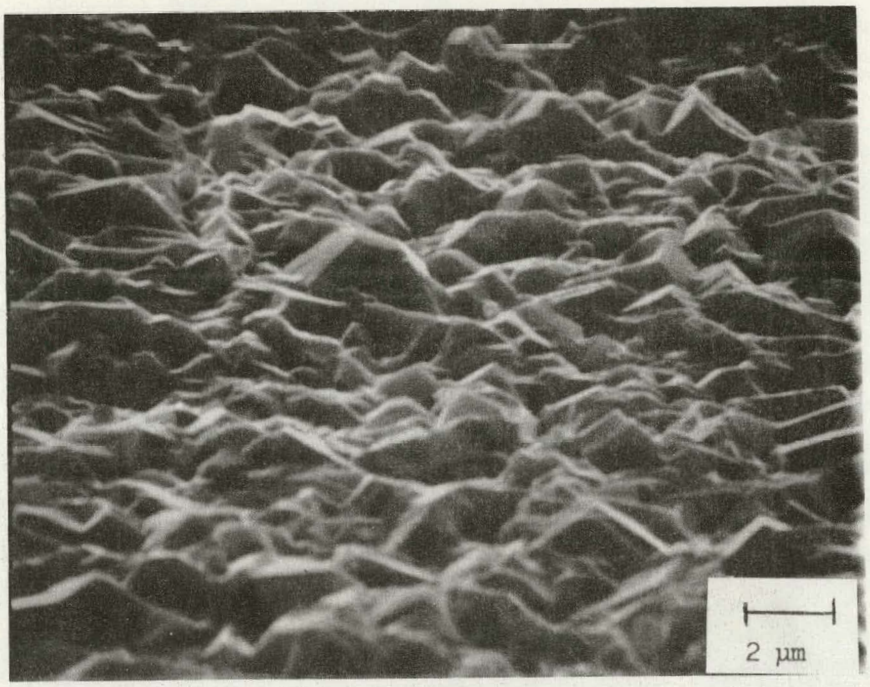

(c)

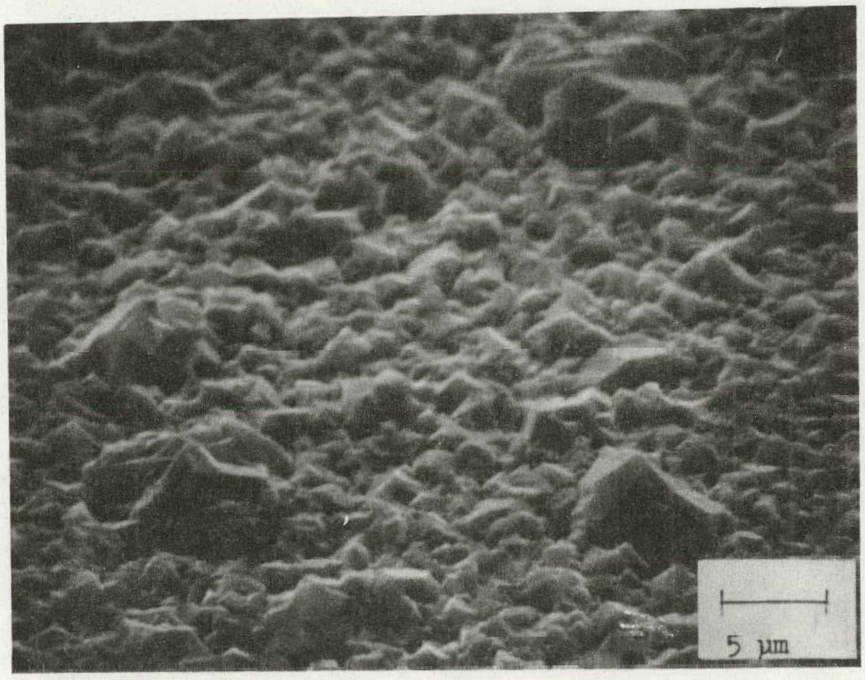

(d)

Figure 2-8. (Continued)

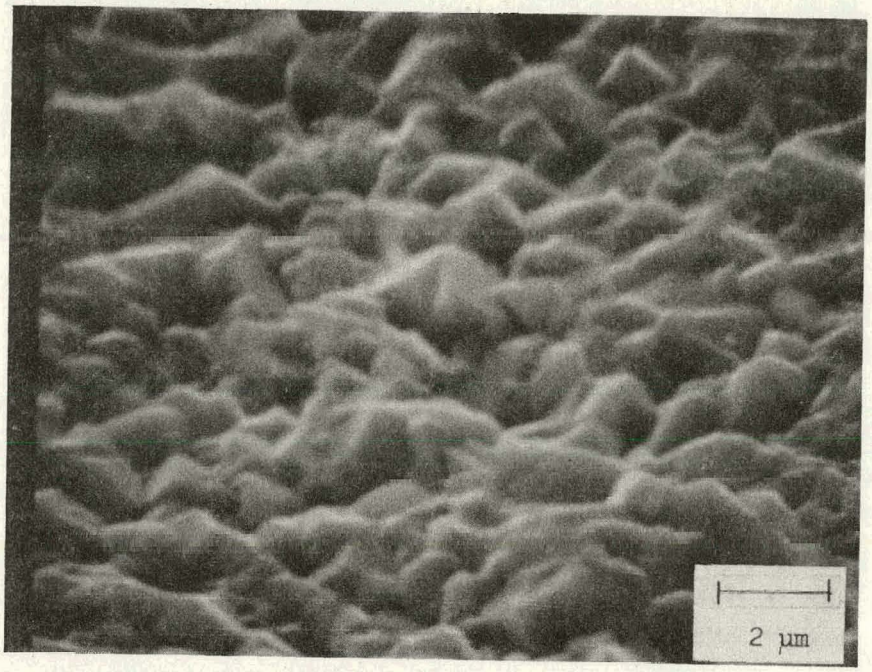

(a)

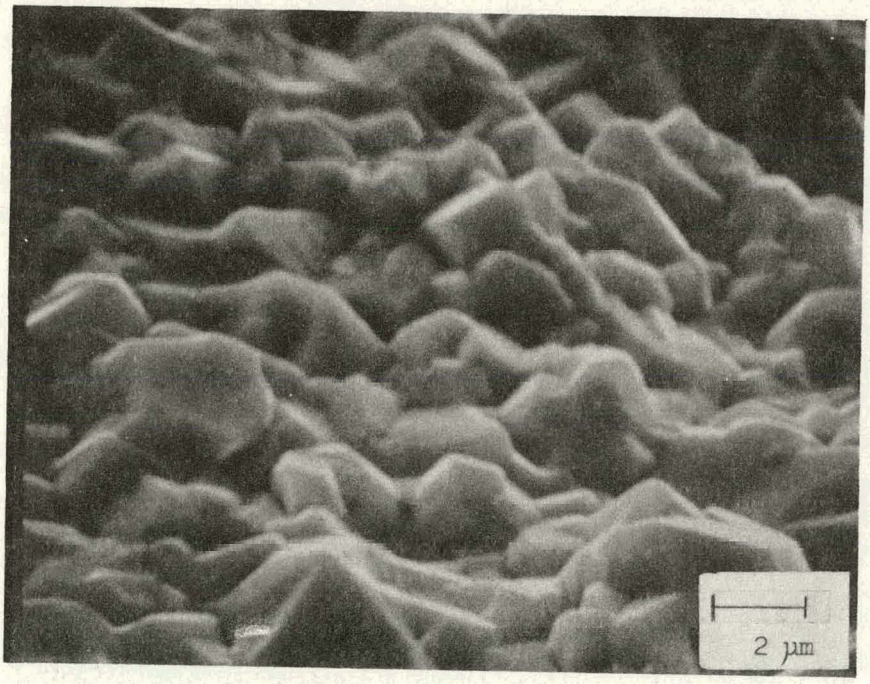

(b)

Figure 2-9. SEM Photographs of Polycrystalline GaAs Films Grown by MO-CVD on (a) Tungsten Sheet, (b) Carbon (Graphite) Wafer, (c) Rodar Plate (see text)

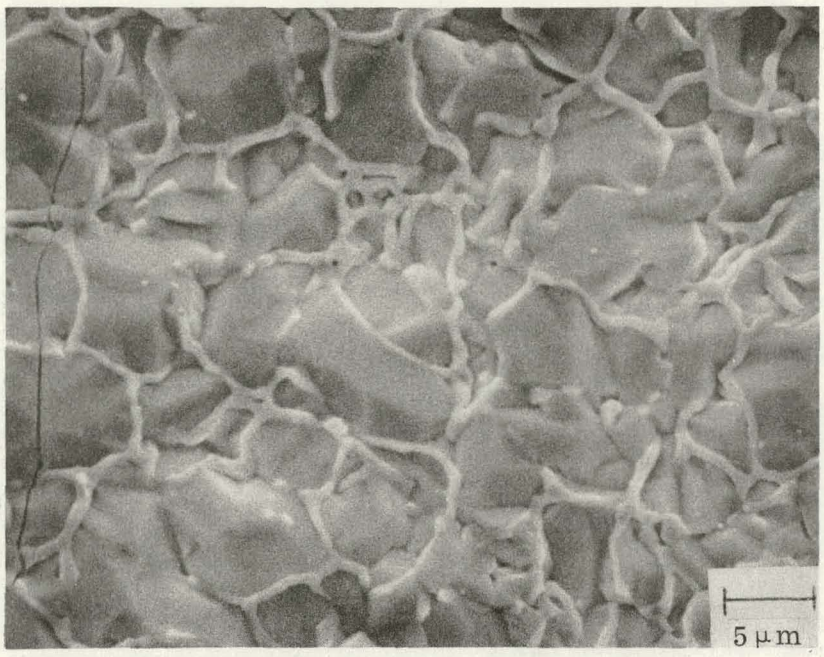

(c)

Figure 2-9. (Continued)

addition, many devices fabricated in GaAs films on composite substrates of Ge on other materials have yielded very poor operating characteristics (see Section 2.4). Some of these problems may be related to the physical characteristics of the GaAs films.

Figure 2-10 illustrates the physical characteristics of GaAs films grown on Mo/glass and Mo/ceramic composite substrates. Note the similarity in the physical properties of the GaAs films in the cases shown; this is to be expected, since the Mo film dominates the characteristics of the growth. In the case of the Mo/ceramic substrate (Figure 2-10d) there are, however, many large crystallites (10-20 μm) which protrude above the film. The origin of these large growths is not known. Figure 2-11 shows the GaAs films on the Mo/glass composite substrates of Figures 2-10a and b viewed in cross-section. It can be seen that in both cases the GaAs film is continuous at the interface, with only a few submicron voids detectable. Films grown on Mo-coated substrates thus are essentially the same in physical appearance as those grown directly on Mo sheet. This uniform fine-grained polycrystalline material has been a useful baseline substrate material for initial solar cell studies.

Ge was deposited by CVD (using GeH_4) on all of the candidate insulator substrates, and GaAs was subsequently deposited on all of the resulting Ge composites. Figure 2-12 shows Ge deposits on three different substrates on the left and the corresponding GaAs deposits on these Ge composites on the right. For composites based on aluminas (Figure 2-12 a and b) the GaAs growth on the Ge resulted in more angular surface features with definite crystalline facets. In fact, compared with

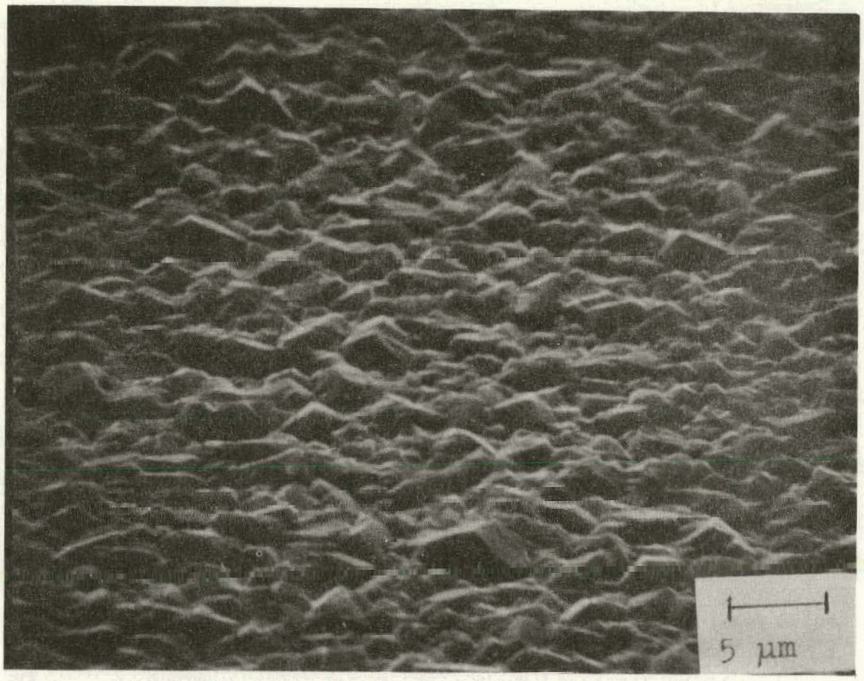

(a)

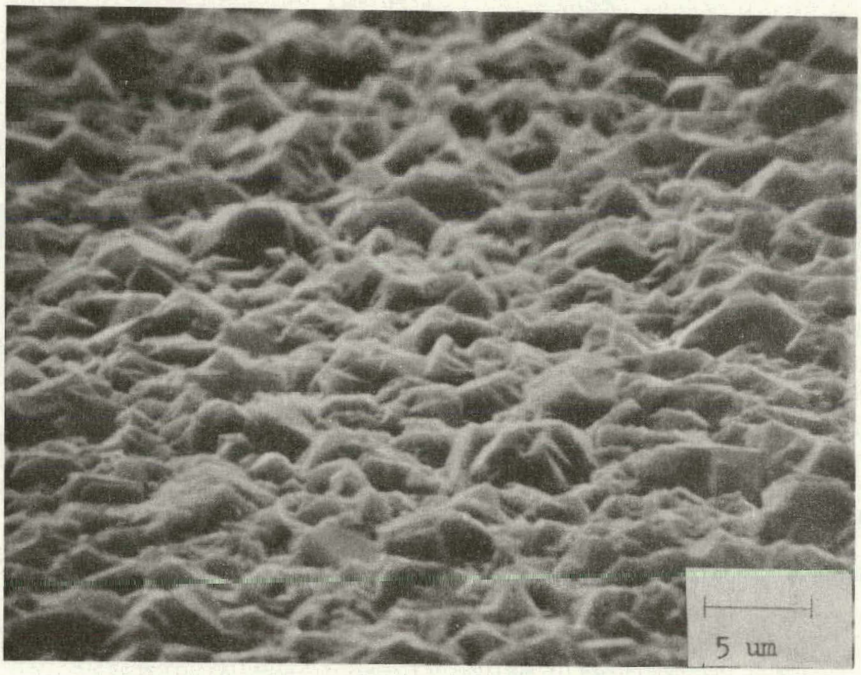

(b)

Figure 2-10. SEM Photographs of MO-CVD GaAs Films Grown on Composite Substrates Involving Mo Films. (a) Mo/Corning Code 0317 Glass, (b) Mo/Corning Code 7059 Glass, (c) Mo/Vistal 5 Refired Alumina (polished), (d) Mo/Vistal Commercial Grade Alumina (polished)

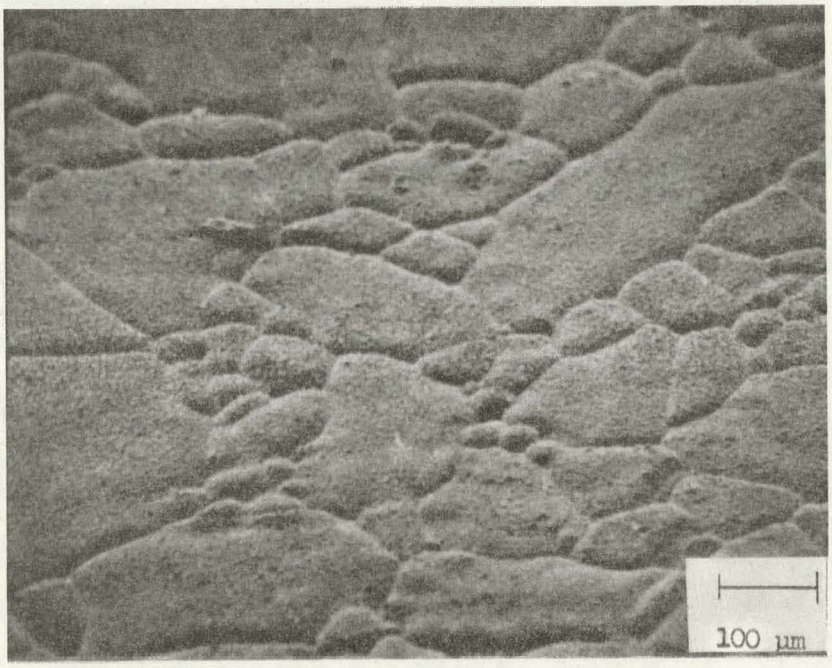

(c)

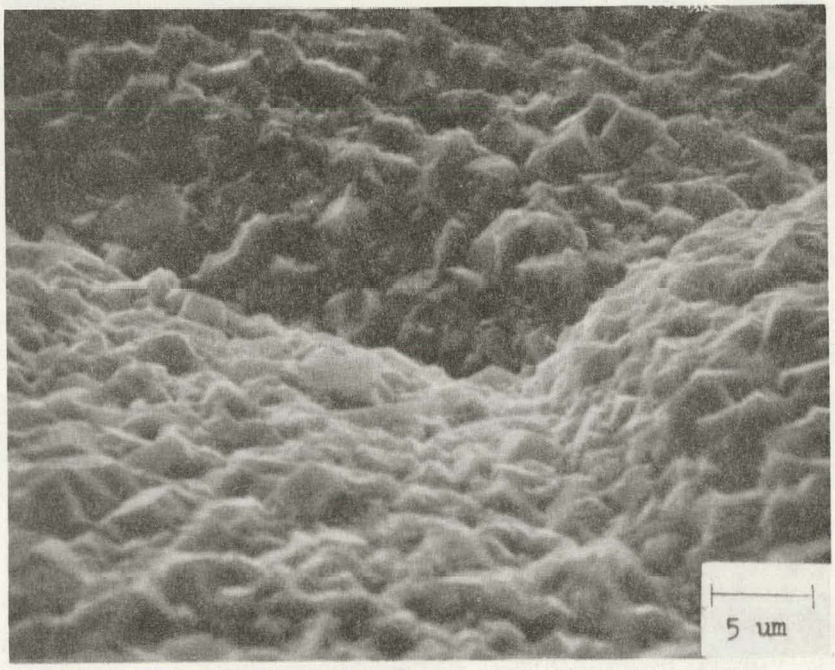

(d)

Figure 2-10. (Continued)

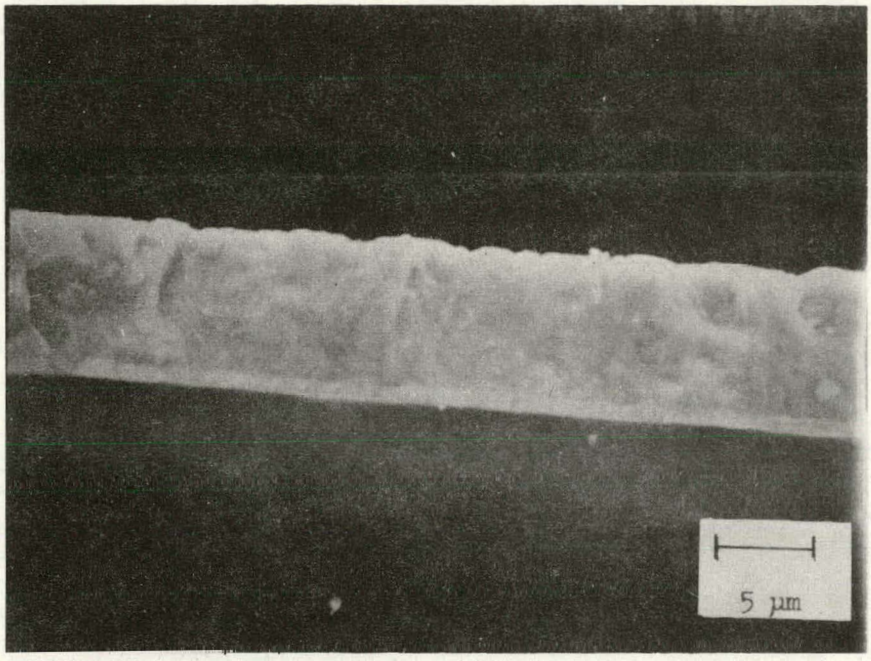

(a)

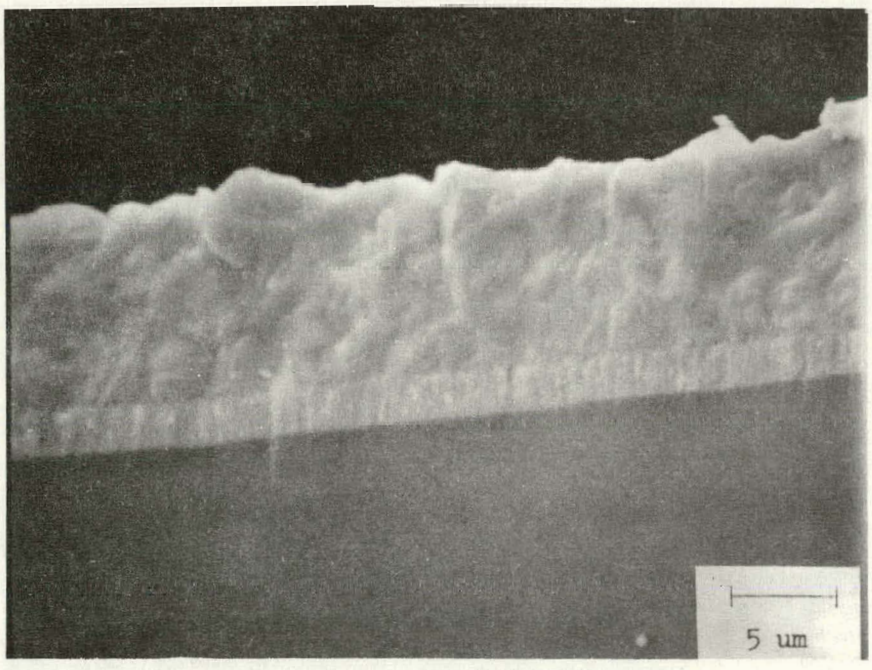

(b)

Figure 2-11. SEM Photographs of GaAs Films Grown on Composite Mo/Glass Substrates, Viewed in Fracture Cross-section. (a) Mo/Corning Code 0317 Glass, (b) Mo/Corning Code 7059 Glass

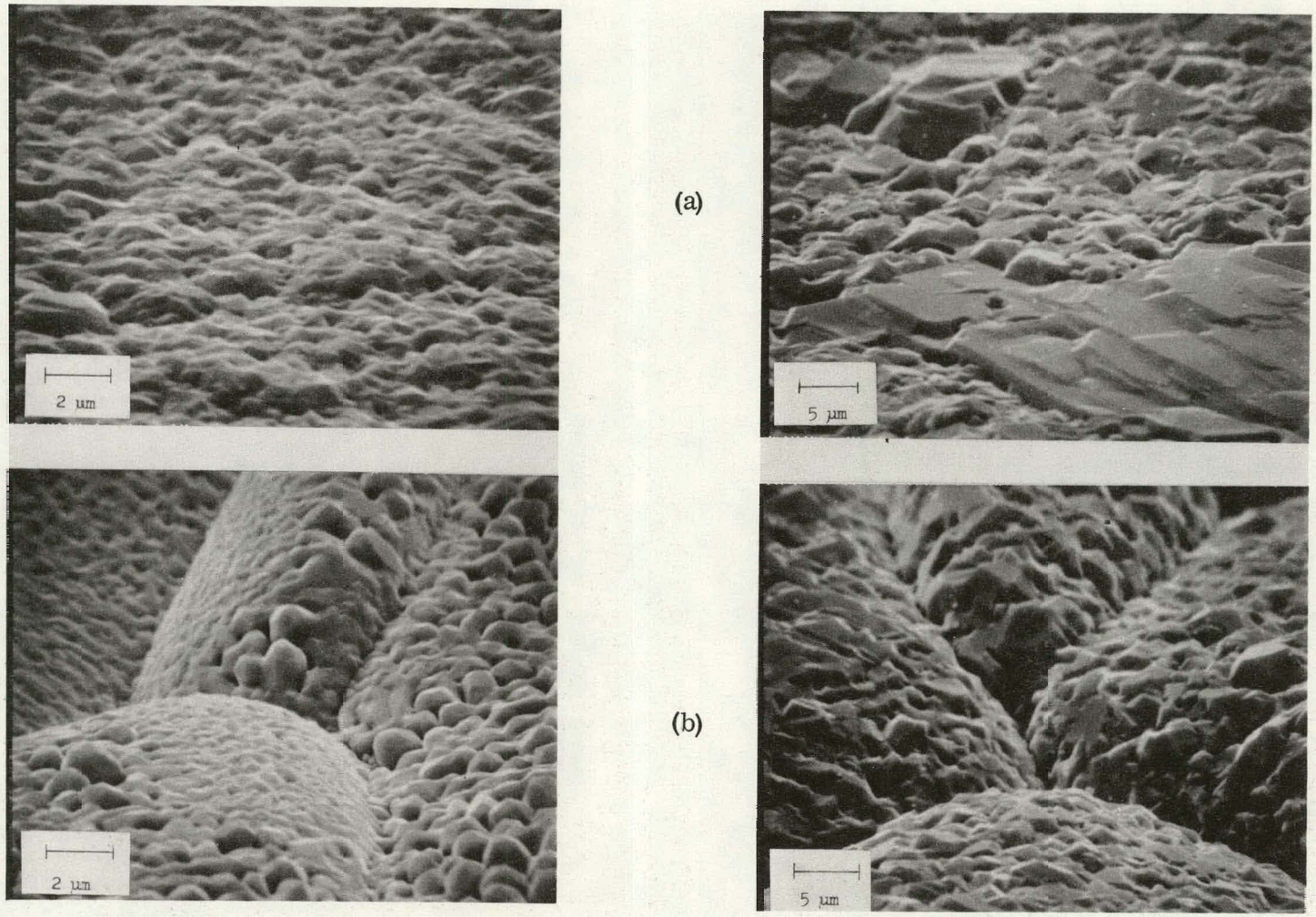

Figure 2-12. SEM Photographs of (left) CVD Ge Deposits on Three Insulating Substrate Materials and (right) MO-CVD GaAs Grown on the Ge Deposits. (a) Refired ASM805 Alumina Substrate, (b) Refired Vistal 5 Alumina Substrate, (c) Corning Code 0317 Glass Substrate

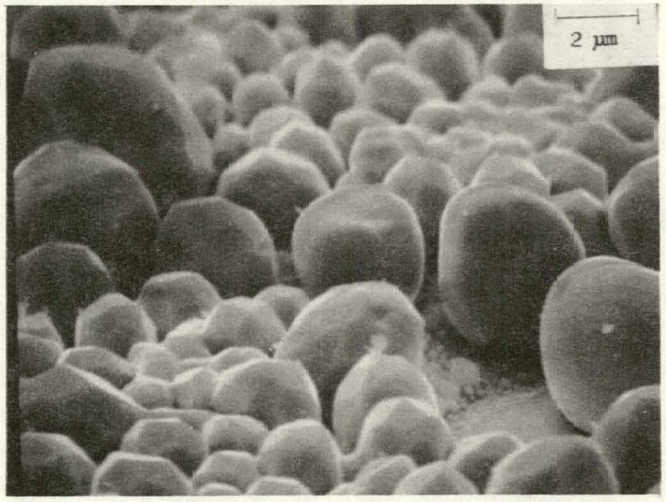

(c)

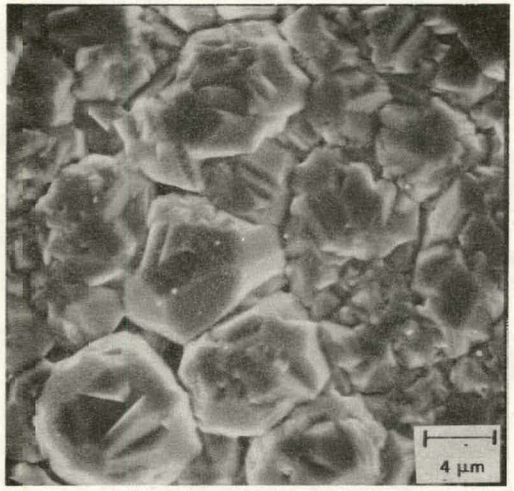

Figure 2-12. (Cont)

growths of GaAs directly on the same ceramics, the growths on Ge appeared to be more preferentially oriented crystallographically, although this was not confirmed by x-ray measurements.

Ge films completely covering the glass substrates, free of voids at the interface, have not yet been achieved. For film growth times that were sufficiently long to produce 2-5 μm films on aluminas the Ge films on glass showed sparsely distributed crystallite growths with $\sim$5 μm separation and 1-5 μm island diameters. These crystallites then served as preferential growth sites for subsequent GaAs growth, as shown in Figure 2-12c (on the right). The GaAs overgrowths were correspondingly discontinuous and displayed rosette structure, obviously the result of growth on the separate Ge crystallites. It is worth noting, however, the uniform size of the rosettes, indicating that a partial-coverage Ge overgrowth may be an excellent nucleating layer. However, as will be discussed further in later sections, an incomplete Ge film on an insulator is not thought to be a practical composite substrate for this program because of the high resistivity of most GaAs polycrystalline films.

These results indicate that if Ge is to be used as a conductive nucleation layer for GaAs then the substrate upon which it is deposited must be conducive to complete coverage by the Ge or the substrate itself must be electrically conductive to overcome the high resistivity of polycrystalline GaAs films. One such substrate is Corning Code 9606 glass-ceramic. Figure 2-13a shows a CVD Ge film on this material, and Figure 2-13b shows the surface of a GaAs film grown on Ge on 9606. Note that although the Ge film incompletely covered the substrate the various regions were interconnected, and the subsequent GaAs film developed to become a complete continuous layer. Figure 2-13c shows a portion of the sample in which the GaAs film was etched off with a 2 percent Br_2-in-methanol etch to reveal the remaining Ge underlayer. The GaAs film (Figure 2-13b) exhibited relatively larger crystallite growth (5 μm) than was found in the Ge layer below it. Attempts to anneal the Ge film near the melting point of Ge yielded GaAs films with somewhat larger apparent grain sizes on occasion, but a systematic study of this effect has not been performed.

In summary, the physical characteristics of GaAs films on a variety of substrates depend strongly on the nature of the substrate. Single-crystal or polycrystalline substrates induce epitaxial GaAs growth on the individual crystallites, with the resulting grain sizes being determined by those of the substrate. Amorphous and non-crystalline substrates induce random nucleation and growth of small crystallites and thus result in a fine-grained (2-5 μm) GaAs film for 5-8μm-thick films. In those cases where the surface of the substrate is not at all conducive to nucleation the result is an incomplete-coverage film. Finally, it appears that nucleating layers of Ge may provide a technique for controlling the geometry of the GaAs deposits on appropriate substrates.

2.3.2 Structural Properties of GaAs Layers on Various Substrates

Several different techniques were used in this program for determining the structural properties of the MO-CVD films. Of particular importance were the crystallographic orientation characteristics and the average grain sizes in the polycrystalline films. Established general procedures exist for determining both properties, but they required adaptation for use on polycrystalline GaAs. For example, an appropriate standard for the x-ray diffraction determination of preferred orientation

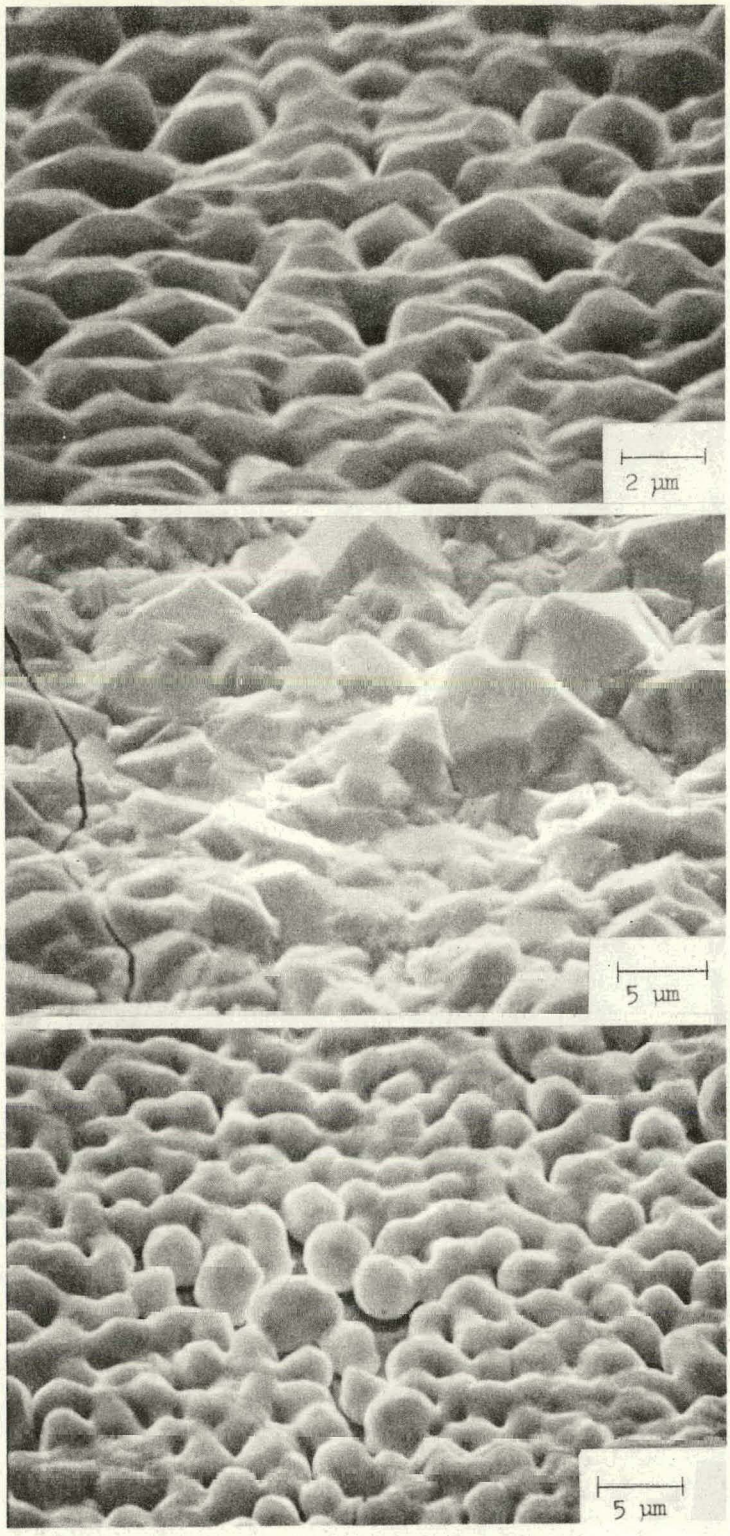

Figure 2-13. SEM Photographs of GaAs and Ge CVD Films on Corning Code 9606 Glass-ceramic Substrate. (a) Ge Film, (b) MO-CVD GaAs Film on Ge Layer, (c) Ge Underlayer after Deposited GaAs Film was Removed with Br_2-Methanol Etch

had to be developed before the results of measurements with this technique could be properly analyzed. These procedures and the results of their application are discussed below.

2.3.2.1 Crystallographic Orientation of Polycrystalline Films

Measurements of the intensities of x-ray diffraction line peaks for GaAs films grown on a variety of candidate substrate materials under a variety of conditions were performed and compared with the ASTM Standard Card Index intensities for randomly oriented polycrystalline GaAs. However, considerable difficulty was experienced early in these investigations in producing a randomly oriented sample of polycrystalline material that gave results that agreed with the ASTM data.

As a result of these studies it was discovered that work that had been previously reported by investigators at the National Bureau of Standards does not agree with the published ASTM data, but does agree with theoretical calculations of expected intensities for polycrystalline GaAs. It was also found that the polycrystalline GaAs reference standards prepared at Rockwell agree with both the NBS work and the theoretical expectations.

The standard GaAs reference sample that was used in these studies was prepared by grinding single-crystal high-purity GaAs with a mortar and pestle and sieving the resultant powder successively with 20 μm and 5 μm sieves. The powder remaining on the 5 μm sieve was then gently mixed with Krylon which had been sprayed on a glass slide. The resulting slurry was then allowed to dry, and the deposit was then used as a diffractometer specimen.

The relative intensities of the principal low-index x-ray diffraction lines for GaAs were obtained using the diffractometer with a focusing monochromator. After locating the positions of the diffraction peaks and taking into account the background correction a step-scanning method was employed. A Philips Model 3181S Angle Mode Programmer system with teletypewriter output was used to obtain the line profile data.

The procedure used for the analysis was to step-scan in Bragg angle in increments of 0.1 deg (for 2θ) through the peak, counting at each step for a fixed time (10 sec). The data obtained in this manner were simultaneously printed out on the teletypewriter and punched out on paper tape. The programmer then traversed to the next peak, and the complete process was repeated until all the required diffraction line profile data had been obtained. The sample was then rotated about an axis normal to its surface, in 90 deg increments, and the data again obtained.

The line peak intensities and the "integrated" (i.e., summed) intensities under the curves were each corrected for background. The values for a given diffraction line were then averaged, and the results were compared with those listed in the ASTM Card No. 14-450 and the National Bureau of Standards Bulletin No. 25, Section 3. The results of this comparison are shown in Table 2-1.

The peak intensities obtained by this procedure are seen to be in good agreement with experimental values reported by NBS and with calculated theoretical values. The data reported in the ASTM Card Index appear to be in error in the intensity listed for the (220) reflection.

Table 2-1. Comparison of Relative Intensities of X-Ray Diffraction Lines for Polycrystalline GaAs

	MILLER INDICES OF DIFFRACTION LINE				
	(111)	(220)	(311)	(400)	(331)
Rockwell Standard Sample					
Peak	100	74	36	7.4	9.8
Area	100	103	49	12	17
ASTM Card Index	100	35	35	6	8
NBS Data	100	61	29	7	11
Theoretical Intensities	100	70	40	10	15

As a result of this work a good reference standard became available with which to compare experimental samples for determination of preferred orientation and grain size. In addition, the experimental technique for determination of preferred orientation was fully specified.

Most of the GaAs films grown early in the program and a selection of films grown later were subjected to preferred orientation analysis, and a representative sample of these results is shown in Table 2-2. As can be seen, most of the films show a marked tendency to $\{111\}$ preferred orientation, with the films grown on glass showing a greater tendency for random orientation.

2.3.2.2 Grain Size in Polycrystalline Films

For successful operation of a polycrystalline thin-film GaAs photovoltaic device it is considered necessary to have average grain sizes of at least 2-5 μm. This is deduced from the curve shown in Figure 2-14, which is based on calculations of Hovel (Ref 11) for the inherent efficiencies of polycrystalline GaAs solar cells as a function of grain size. Clearly, grains as large as possible are desirable but grains of $\sim 10\,\mu$m are seen to provide near maximum efficiency.

Johnston (Ref 12) found that the grain size in CVD GaAs films grown on graphite varied linearly with film thickness. However, for large-scale utilization of GaAs solar arrays the films must be kept as thin as possible - certainly less than 5 μm thick to minimize the amount of Ga used. Thus, one of the main concerns of this program has been to assess the grain size of GaAs films grown on various substrates and to determine ways of increasing the grain size without utilizing more Ga than is contained in a 5 μm film.

A variety of techniques was considered for the determination of grain size. The most straightforward method is the assignment of grain size by the size of crystalline features on the surface of the film. This is also the most widely used technique, but it is fraught with difficulties. For example, consider in Figure 2-8b the large crystallites on Corning 0211 glass. The tops of these crystallites are quite irregular, and these features would probably be taken as indicative of the grain size if the film completely covered the substrate. On the other hand, techniques which work well for either large-size (20 - 100 μm) grains or small-size ($\sim 0.1\,\mu$m) grains do not work well in the 1 - 10 μm regime. For example, x-ray line broadening is an excellent technique for determining very fine grain sizes ($\leq 0.1\,\mu$m) but is ineffective in the range of interest here.

Table 2-2. X-ray Diffraction Line Intensities (Peak Heights) for Polycrystalline GaAs Films Grown by MO-CVD on Various Substrate Materials

SAMPLE DESIGNATION	SUBSTRATE MATERIAL	DEPOSITION TEMP (°C)	RELATIVE INTENSITIES* (111)	(220)	(311)	(400)	(331)
ASTM GaAs Standard	–	–	100	74	36	7.4	9.8
EA60727D1	Rodar**	610	100	11	6.9	1.1	2.7
EA60727D2	Kovar	610	100	11	6.5	1.1	2.8
EA60728A1	Rodar**	615	100	14	6	0.96	2.7
EA60728A2	Kovar	615	100	12	5.4	0.83	2.6
EA60728B1	Rodar**	536	100	44	24	4.2	5.4
EA60728B2	Kovar	536	100	36	17	2.8	3.7
EA60811C1	Mo	653	100	4.9	11	5.3	–
EA60811C2	Mo	653	100	20	19	5.9	–
EA60811B1	Mo	725	100	16	24	8.6	6.1
EA60811B2	Mo	725	100	14	19	6.8	3.8
EA60812A1	Mo	778	100	18	19	6.0	6.2
EA60812A2	Mo	778	100	20	21	6.3	5.8
EA60816A1	Mo	740	100	8.7	18	7.3	43
EA60816B1	Mo	836	100	54	26	0.6	11
EA60813A1	ASM 805†	736	100	19	21	5.6	–
EA60813A2	ASM 838†	736	100	28	24	5.8	–
EA60814A1	ASM 805†	737	100	5	16	6.6	–
EA60814A2	ASM 838†	737	100	17	22	6.2	–
EA60812D1	ASM 805†	729	100	28	17	4	7.6
EA60312D2	ASM 838†	729	100	43	22	4.3	8.0
EA61103A2	Vistal 4††	725	100	13	24	7.4	8.7
EA61103A3	Vistal 4††	725	100	16	16	12	6.0
EA60825B3	Corning 1723 •	706	100	33	35	9.2	–
EA60826A	Corning 0317 •	730	100	53	39	8.6	–
EA60826B	Corning 1723 •	750	100	58	28	5.8	12
EA60826C1	Corning 1723 •	725	100	42	22	5.2	14

* Experimental relative intensities (refer to peak intensities)

** Rodar is an alloy of Fe, Ni, and Co similar in composition to Kovar.

† Polycrystalline alumina.

†† Vistal 4 is Vistal polycrystalline alumina refired four times.

• Glasses.

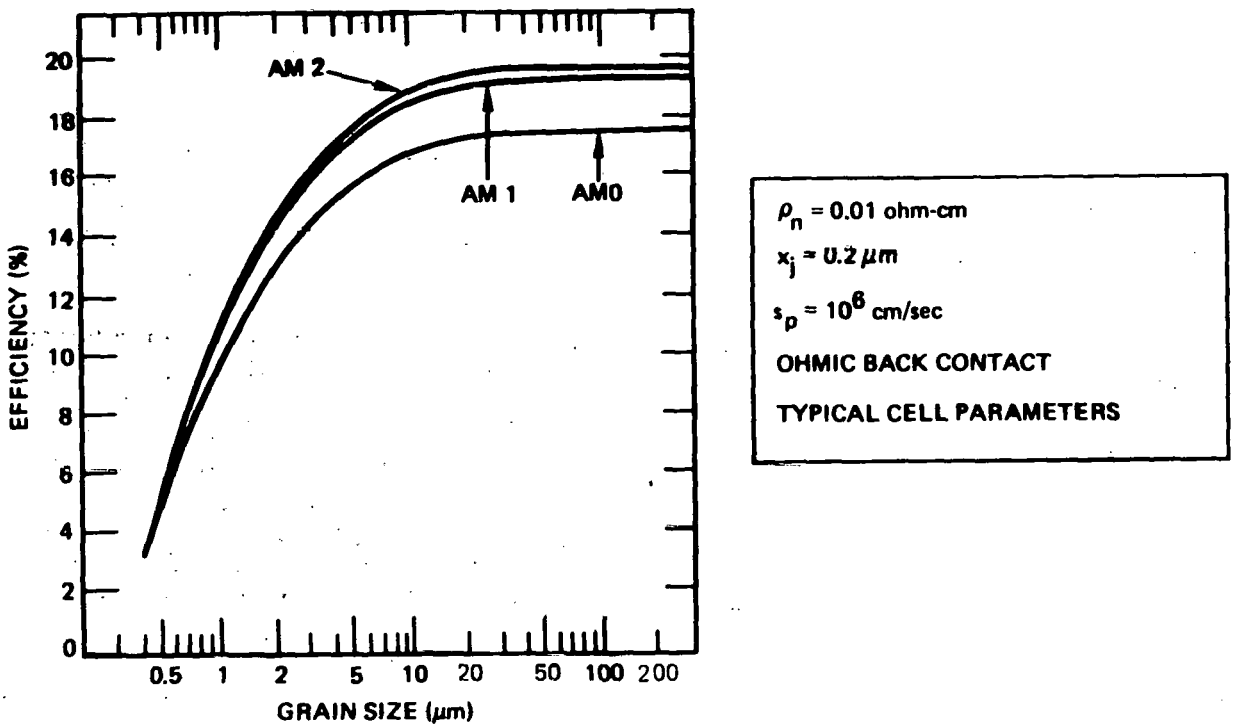

Figure 2-14. Inherent Conversion Efficiencies of Polycrystalline p/n GaAs Solar Cells 1 μm Thick as Function of Grain Size for AM0, AM1, and AM2 Solar Spectra, with Allowance for Lifetimes and Diffusion Lengths Decreasing with Grain Size. (After Hovel, Ref 11.)

So also chemical etching of grain boundaries with preferential defect etches works well for large grains but was ineffective for the films grown in this program. The etches tend to round otherwise sharp geometric features, and grain boundaries thus were etched with groove widths comparable with the grain size. Numerous defect etches were tested on as-grown films, with no satisfactory results.

The techniques which yielded the best, although not completely satisfactory, results involved etching a smoother surface with a dilute defect etch or using electron-beam-induced current (EBIC) measurements on thin Schottky-barrier samples. These techniques were applied as follows.

The as-grown surfaces of polycrystalline GaAs are quite rough. Two procedures were used to smooth the surface. Mechanical polishing of either the top surface or a beveled surface (using a shallow-angle lap) provided a mirrored surface which could be etched with dilute A-B etch to yield apparent crystalline structure in the film. (See Figure 2-15.) It is not clear how much of the linear structure shown in the photographs is the result of etching residual polishing damage. Notice, however, that the size of the etched features (Figure 2-15b) corresponds well with the estimate of grain size based on unpolished surface features (Figure 2-15a).

During the fourth quarter of the program it was discovered that etching polycrystalline GaAs with a Br_2-MeOH solution resulted in considerable smoothing of the surface, presumably because the etch is isotropic and tends to round the edges of

angular features. The polycrustalline GaAs film shown in Figure 2-15 was 10 μm thick as grown; 5 μm of GaAs was removed to produce the surface shown in Figure 2-15b. Note the appreciable smoothing of the surface.

With continued etching angular grain features became visible in some films. Figure 2-16 shows examples for polycrystalline GaAs films grown on Corning Code 7059 and 1723 glasses. The characteristic grain size delineated in both cases again corresponds well to the size of surface features (2-5 μm) found to be typical of these films when examined in the SEM.

EBIC techniques are attractive as a means for determining grain size because they also reveal the effects of grain boundaries on current collection. Grain boundaries should act as planes of high surface recombination velocity and, as such, collect carriers from within a diffusion length of the boundary. Thus, an EBIC image of a structure in which the collecting junction is normal to a grain boundary should show a dark region near any such grain boundaries. In general, it was found not possible to apply the EBIC technique to unprocessed samples, because the surfaces were too rough. The rough protrusions affect the collection of current as effectively as do the grain boundaries, and thus give spurious features to an EBIC image. However, it was found that the polishing etch described above could be applied to provide a much smoother surface for EBIC measurements. After the etching, Au Schottky barriers 50Å thick were deposited on the film surface. The sample was then mounted and bonded with wire bonds.

Figure 2-17 shows SEM photographs of an EBIC sample in the secondary-electron mode and in the EBIC mode. The bonding pad is Au 2000Å thick. Note that the EBIC image is generally more mottled than that of the secondary mode. This mottling is believed to be the result of darker grain boundaries in the image. The general dimensions of this mottled pattern again agree with the typical dimensions of surface features, i.e., 2-5 μm.

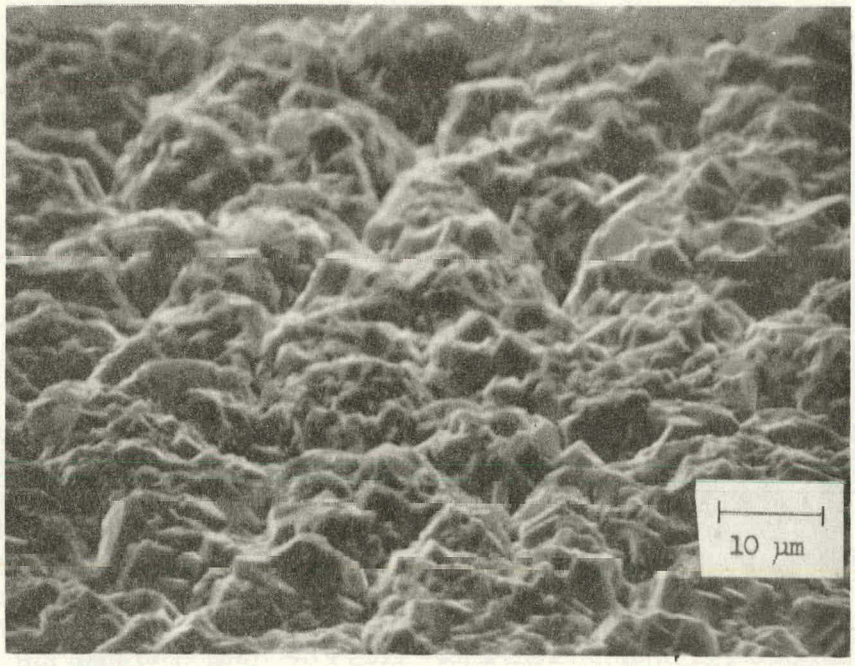

(a)

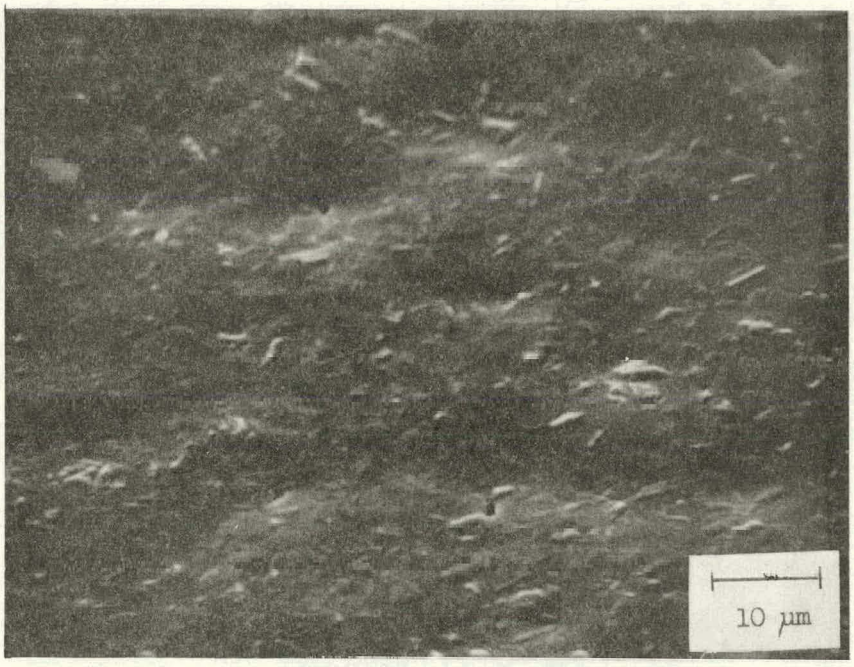

(b)

Figure 2-15. Structure of Polycrystalline GaAs Film Grown by MO-CVD. (a) As-deposited Surface, Showing Crystallographic Surface Features; (b) Surface after Use of Dilute A-B Etch, Delineating Individual Grains and Producing a Relatively Smooth Surface.

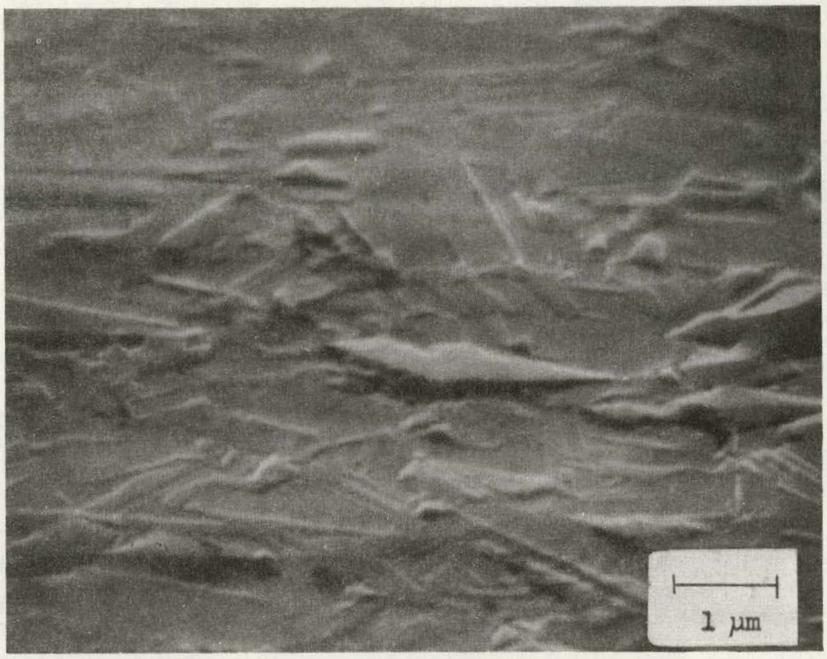

(a)

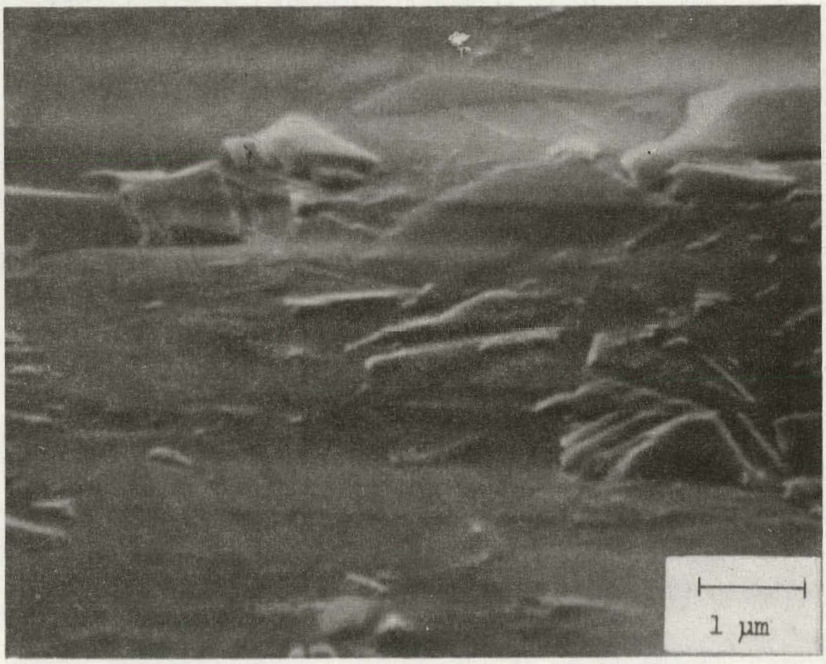

(b)

Figure 2-16. Polycrystalline MO-CVD GaAs Films Grown on Two Corning Glasses, Shown after Films Were Etched to Delineate Individual Grains. (a) Code 1723 Glass Substrate, (b) Code 7059 Glass Substrate.

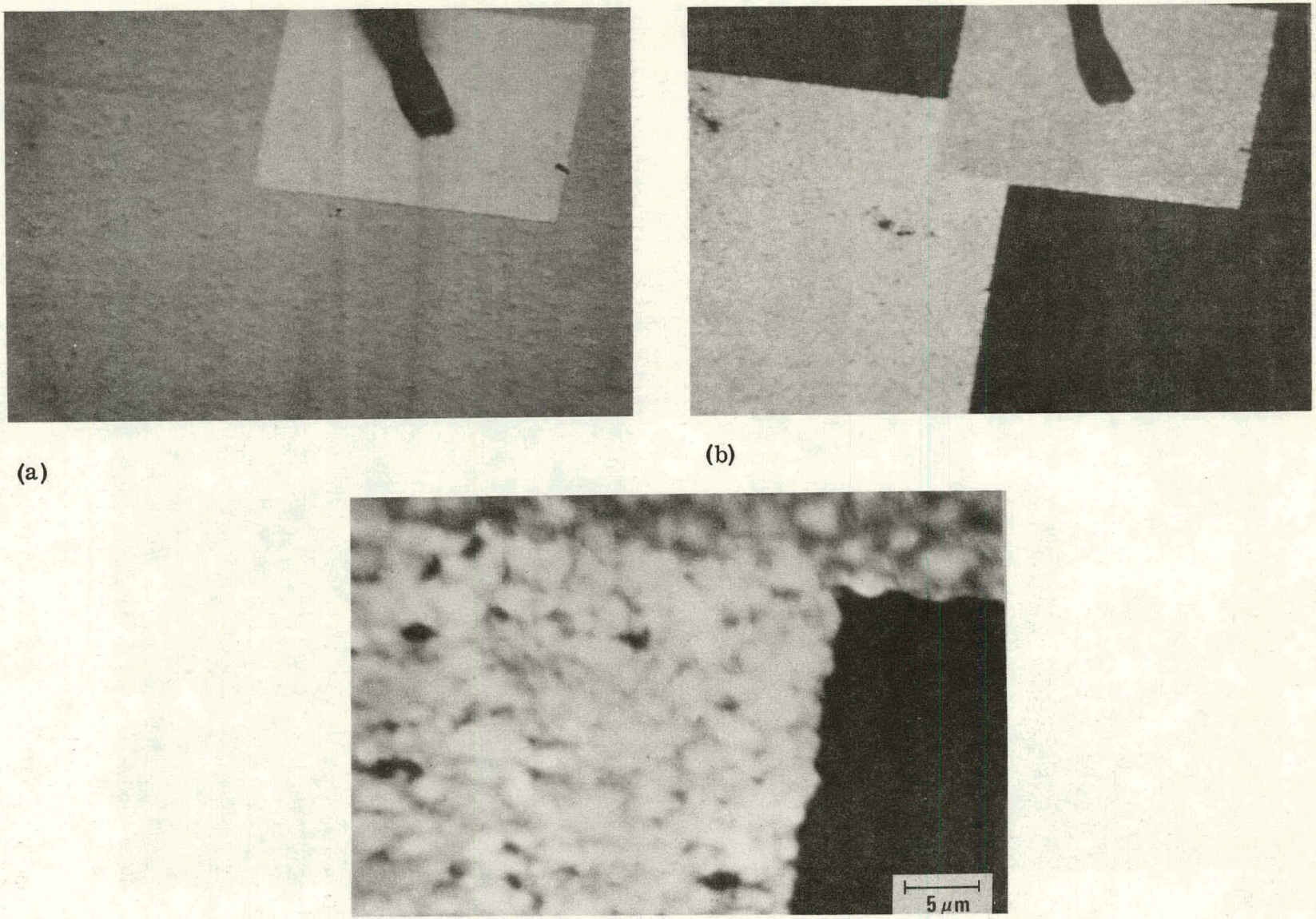

Figure 2-17. SEM Photographs of Polycrystalline GaAs Film Sample Prepared for EBIC-mode Examination by Etch-polishing and Application of 50Å Au Schottky Barriers. (a) Secondary-electron Mode, Showing Au Bonding Pad; (b) EBIC Mode, Showing Au Schottky Barrier (lower left) and Bonding Pad; (c) EBIC Mode, High Magnification, Showing Mottled Pattern in Schottky-barrier Region Associated with Individual Grains

The EBIC technique is very powerful and will be emphasized in the follow-on program to study grain boundaries and their effects on the photovoltaic properties of GaAs polycrystalline film cells.

2.3.3 Electrical Properties of Polycrystalline GaAs Films on Various Substrates

The electrical properties of polycrystalline GaAs is an area of research in which very little work has been reported, and yet it is one of crucial importance to solar cell performance. For example, consider a p-n junction structure (Figure 2-18a) with a top layer 1 μm thick – a reasonable thickness for a GaAs solar cell. For a contact geometry as shown in Figure 2-18b the resistance contributed to the device by each region of the top layer contacted by a finger (that is, the region within the dashed outline in Figure 2-18b) is given by

$$R = \frac{\mathscr{R}s}{8h} \quad .$$

As a result, for material with a sheet resistance $\mathscr{R}$ of 10^6 ohms/square 36 percent of the top surface would have to be covered with contact to achieve 10 ohms series resistance – an unacceptably large coverage factor. For a sheet resistance of 10^4 ohms/square the coverage would be an acceptable 5 percent to achieve 10 ohms resistance.

The relationship between top-layer resistivity and the required contact area coverage is shown in Figure 2-19 for various values of device series resistance, for a film 1 μm thick with contact line width of 50 μm. The specific contact resistance is assumed to be negligible. To achieve a device with resistance of 1 ohm due to the top layer and still limit contact coverage to less than 10 percent the resistivity of the top layer material (1 μm thick) must be less than 0.3 ohm-cm, and for 10 ohms resistance it must be less than 3 ohm-cm.

The electrical properties of single-crystal and polycrystalline GaAs were measured by means of the Hall effect, using the van der Pauw technique, and by C-V analysis of Schottky barriers deposited on the films. Typically a sample was prepared for Hall measurements by alloying In dots (Ref 13) into the surface and measuring the parameters in the usual way. Capacitance behavior of Schottky barriers was measured either by the use of a capacitance bridge to measure C vs V and analyzing the results on a computer or by using a Miller Feedback Profiler to plot n vs x directly.

Undoped films grown early in the program on insulating substrates showed exeeedingly high resistivities (~10^6 ohm-cm). These results prompted a thorough study of resistivity vs doping level for both n- and p-type crystals of GaAs. A variety of substrates were used in this study, including large-grained Vistal alumina to promote large-grained GaAs growth and amorphous substrates such as glasses. In this way a variation in film grain size could be effected and the effect of grain size on resistivity determined. Each of the deposition runs included a single-crystal sapphire substrate to act as a control and to permit determination of the carrier concentration.

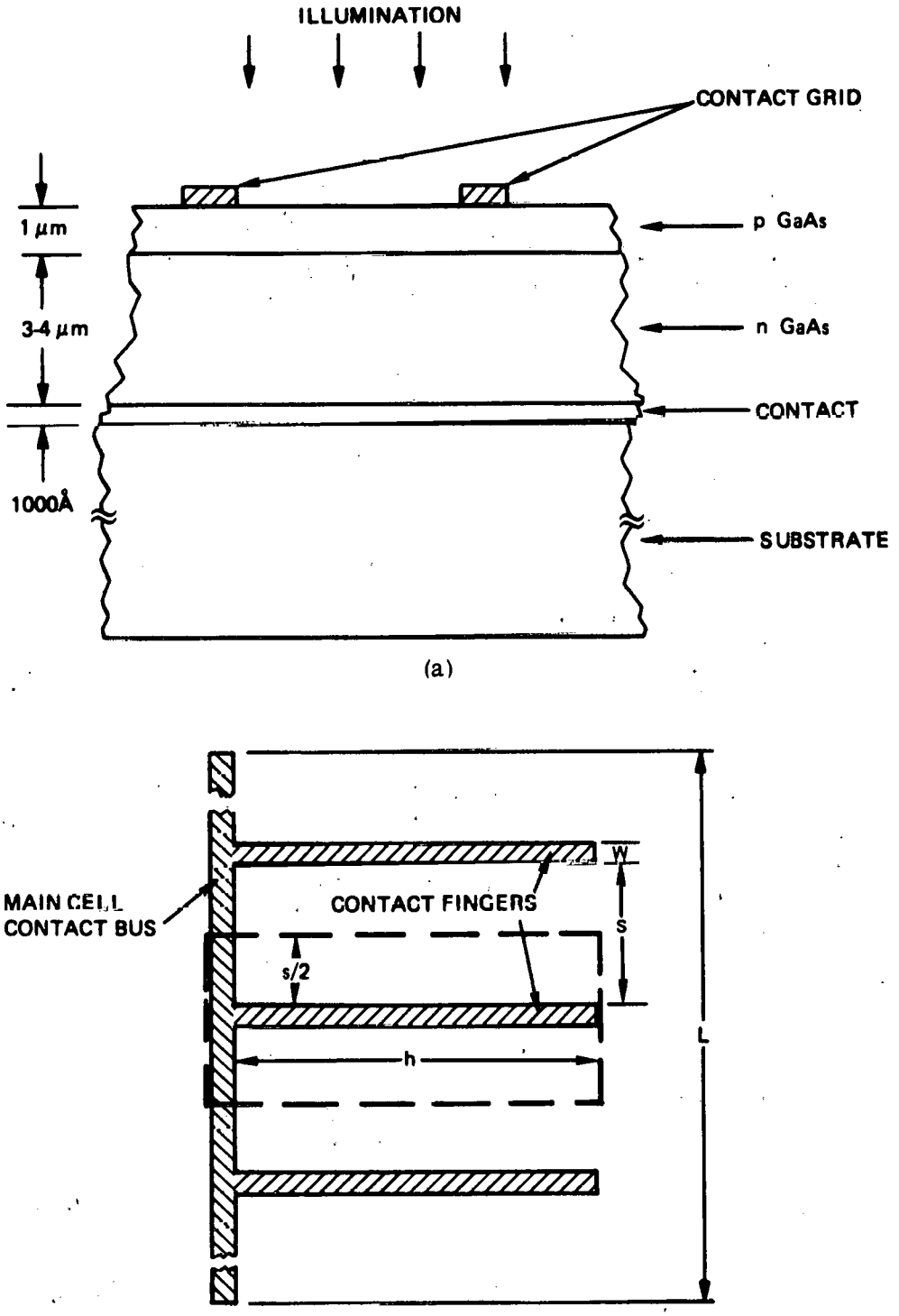

Figure 2-18. Typical (a) Layer Structure and (b) Contact Configuration for GaAs Solar Cell.

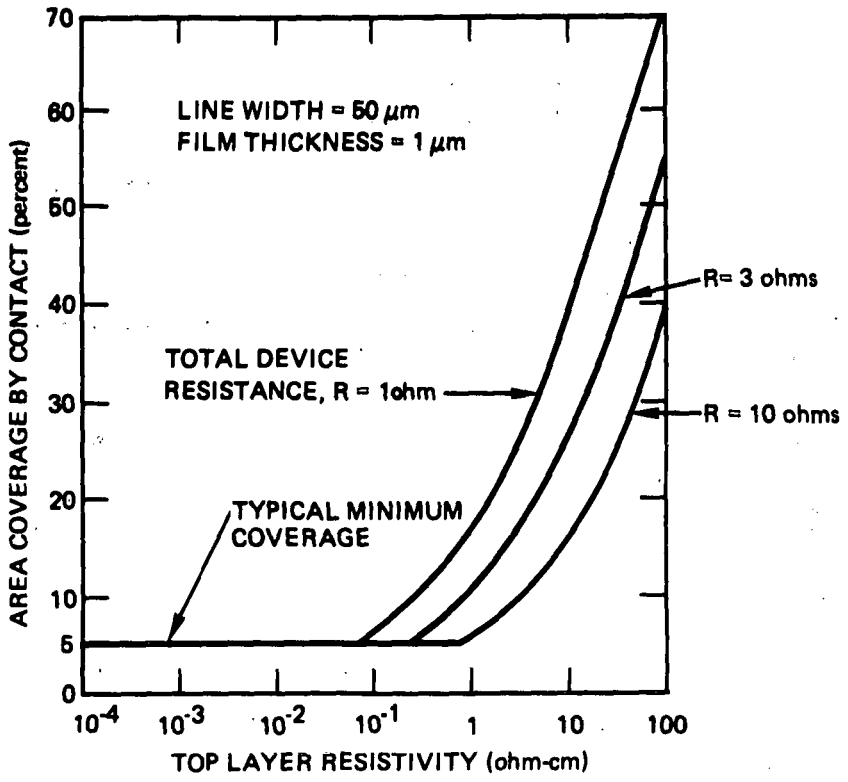

Figure 2-19. Calculated Relationship between Resistivity of Top Layer in Cell Structure and Required Contact Area Coverage, for Various Values of Device Series Resistance.

In all samples of polycrystalline GaAs except the most highly doped p-type layers no measurable Hall effect could be detected with the apparatus in use at the time. Figures 2-20 and 2-21 show the measured resistivity of polycrystalline GaAs p- and n-type material, respectively, versus the carrier concentration measured in the epitaxial film on sapphire. In cases where the carrier concentration of the polycrystalline film itself could be measured this was used as the abscissa; in none of those cases was there a large discrepancy in carrier concentration between the measured value in the polycrystalline film and that in the epitaxial layer.

There are several observations to be made about the data shown in these two graphs:

1. The resistivities of the polycrystalline films are 1-2 orders of magnitude greater than those of equivalently doped single-crystal films.

2. The resistivities of n- and p-type material are roughly equal at the same doping level.

3. Material with larger grain size generally has lower resistivity than that of fine-grained material.

4. The resistivity of p-type material varies as $(1/p)^{1.5}$.

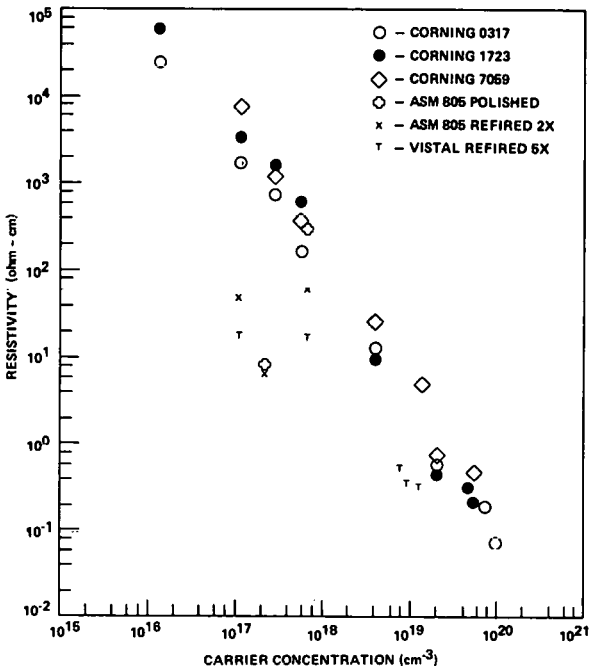

Figure 2-20. Resistivity of Polycrystalline p-type GaAs on Variety of Substrates as Function of Measured or Inferred Carrier Concentration (measured on films grown on companion single-crystal sapphire substrates).

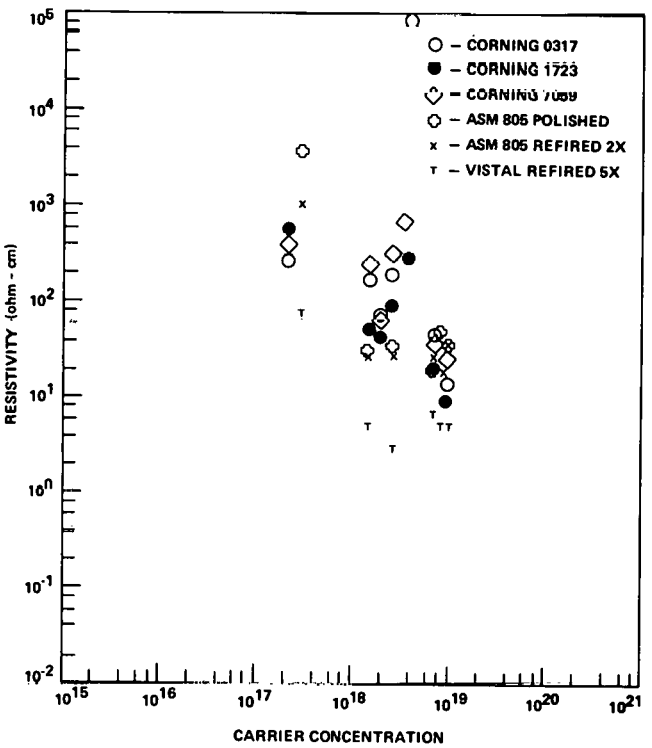

Figure 2-21. Resistivity of Polycrystalline n-type GaAs on Variety of Substrates as Function of Carrier Concentration Measured on Companion Single- crystal Sapphire Substrates.

Based on these observations the following conclusions were reached. First, it is clear that grain boundaries dominate the electrical properties of polycrystalline GaAs films at all doping levels. This contrasts with the behavior of polycrystalline Si (Ref 14), in which the resistivity drops several orders of magnitude above a critical doping level and approaches the resistivity of single-crystal material at high doping. Second, intragrain mobilities appear to play little role in determining the resistivity (cf the equivalent resistivities of n- and p-type materials). Measured mobilities for p-type material with hole concentrations greater than 10^{19} cm^{-3} are on the order of 0.1 to 1 $cm^2/V\text{-sec}$.

The third conclusion is that n-type material is too resistive to be used as a top layer in a p-n junction solar cell structure because the lowest resistivity that was achieved was the order of 2 ohm-cm at $6 \times 10^{18} cm^{-3}$. Single-crystal n-type material of this doping concentration has exceedingly small diffusion lengths. As a result, layers thinner than $1\mu m$ would have to be used to achieve reasonable collection efficiency in a cell, causing the sheet resistance to be too high to be practical unless a transparent contact could be developed for application to the top layer.

The major question as to the validity of the data shown in Figures 2-20 and 21 relates to the use of the carrier concentrations of single-crystal films as representative of those in simultaneously grown polycrystalline material. The only check of this point was in the high doping region for the p-type material, where the carrier concentration could be measured in the polycrystalline material as well as in the epitaxial material. Here good agreement was attained between the resistivities of the polycrystalline and the single-crystal films. In an attempt to resolve this question, capacitance-voltage characteristics of some polycrystalline films were measured. Again, however, only a limited range of doping could be explored because the background doping was the order of 10^{15} cm^{-3} and the maximum doping level for fabrication of low-leakage Schottky barriers is $\sim 5 \times 10^{16}$ cm^{-3}. In addition, the material must be deposited on a conducting substrate to obtain meaningful measurements, as discussed below.

The capacitance bridge used in C-V analysis measures an effective parallel combination of a capacitance and resistance, such as is shown in Figure 2-22a. The equivalent circuit of the actual sample is shown in Figure 2-22b, where C_o is the actual Schottky barrier capacitance, $1/R_o$ the conductance, and R_s the series resistance. The measured capacitance C_p is related to the actual capacitance by

$$C_p = C_o \frac{1}{\left(1 + \frac{R_s}{R_o}\right)^2 + \omega^2 C_o^2 R_s^2} .$$

For $\omega = 2\pi \times 10^6$ sec^{-1}, $C_o \approx 100$ pf, and $R_s \approx 10^4$ ohms, it follows that $C_p \approx 0.01\ C_o$. Thus, the doping level would be interpreted as being much lower than the actual doping level under these conditions.

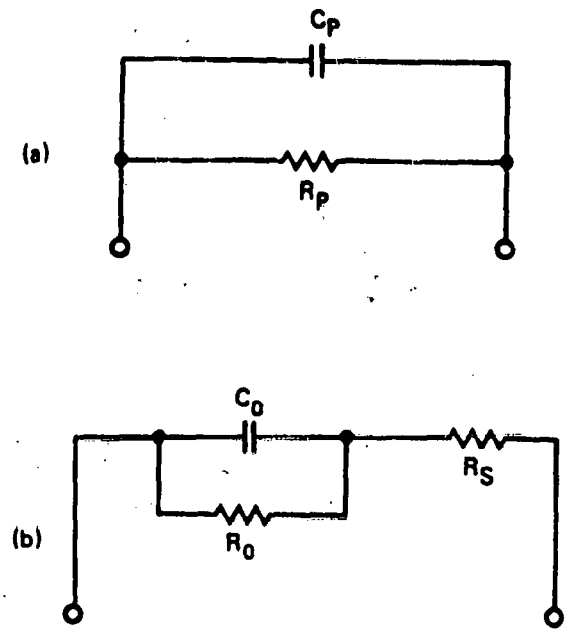

Figure 2-22. Equivalent Circuit of Sample in C-V Bridge Measurement of Carrier Concentration Using Schottky Barrier Method. (a) Effective Circuit Seen by Bridge, (b) Actual Equivalent Circuit of Sample.

In fact, when samples grown on insulators were measured by C-V analysis the deduced carrier concentration was typically two orders of magnitude lower than expected. However, good correlation was observed between C-V measurements on polycrystalline films grown on conducting substrates and van der Pauw measurements on films grown on single-crystal sapphire in the same way. This gave added credibility to the use of films on sapphire monitors to obtain a measure of carrier concentrations in polycrystalline films.

Figure 2-23 shows a carrier concentration profile of a GaAs n/n^+ sample grown on a Mo/glass composite substrate, as obtained with the Miller Feedback Profiler. The films were grown by doping the initial portions of the film to 2-4 x 10^{18} cm^{-3} with Se and shutting off the H_2Se flow while growth continued for approximately 2 m more. The profile shows a 2 μm n layer doped to approximately 10^{15} cm^{-3} followed by a gradually increasing doping level which exceeds 10^{17} cm^{-3} on this plot.

The results indicate that both Hall and C-V measurements are useful but limited in their range of applicability for polycrystalline GaAs. More sensitive Hall-effect measurements must be achieved to allow measurement of all the appropriate properties of the polycrystalline GaAs.

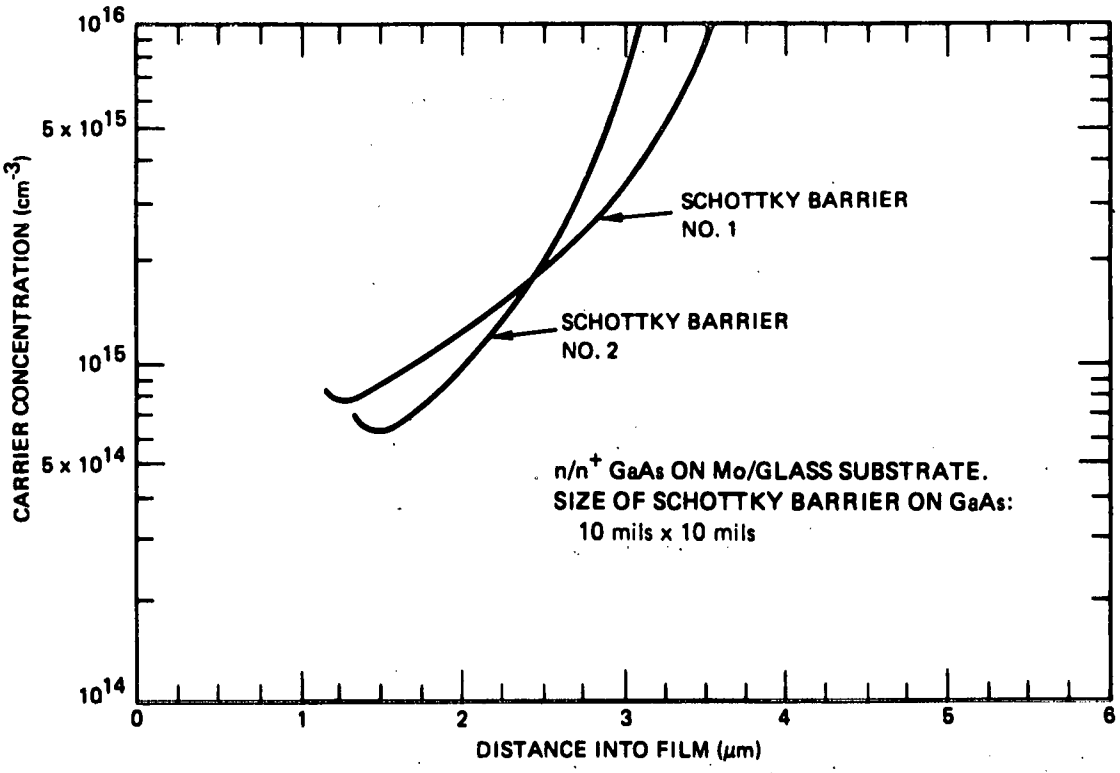

Figure 2-23. Carrier Concentration Profile in n/n^+ MO-CVD GaAs Sample Grown on Composite Mo/Glass Substrate, as Obtained with Miller Feedback Profiler.

2.3.4 Determination of Aℓ Concentration in Ga_{1-x} $Aℓ_x$ As Films

The determination of the Aℓ concentration in GaAℓAs films is required to permit correlation of the observed performance of GaAs window-type solar cells with the theoretically predicted characteristics. A routine, easy to use, non-destructive technique is needed.

One such method is centered on determination of Aℓ concentration in GaAℓAs films by x-ray measurement of lattice constants. Measurement of the difference in lattice constants of an epitaxial film and its substrate is routine at Rockwell; it is commonly used in adjustment of the composition of magnetic bubble films to the correct proportions. The technique is capable of yielding the $\Delta a/a_0$ ratio with sufficient accuracy to permit the determination of the Aℓ concentration of GaAℓAs films grown on GaAs. It should be possible, by establishing a series of standard GaAℓAs films of known composition on GaAs, to use the $\Delta a/a_0$ measurement as a routine technique for determining Aℓ concentration in other films. The preliminary work done toward establishing this procedure is described here.

A series of CVD $Ga_{1-x}Aℓ_xAs$ films was prepared with the Aℓ concentration ranging from 0 to 100 mole percent, i.e., from GaAs/GaAs to AℓAs/GaAs. The AℓAs/GaAs samples were kept in a N_2 atmosphere to prevent any oxidation of the film, and were removed just prior to analysis. The films were analyzed using double-crystal x-ray diffractometry, conventional x-ray diffractometry, and

electron microprobe analysis. Analysis of the data and further experimental work are being pursued separately, under company sponsorship, to complete the project. The data and analysis reported here thus represent a progress report on the work accomplished to date.

2.3.4.1 Double-Crystal X-ray Diffractometry

For (100)GaAs substrates, rocking curves were obtained using Cu K-alpha radiation and the (400) symmetrical and (620) asymmetrical x-ray reflections. In the double-crystal diffractometer the first crystal reference was the (400) reflection from GaAs:Si in the symmetrical case and the (888) reflection from $Gd_3Ga_5O_{12}$ in the asymmetrical case. Rocking curves (plots of diffracted intensity versus rotation angle recorded as the specimen is rocked through the diffraction (Bragg) angle) obtained on this series of samples showed two peaks, one peak corresponding to diffraction by the film and the other to diffraction by the substrate. The separation of the two peaks measured the difference in lattice parameter of the film and substrate. The measured difference for these samples ranged from 0.003 to 0.012Å.

A Cu K-alpha (620) rocking curve of a MO-CVD film of GaAlAs on a (100)-oriented GaAs:Si substrate is shown in Figure 2-24. The curve consists of two peaks,

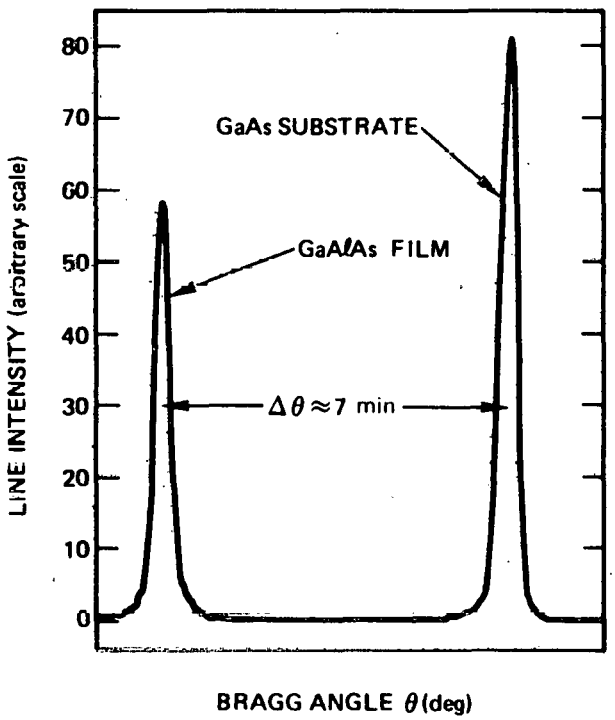

Figure 2-24. X-ray Diffraction Rocking Curve Obtained for MO-CVD GaAlAs Film on (100)-oriented GaAs:Si Single-crystal Substrate, Showing Substrate Peak on Right and Film Peak on Left.

the strong substrate peak and the weak film peak. The peak separation corresponds to an effective lattice parameter difference of about 0.007Å. The film had the larger lattice parameter in this case and was in compression.

2.3.4.2 Conventional X-ray Diffractometry

The other x-ray technique investigated involves conventional x-ray diffractometry. The experimental arrangement is the same as that used in determining preferred orientation in polycrystalline films. The relative intensities of the (600) reflections from both the substrate and the film were determined by using the angle mode programmer and step-scanning in 2θ increments of 0.01 deg over the line profile. At this high Bragg angle (2θ ≈109 deg for Cu K-alpha) the a_1 and a_2 doublet was resolved in most cases, resulting in four peaks – two from the substrate and two from the film. This technique is not as accurate as double-crystal diffractometry but is more applicable to the analysis of polycrystalline films. It is hoped that continued examination of this method will define its limits of applicability.

2.3.4.3 Electron Microprobe Analysis

The analyses using the electron microprobe involved the K-alpha x-ray spectrum of the elemental components in the films - Ga, As, and Aℓ. GaAs was used as a compound standard for the Ga composition determination and elemental Aℓ and As were used as standards for the Aℓ and As composition determinations. The observed intensities were corrected for absorption, atomic number, background, and fluorescence using computer program MAGIC 1 (Ref 15).

The initial results obtained for Aℓ and Ga compositions were in error. The result for Aℓ was affected by the absorption due to Ga and As, and since the film thicknesses were approximately 2μm the Ga concentration value was increased by excitation of the Ga in the substrate by the K-alpha radiation from the As.

To eliminate the effect of As or Ga on the observed Aℓ intensity the excitation voltage of the probe instrument was kept at 5 keV so that the Aℓ K-alpha could be excited but the As or Ga K-alpha could not. The Aℓ intensity in the film was compared against the intensity obtained on an Aℓ elemental standard. The intensities were manually corrected for absorption, backscatter, and stopping power.

2.3.4.4 Results of Aℓ Composition Measurements

The initial results obtained with the three techniques are given for four representative samples in Table 2-3.

The measured values $(\Delta a/a_s)_m$ must be corrected for strain induced in the films and substrates by differences in the lattice constants and the linear thermal expansion coefficients of GaAℓAs and GaAs. This can accurately be done only by measuring the radius of curvature ρ of the film/substrate couple and using the following relations:

$$\left(\frac{\Delta a}{a_s}\right)_o = \left(\frac{\Delta a}{a_s}\right)_m + \frac{2\gamma}{E}\sigma_f - \frac{2\gamma}{E}\sigma_s \quad , \tag{1}$$

Table 2-3. Values for Aℓ Concentration in Four $Ga_{1-x}A\ell_xAs$ MO-CVD Films Determined by X-ray Diffraction and Electron Microprobe Techniques

Sample	$\left(\frac{\Delta a}{a_s}\right)^*$	$\left(\frac{\Delta a}{a_s}\right)_m^\dagger$	Aℓ Concentration†† (mole fraction)
A	5.3×10^{-4}	3.5×10^{-4}	0.32
B	1.24×10^{-3}	9.7×10^{-4}	0.57
C	1.77×10^{-3}	1.52×10^{-3}	0.96
D	2.12×10^{-3}	1.76×10^{-3}	0.98

*Measured values based on conventional x-ray diffraction
†Measured values based on double-crystal diffraction
††Electron microprobe analysis

where the stress in the film (σ_f) and the stress in the substrate (σ_s) are related to the thicknesses t_f and t_s and ρ by

$$\sigma_f = \frac{-E}{6\rho(1-\gamma)} \frac{t_s^2}{t_f} , \tag{2}$$

and

$$\sigma_s = -4\frac{t_f}{t_s} \sigma_f . \tag{3}$$

where E is Young's modulus (10^{12} dynes/cm^2) and γ is Poisson's ratio (0.3).

If all of the differences in lattice constant are accommodated elastically, then ρ can be expressed in terms of the thickness and $\Delta a/a_s$. When the appropriate relation is substituted into the equations above and it is recalled that $t_f \ll t_s$, the following relationship results:

$$(\Delta a/a_s)_o = (\Delta a/a_s)_m \Big/ 1.9 . \tag{4}$$

That is, the measured value is almost twice the actual value of $(\Delta a/a_s)_o$.

Using Eq (4) and comparing the measured $(\Delta a/a_s)_o$ from Table 2-3 with the results of Estop et al (Ref 16), it is seen that there is poor agreement between the composition determined by x-ray means and that determined by microprobe analysis,

with the $\Delta a/a_s$ measurements indicating a lower value of x. There are two possible explanations for this. One is that the microprobe results are incorrect; this cannot be ruled out owing to the many interactions among the components of the films. The other possibility is that the lattice constant difference was not all being accommodated elastically and misfit dislocations resulted in a lower-than-expected ratio of $(\Delta a/a_s)_m$ to $(\Delta a/a_s)_o$. Use of Eq. (4) would then underestimate the A concentration.

Precise determination of the radius of curvature of the sample must be accomplished to test this possibility, and such measurements are planned. In addition, comparison of the $(\Delta a/a)$ measurements indicates a discrepancy between the values determined by double-crystal diffractometry and those by conventional diffractometry. This difference may be due to the fact that different reflections were used for the two measurements. Measurements of $(\Delta a/a)$ on the double-crystal instrument for two different reflections showed some differences, which may be an indication of the formation of misfit dislocations. Proper corrections for strain in the films, obtained by measurement of the radii of curvature of the samples, should account for the occurrence of dislocations, as indicated above.

2.4 TASK 4. EXPERIMENTAL PHOTOVOLTAIC DEVICE FABRICATION AND EVALUATION

This task was summarized as follows at the start of the program:

> Prototype heterostructure and Schottky-barrier solar cells will be fabricated to provide an ultimate test for the CVD films grown on various low-cost substrates. Appropriate device designs will be developed for both transparent and opaque substrate materials, and experimental structures will be made for each case. In addition to determining the suitability of the films for solar cell applications, detailed characterization of these devices will provide the needed information on various aspects of the device fabrication technology itself -- e.g., layer dimensions, doping concentrations, contact materials and processing. Characterization methods will include determination of detailed I-V curves (light and dark) and determination of the usual solar cell properties (V_{oc}, I_{sc}, curve fill-factor, efficiency) both under laboratory illumination and in an AM1 solar simulator.

The activities of this task were concentrated primarily in the third and fourth quarters. The limited work on this task in the first quarter involved the design of an experimental solar cell contact mask and the verification of single-crystal contact technology for window-type heterojunction solar cell fabrication.

Relatively little further work was done in the second quarter, primarily because of problems that were encountered in obtaining good quality GaAlAs films (Ref 9). However, all of the apparatus required for complete characterization of GaAs solar cells was acquired, assembled, and made operational. Also, the ohmic contact technology for both n- and p-type GaAs was tested and found fully satisfactory. For n-type GaAs contacts of Au-12 percent Ge were used, and contacts to p-type GaAs were either In-Ag-Zn or Au-Zn. The development of a specific contact material for GaAlAs was hampered by the lack of doped GaAlAs material of adequate quality in the first two quarters.

Significant progress was made in the third quarter toward the goal of producing low-cost GaAs solar cells. Results obtained on single-crystal heterostructure window cells grown by the MO-CVD technique clearly established that the technique is capable of producing high-efficiency GaAs solar cells. This development was a necessary one to establish confidence that the ultimate goal of fabricating low-cost large-area polycrystalline solar cells could be met. In addition to the single-crystal results, initial attempts to produce polycrystalline GaAs solar cells were also successful.

During the third quarter single-crystal window-type heterostructure cells in GaAlAs/GaAs multilayers were fabricated and evaluated (with no AR coating) under simulated AM0 illumination and found to have conversion efficiencies as high as 12.8 percent. Devices with all-epitaxial junctions were found to have much higher efficiencies than those with junctions at the film-substrate interface. Open-circuit photovoltages as high as 0.99 V, short-circuit current densities as high as 24.5 mA/cm^2, and curve fill-factors up to 0.74 were achieved. The polycrystalline cells that were fabricated were mainly of the Schottky-barrier type. Initial results on Schottky-barrier cells formed on films grown on Mo/glass composite substrates indicated efficiencies of 1.35 percent under simulated AM0 illumination. Other composite substrates were used for fabrication of additional Schottky-barrier devices, and some junction-type polycrystalline cell structures were also fabricated.

During the fourth quarter the fabrication of Schottky-barrier devices on various polycrystalline GaAs structures - e.g., n/n^+/Mo/glass, n/n^+/graphite, and n/n^+/tungsten - continued, with variations introduced in n-layer and total GaAs film thickness, Mo film configuration (including patterned grid), and metal thickness to attempt to obtain improved results. Efficiencies of uncoated cells of up to 2.75 percent (AM0) were achieved. The nature of the contact between GaAs and thin-film Mo was also examined experimentally and found to be non-ohmic for both n and n^+ GaAs unless the doping level in the GaAs is above $\sim 1 \times 10^{18}$ cm^{-3}, in which case an ohmic contact is achieved.

Polycrystalline GaAs p-n junctions were also examined further in the fourth quarter. Reasonable I-V characteristics were found for the n/p configuration, but p/n structures had poor junction properties, with an apparent shunt resistance of only ~100 ohms. It is believed that the cause of this difference in performance in the two cases is diffusion of Zn along the grain boundaries of the polycrystalline GaAs films.

Details of these investigations are given in the following sections.

2.4.1 Single-crystal GaAlAs/GaAs Heterostructure Solar Cells

The first single-crystal solar cells fabricated in this program were similar in structure to those which have yielded high efficiencies in devices grown by liquid-phase epitaxy (LPE) (Ref 17). The structure was a p/p/n composite of $Ga_{(1-x)}Al_xAs$/GaAs/GaAs, with $x \approx 0.8$.

The initial structures were formed by sequentially growing p-type GaAs and p-type GaAlAs on an n-type single-crystal GaAs substrate, thus forming a p-n junction at the interface of the epitaxial material and the bulk substrate. The best devices, however, had an all-epitaxial junction, involving an n-type GaAs epitaxial layer grown before the p-type layers but during the same CVD run. The typical layer thicknesses were GaAlAs 500Å, p-type GaAs 1.4 to 1.5 μm, and n-type GaAs 4 to 6 μm.

The cells were fabricated by depositing a Au-Ge (12 percent Ge) contact on the back surface of the device, defining a square grid pattern in photoresist on the top surface, etching the pattern lightly to remove the GaAlAs where the contact deposition was to take place, depositing a Au-Zn-Au (2 percent Zn) layer over the whole surface, and removing the photoresist to define the grid contact. The structure was then alloyed at 425°C for 1 to 2 min. The samples were then cleaved into portions having a maximum area of 0.5 cm^2. This was done to allow mounting the devices on the headers that were available.

The resulting devices were evaluated by measuring the I-V characteristics under illumination by an uncalibrated AM0 solar simulator. A Canrad-Hanovia Model 976C-0010 Xe high-pressure arc lamp, powered by an Oriel Model 6117 Universal Arc Lamp Source, was used unfiltered for the measurements. The lamp was operated at 1 Kw, and the resultant illumination at the sample was measured by a calibrated Eppley Bi-Ag thermopile. Incident intensities in the range 128 to 135 mw/cm^2 were used. The measurements on some of the devices were subsequently checked by additional measurements using a balloon-flight-calibrated AM0 solar simulator at the Photoelectronics Group of OCLI (City of Industry, CA) and found to be quite accurate.

Figure 2-25 shows the I-V characteristics, both dark and under simulated AM0 excitation, for a heterostructure solar cell with the p-n junction at the film substrate interface. The open-circuit voltage (V_{OC}) and the curve fill factor (FF) are somewhat lower than the best values for these parameters obtained on LPE devices. Similarly, the short-circuit current density (J_{SC}) is about 20 percent lower than expected for the best devices. The CVD device involved here had no antireflection (AR) coating.

The device represented in Figure 2-25 is one of the better devices obtained with the junction at the epitaxial film-substrate interface. Figure 2-26 shows similar characteristics for a device with an all-epitaxial grown junction. Note the increased V_{OC} and J_{SC} values for this device, which is the best of those fabricated during the period covered by this report. The conversion efficiency of the device was 12.8 percent with no AR coating, under simulated AM0 conditions. With an appropriate AR coating an efficiency comparable with the best reported values for LPE devices would be expected.

Table 2-4 compares the ranges of properties obtained for all-epitaxial-junction devices with those obtained for devices with junctions at the film-substrate interface. The devices with all-epitaxial junctions are improved in almost every respect.

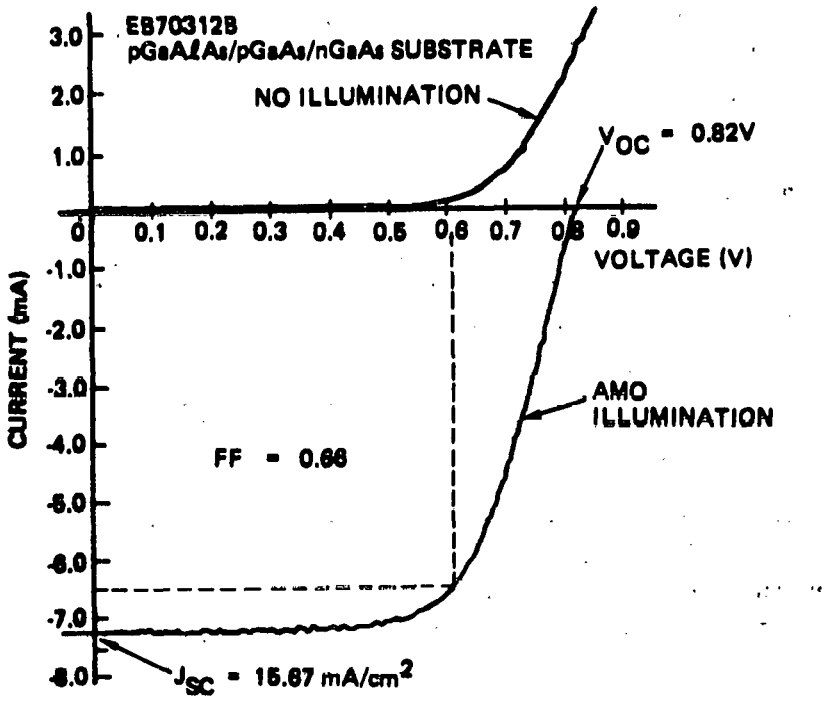

Figure 2-25. Dark and Light I-V Characteristics for MO-CVD GaAlAs/GaAs Heterostructure Solar Cell with Junction at Film-substrate Interface.

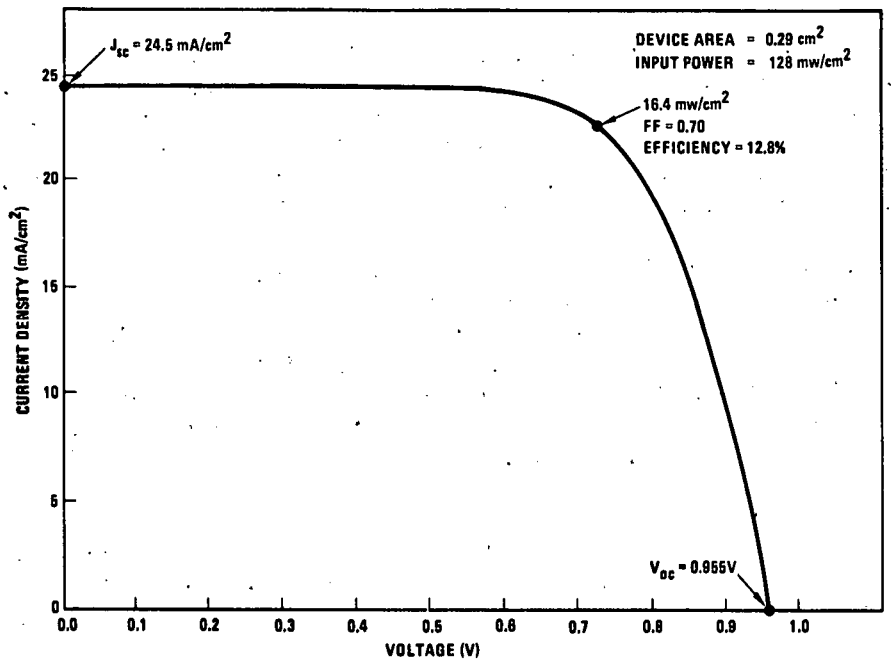

Figure 2-26. Fourth Quadrant of I-V Characteristic of MO-CVD GaAℓAs/GaAs Heterostructure Solar Cell under 128 mw/cm^2 Illumination (uncorrected for contact area or reflection from uncoated GaAℓAs window).

Table 2-4. Comparison of Film-substrate and All-epitaxial Heterobarrier Solar Cells

Structure	Maximum Efficiency*	V_{oc} (max)*	J_{so} (max)*	FF (max)*
pGaAℓAs/pGaAs/n Substrate	8%	0.82V	17 mA/cm^2	0.72
pGaAℓAs/pGaAs/nGaAs/n Substrate	12.8%	0.99V	24.5 mA/cm^2	0.74

*Measured under simulated AMO conditions with no AR coating.

These results indicate that MO-CVD is a potential high-volume fabrication technique for high-efficiency single-crystal solar cells for use in concentrator systems, such as would be used in either terrestrial systems or orbiting space power supplies. The results also strongly indicate that the MO-CVD technique should be applicable to the successful fabrication of polycrystalline solar cells of good efficiencies for non-concentrator terrestrial use - the goal of this program.

2.4.2 Single-crystal and Polycrystalline Thin-film Schottky-barrier Solar Cells

It was decided early in the program that emphasis would be placed upon evaluation of Schottky-barrier solar cells to obtain a measure of the quality of the polycrystalline materials being prepared. This was particularly important prior to attempting to fabricate p-n junction cells in polycrystalline material, so that potential problems with junction formation would not be obscured by problems of materials nonuniformity.

2.4.2.1 Cells on Films on Bulk Single-crystal and Polycrystalline Substrates

As a calibration of the materials quality and to investigate potential problems that might occur with solar cells fabricated in polycrystalline materials, Schottky-barrier solar cells were fabricated on epitaxial GaAs layers grown on bulk single-crystal and large-grained polycrystalline substrates.

The structures employed were n/n^+/substrate, where the n region was undoped and the n^+ region was doped above 10^{18} cm^{-3}. The undoped region typically had a net carrier concentration in the range 5×10^{14} - 2×10^{15} cm^{-3}. The films were deposited at 725°C in the usual way. Au-Ge ohmic contacts were applied to the backs of the samples, and 50 mil x 50 mil Au Schottky-barrier pads 50Å thick were deposited on the front surfaces. A thick Au pad 10 mils x 10 mils was deposited in one corner of each Schottky barrier, for bonding and probing.

Figure 2-27 shows the I-V characteristics of a Schottky-barrier cell fabricated on epitaxial n/n^+ GaAs layers grown on GaAs:Si single-crystal wafers. The open-circuit voltage for this cell was 0.4 V, with short-circuit current density ~15 mA/cm^2 and a 0.62 fill factor, for a total efficiency of 2.7 percent. This value of efficiency is low for this type of cell.

Cells were fabricated in the same way on polycrystalline layers grown on bulk polycrystalline GaAs substrate wafers. After deposition of the film the surface was observed to have discrete steps at the boundaries between grains, resulting from differing growth rates on the various orientations. No attempts were made to analyze Schottky barriers which straddled one of these boundaries because the barrier would be discontinuous across the boundary.

Figure 2-28 shows the light and dark I-V characteristics of one of these Schottky-barrier cells. The characteristics of the cell are actually superior to those of cells in the films grown on single-crystal material: V_{oc} = 0.51 V, J_{sc} = 18.8 mA/cm^2, and fill factor = 0.74. The efficiency of this cell was 5.2 percent. This is the efficiency value against which the performance of other polycrystalline cells fabricated later in the program were compared.

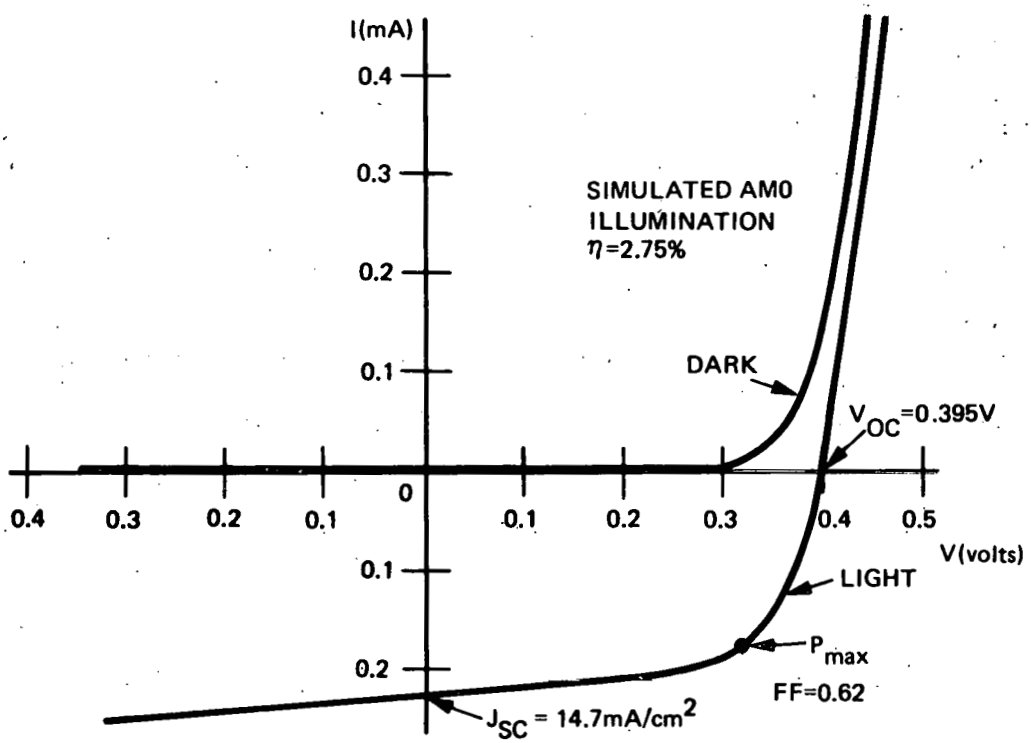

Figure 2-27. Light and Dark I-V Characteristics of Schottky-barrier Solar Cell Fabricated on Epitaxial n/n$^+$ GaAs Grown by MO-CVD on Single-crystal GaAs:Si Substrate.

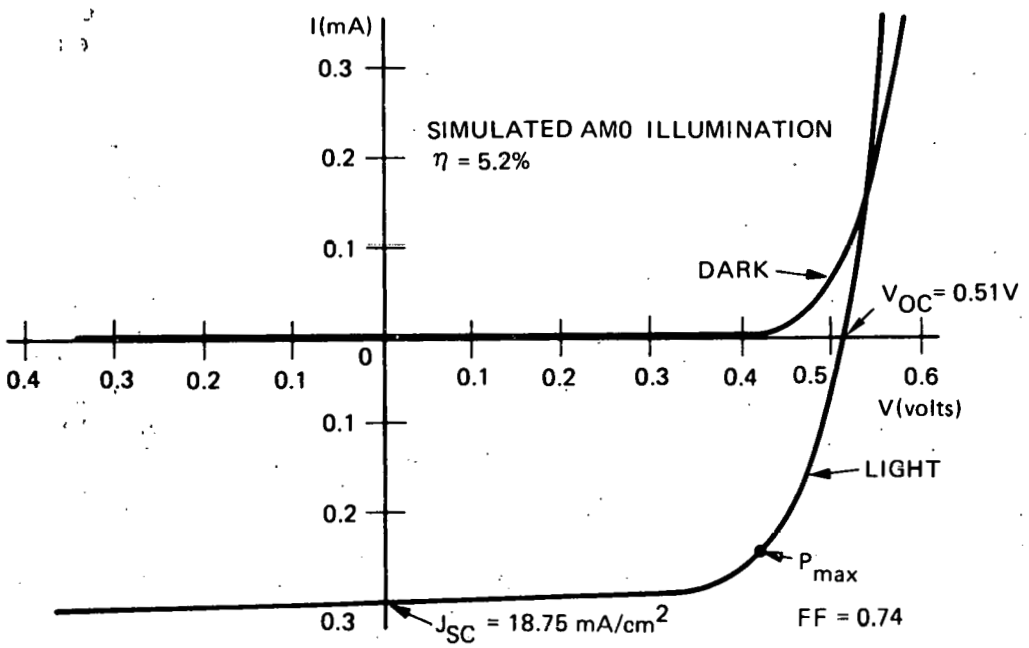

Figure 2-28. Light and Dark I-V Characteristics of Schottky-barrier Solar Cell Fabricated on Polycrystalline n/n$^+$ MO-CVD GaAs on Bulk Polycrystalline GaAs Wafer.

2.4.2.2 Polycrystalline Cells on Low-cost Substrates

The emphasis of this program is to produce solar cells on potentially low-cost substrates, evaluate their performance, and improve them to the point that they meet the goals of the national photovoltaic energy conversion program. The initial cells of this type involved a series of n/n^+ deposits made on potentially low-cost substrates or prototypes for these substrates. Among these materials were Mo, W, carbon, Mo films on glass, and Ge films on a variety of substrates.

Of these, the most success was achieved with cells grown on the Mo/glass composite substrate. Here two options were investigated: (1) a Mo/glass composite with full-surface Mo coverage, and (2) a composite involving only a grid of Mo on the glass. Results better by a factor of five were obtained for substrates with full Mo coverage.

The I-V characteristics of such a cell are shown in Figure 2-29. The cell represented there had an efficiency of 2.25 percent under simulated AM0 illumination, with the short-circuit current density J_{SC} = 12.5 mA/cm^2. The open-circuit voltage V_{OC} (0.46 V), the short-circuit current density, and the fill factor (0.53) are all substantially below the corresponding parameters for the cells on single-crystal material. Similar results were achieved with substrates consisting of Mo layers on other substrate materials, such as polycrystalline alumina.

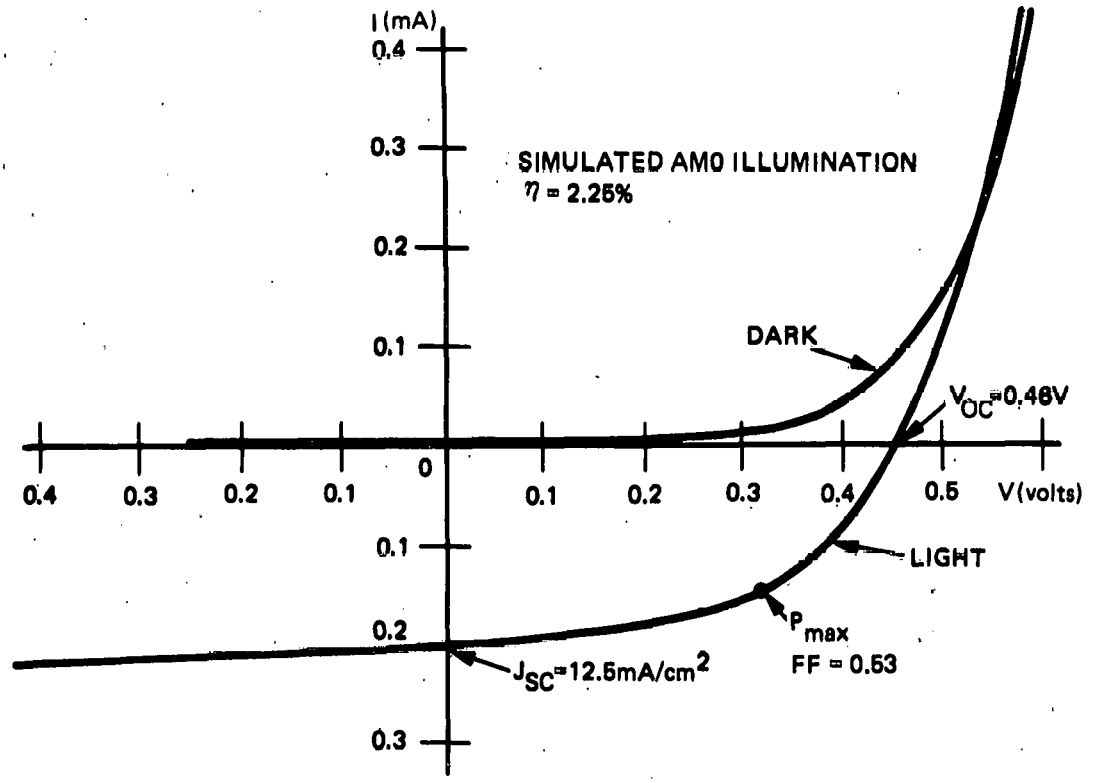

Figure 2-29. Dark and Light I-V Characteristics of Schottky-barrier Solar Cell Fabricated on Polycrystalline n/n^+ MO-CVD GaAs Grown on Mo/Glass Composite Substrate.

A study was made to determine whether the bulk GaAs or the GaAs/Mo interface caused the high resistance of these devices. It was discovered that as long as the doping of the n^+ layer was greater than 1-2 x 10^{18} cm^{-3} the contact between the Mo and the GaAs was ohmic, with negligible resistance. Further, most of the cell resistance was contributed by the film of GaAs.

A variety of other substrates were also used for the fabrication of Schottky-barrier cells. In most cases the performances were inferior to that obtained with films on the Mo/glass composite. Figures 2-30 and 2-31 show the I-V characteristics of two of these devices, on carbon (graphite) and tungsten substrates, respectively. In neither case was there any measurable photovoltaic effect. The W-GaAs interface was found to be non-ohmic at carrier concentrations $n \approx 2 \times 10^{18}$ cm^{-3}, as is shown by the dashed curve, which is the I-V characteristic obtained between the W substrate and an ohmic contact on the GaAs (Figure 2-31).

Ge was deposited on a variety of substrates by CVD (using germane, GeH_4), either as the first step in a GaAs MO-CVD experiment or as a separate deposition experiment prior to loading the reactor for the GaAs deposition. The devices fabricated on GaAs films grown on these Ge underlayers all showed very poor I-V characteristics; many of them were shorted. The cause of the difficulties may have been a

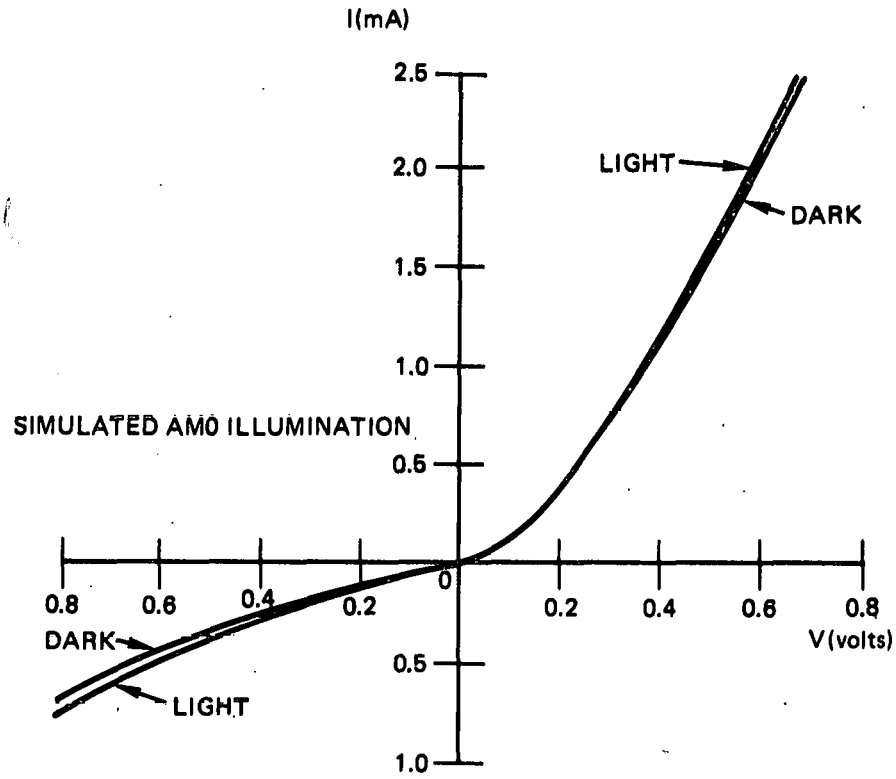

Figure 2-30. Dark and Light I-V Characteristics of Schottky-barrier Solar Cell Fabricated on Polycrystalline GaAs Film Grown by MO-CVD on Graphite Substrate.

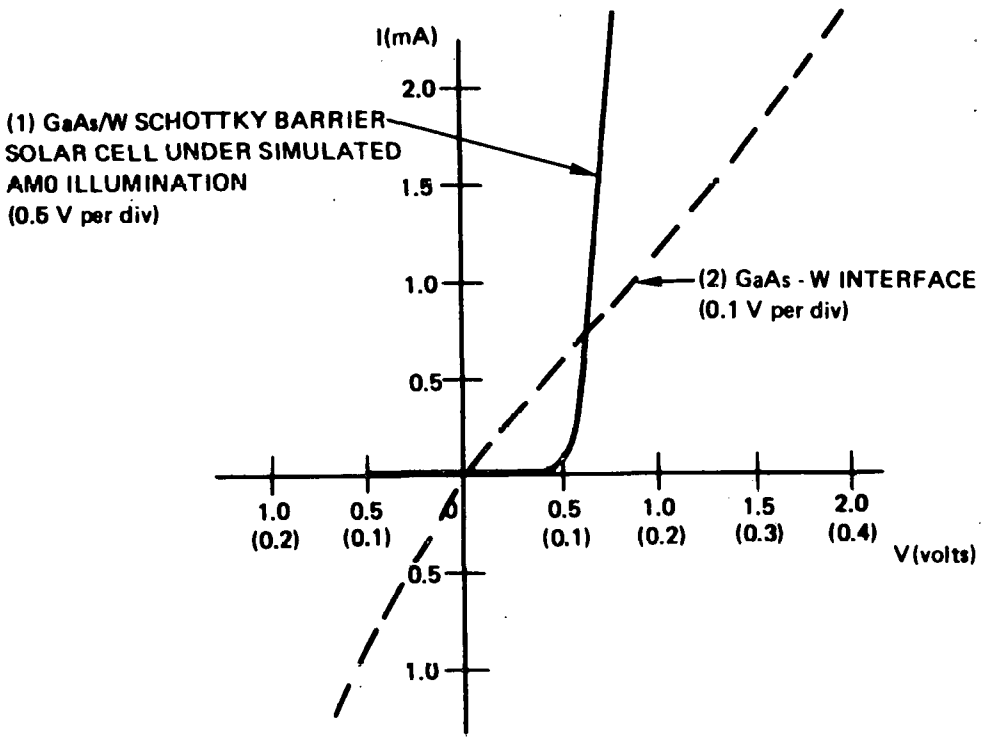

Figure 2-31. I-V Characteristics of (1) Illuminated Schottky-barrier Solar Cell Fabricated on Polycrystalline GaAs Film Grown by MO-CVD on W Substrate, and (2) GaAs-W Interface

doping concentration that was too high, due to counterdoping by Ge in the reactor system, or incomplete coverage of the substrates by the deposited films. Further analysis of these films and the devices fabricated on them will be performed in later phases of the program.

2.4.3 Junction Devices in Polycrystalline Films

Polycrystalline GaAs p-n junction structures were grown by MO-CVD on a number of substrate materials. The structures were grown to have n layers of 5 μm thickness and a doping level of 2×10^{17} cm^{-3}. The p layers were also typically 5 μm thick and doped to a level of 2×10^{18} cm^{-3}. All of the samples discussed in this report were grown with these approximate parameters. Other samples were grown with higher n-type doping, lower p-type doping, and thinner p layers, but these samples were not evaluated prior to the end of the period covered by this report.

The "standard" samples described above had impurity doping concentrations comparable with those used in the high-efficiency single-crystal cells (Section 2.4.2.1). The junction-type polycrystalline structures were grown on substrates of bulk polycrystalline GaAs, Mo/glass composites, Ge/glass composites, Ge/glass-ceramic (Corning Code 9606) composites, patterned Mo/alumina composites, and patterned Mo/refired-alumina (Vistal) composites.

Figure 2-32 shows the I-V characteristics of two mesa-type junction devices in a film grown on a polycrystalline GaAs substrate. The mesa of one of the devices was fully contained within a single grain of the polycrystalline film, while the mesa of the other contained an additional small grain so that the grain boundary between the two grains was included within the area of the device. The I-V curves clearly show the effects of the increased leakage in the device containing the additional grain and the grain boundary. It is not known if this increased conduction was caused by the grain boundary itself or by the material in the second grain. Mesas in some other large grains on the same sample had shorted junctions. It is interesting to note that the grains with mesas that had shorted junctions also showed a high density of large etch pits after the mesa etch, indicating perhaps the presence of a spike defect of some kind penetrating the two GaAs regions.

Deposited p-n junctions on Mo/glass composites typically showed very poor I-V characteristics. Figure 2-33 shows the dark I-V characteristic of one mesa p-n junction device on Mo/glass. The devices were excessively leaky, as indicated in the figure. The shunt resistance of the device estimated from this I-V characteristic was the order of 150 ohms. It is believed that the low shunt resistance occurred because of diffusion of Zn along grain boundaries in the deposit, causing leakage paths between the front and rear contacts.

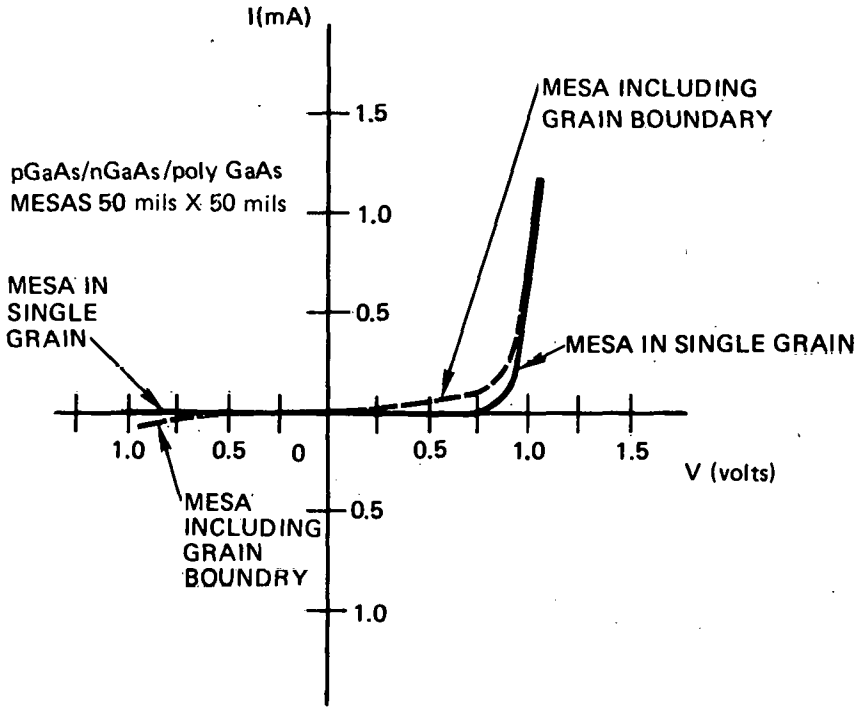

Figure 2-32. Dark I-V Characteristics of Two Mesa-type p-n Junction Devices in Polycrystalline GaAs Grown by MO-CVD on Bulk Polycrystalline GaAs Substrate.

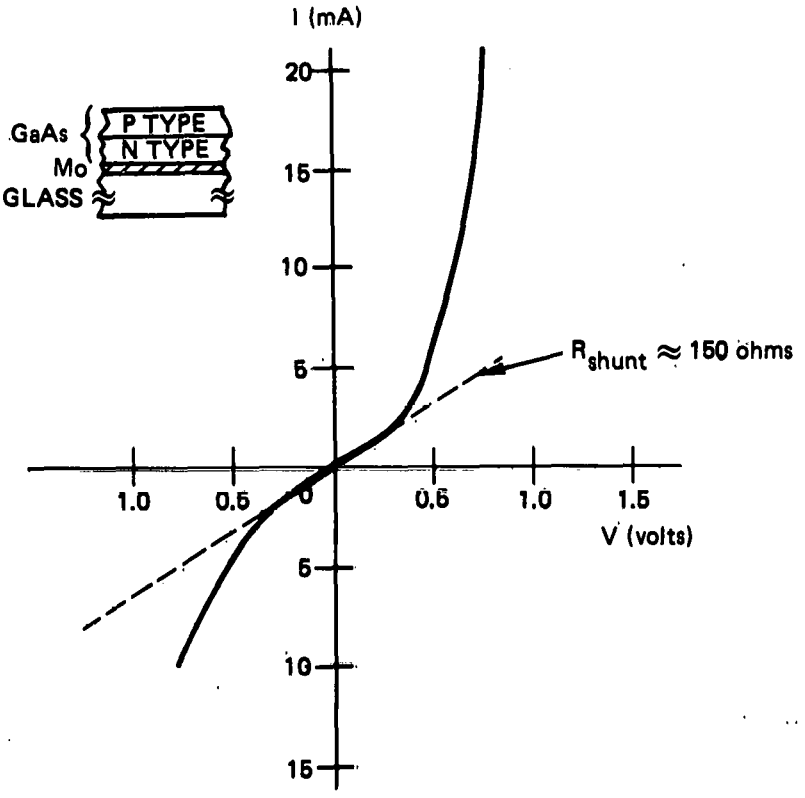

Figure 2-33. Dark I-V Characteristic of Mesa-type Deposited p-n Junction Device in Polycrystalline GaAs Grown by MO-CVD on Mo/Glass Composite Substrate.

This must be confirmed by detailed studies of cross-sectioned samples, but further evidence for this interpretation is provided by comparison of the above results with those for an inverted (n-on-p) structure, shown in Figure 2-34. The p-type doping of this structure was a factor of two lower, but – more significantly – diffusion of Zn had to occur from a solid source rather than from a gaseous source. As a result, the Zn apparently did not penetrate the n layer appreciably. The resultant I-V characteristic shows little or no leakage.

As mentioned previously, many other polycrystalline junction samples were grown, and will be evaluated in the second phase of the program.

During the final quarter additional device masks were designed and fabricated. These new masks provide for a variety of Schottky-barrier solar cell sizes, and also include several sets of contact masks. A contact mask is provided for p-n junction cells to permit low-area-coverage metallization with the required low resistance for both single-crystal and polycrystalline cells. A set of interdigitated finger-type contact masks is also included, to provide not only for metallization patterns for all-one-side contacting of cell structures but also for the required etching to contact the "buried" layer. These mask sets will be used in the device work in subsequent phases of the program.

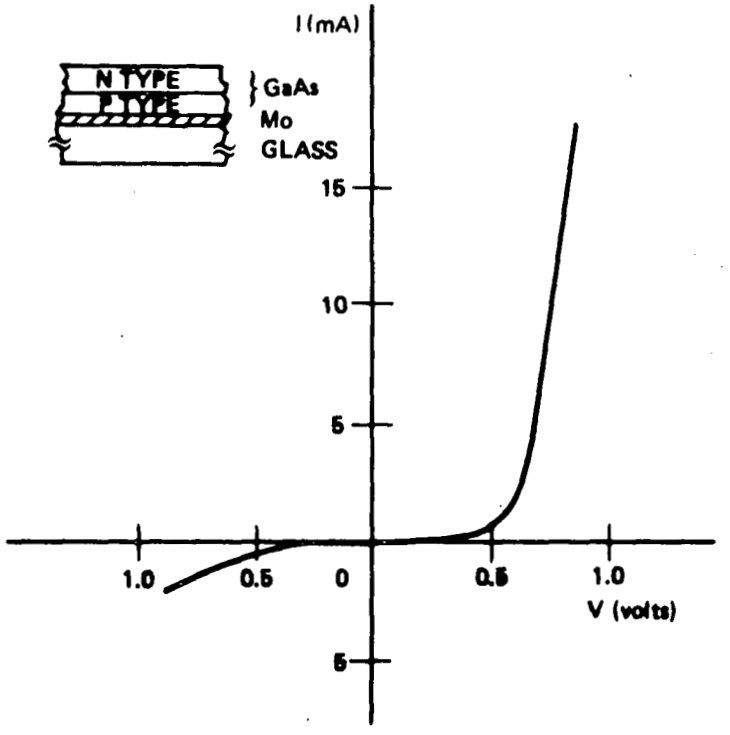

Figure 2-34. Dark I-V Characteristic of Mesa-type Deposited n-p Junction Device in Polycrystalline GaAs Grown by MO-CVD on Mo/Glass Composite Substrate.

2.5 TASK 5. ANALYSIS AND PROJECTION OF CELL FABRICATION COSTS

This task was summarized in the program proposal as follows:

> Present costs for experimental and pilot-line quantities of thin-film GaAs solar cell structures will be analyzed at the start of the program and again during the final month of the contract. Future costs for large-scale production of such cells will be projected during the final month of the contract, based on the analyses of present actual costs of materials, processing costs (including labor), and capital equipment and facilities requirements, compiled from data available from this program, from Rockwell facilities engineers, from materials and equipment vendors, and other sources.

The effort on this task in the first quarter was limited to (1) selection of two conceptual device designs to be used as the basis of cost analyses and projections; (2) acquisition of some materials costs from vendors and the costs of certain facilities and support services (from Rockwell facilities personnel); and (3) outlining of preliminary materials and processing matrices for use in establishing a range of present and projected costs for thin-film GaAs solar cells fabricated by the MO-CVD method. One of the conceptual device designs involved a conventional window-type GaAlAs/GaAs film structure on an opaque substrate and the other involved an inverted structure on a transparent substrate.

It had originally been proposed that the initial analysis of present device fabrication costs and a preliminary projection of future large-scale production costs be completed during the first six weeks of the program. It was intended that this analysis would consist of three parts: (1) determination of the "materials content value" for the two conceptual device designs in terms of present costs, and - to the extent possible - projected future costs; (2) analysis of the total cost of producing a solar cell in each of the two conceptual designs in the laboratory, accounting for all materials costs, processing costs, labor, and facilities and equipment requirements; and (3) projection of total costs for producing these same two cell designs on a limited pilot-line basis, using current cost factors scaled up to the pilot-line level. However, the program schedule was modified, with the intention of carrying out this analysis in the second quarter.

During the second quarter some attention was given to identification of materials and processing costs associated with the two conceptual designs, but it was realized that further details of the actual device designs most likely to be adopted should become established before any extensive cost analyses were carried out. In a preliminary consideration of current costs of materials used in simplified versions of the two conceptual designs of thin-film GaAlAs/GaAs heterostructure devices it appeared that there is a probable lower limit of \$43 - \$52 per m^2 for the total current cost of just the materials used in the proposed configurations. Despite this, it was concluded that thin-film GaAs cells fabricated by the MO-CVD process can probably meet the future cost goals of the ERDA program (see below) provided substrate materials with the necessary properties can be identified and produced inexpensively in practical sizes and very large quantities.

Further consideration was given to the analyses in the third quarter, and some generalizations regarding cost goals for GaAs solar cell fabrication were delineated by reference to the corresponding cost goals of the ERDA Low Cost Silicon Solar Array Project. These are discussed in the following sections, along with some analyses of material availability and material costs developed at the end of the period covered by this report.

2.5.1 Conceptual Solar Cell Designs for Cost Analyses

For purposes of preliminary analysis two different conceptual device designs were developed. They are both heterostructure devices, one involving opaque substrate materials and the other involving transparent substrates and an inverted structure permitting illumination through the substrate. Both designs involve the following basic solar cell components: (1) substrate (opaque or transparent, simple or composite); (2) base-region or backside contact; (3) active base region of cell (probably n-type GaAs); (4) front layer of cell (probably p-type GaAs); (5) window layer (probably p-type $Ga_{1-x}Al_xAs$, with $x \approx 0.9$); (6) front contact. on incident-light surface; and (7) antireflection coating on front surface.

The two configurations are shown in Figure 2-35 in somewhat generalized form. For both designs the front (incident-light surface) contact and the base-region (backside) contact are shown as continuous layers in the diagrams. It is understood, however, that these conducting contact layers may in practice take the form of an open gridwork or a continuous layer, in either instance with an associated high degree of optical transparency for the case of the front contact.

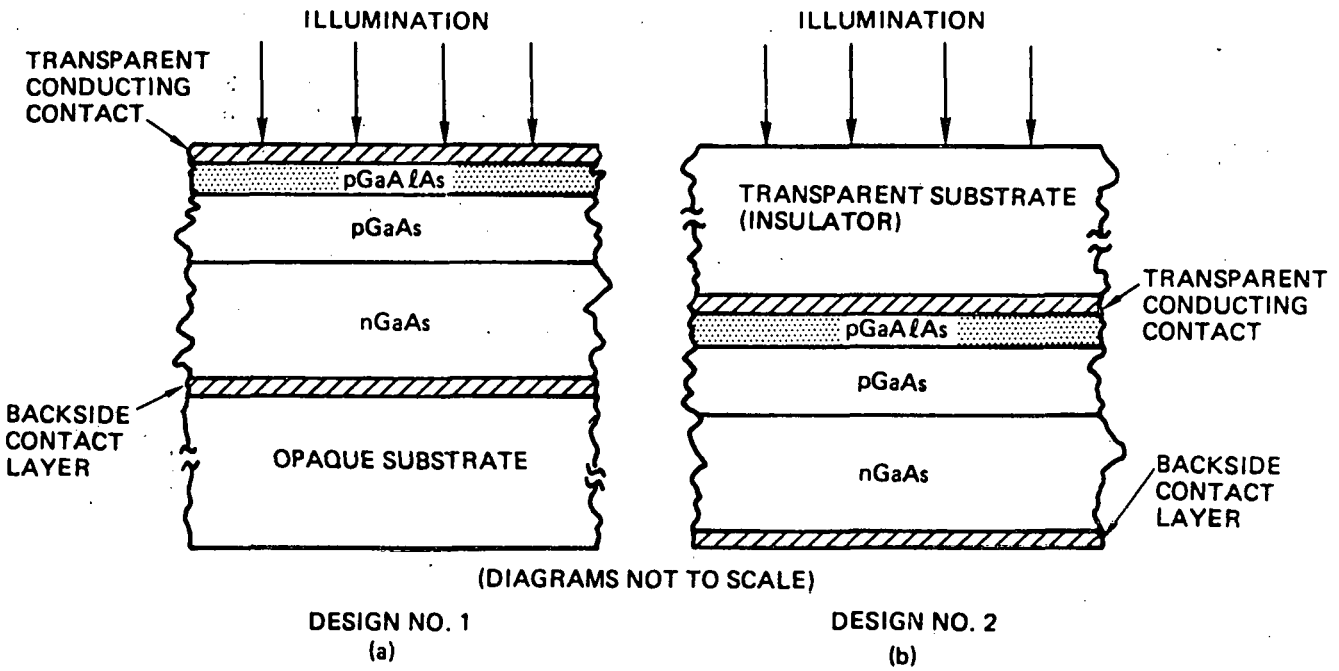

Figure 2-35. Conceptual Designs of Thin-film GaAlAs/GaAs Heterostructure Solar Cells. (a) Conventional Window Structure with Opaque Substrate; (b) Inverted Structure with Transparent Substrate. (AR coating not shown on either configuration.)

Design No. 1, the conventional window structure on an opaque substrate, is shown in Figure 2-35a, and involves deposition of n-type GaAs onto the substrate followed by deposition of p-type GaAs and then p-type $Ga_{1-x}A\ell_xAs$, with $x \approx 0.9$. The junction is formed at the interface of the two GaAs layers. The $A\ell$ concentration must be selected to achieve stable low-contact-resistance devices and good high-energy spectral response, and the thickness of the $GaA\ell As$ layer must be adjusted to provide good spectral transmission and yet allow adequately low series resistance in the cell.

Design No. 2, which involves a transparent substrate, is shown in Figure 2-35b. It consists of an inverted $GaA\ell As$/GaAs window-type heterostructure, and is formed by deposition of p-type $Ga_{1-x}A\ell_xAs$ ($x \approx 0.9$) onto the transparent substrate followed by deposition of p-type GaAs and then n-type GaAs. The junction is again formed at the interface of the two GaAs layers. As with the first design, the $A\ell$ concentration and the thickness of the alloy layer must be chosen for optimum optical and electrical properties. For both configurations the details of the contact designs and the impurity doping concentrations in the layers remain to be determined by experiment and device analysis.

These two basic conceptual designs provide the basis for the various cost estimates that have been developed during the period convered by this report.

2.5.2 General Cost Goals for GaAs Solar Cells on Low-cost Substrate Materials*

As indicated in Section 1 (Introduction), the future cost (i.e., market price) goals for the National Photovoltaic Conversion Program are \$500 per peak kw by 1985 and \$100 to \$300 per peak kw by 2000, with annual production capacities in those years of 500 peak Mw and 5×10^4 peak Mw, respectively. The performance goal of at least 10 percent efficiency for low-cost polycrystalline solar cells in those same years requires that any process to be considered must permit fabrication of large-area cell arrays at total costs not exceeding \$50 per m^2 in 1985 and \$10 to \$30 per m^2 in 2000.

Since the standard of comparison for photovoltaic cells, for both performance and cost, continues to be the Si solar cell, the 1985 goals of the ERDA/JPL Low Cost Silicon Solar Array (LSSA) Project provide a convenient measure of the signficance of the above cost figures. The Si material cost goal for 1985 is \$10 per kg. The cost goal for production of large areas of Si sheet is ~\$17 per m^2 (beyond the Si material cost), while the cost goal for fabricating Si solar arrays (including contacts, interconnects, bonding, encapsulating) is another ~\$17 per m^2 beyond the sheet fabrication cost.

With these 1985 Si solar array cost goals as a guide, upper limits can be set on materials costs, film formation costs, and cell array fabrication costs for thin-film GaAs cells in that same time period. Thus, for GaAs cells to complete with low-cost Si cells (both presumed to operate at 10 percent AM1 efficiency), the materials costs should not exceed ~\$16 per m^2 if the same cost limits are assumed for film production and array fabrication in both cases. On a simple proportional basis, the corresponding figures for the year 2000 - in which the ERDA total cost goal is \$10 to

*All cost figures in this and subsequent sections are in terms of current year (1977) dollars; no allowance is included for inflation effects.

$30 per m^2 - would be $3 to $10 per m^2 for materials, $3.50 to $10 per m^2 for film formation, and another $3.50 to $10 per m^2 for array fabrication, for either GaAs or Si solar cell arrays.

Thus, the cost goals that have been established (and generally accepted as stringent but feasible) for Si solar arrays in the LSSA Project can also serve at least as guidelines for development of low-cost GaAs solar arrays. Major differences exist, however, in the nature and the maturity of present technologies involved in the three principal cost categories - (1) processed/purified material, (2) film or sheet fabrication, and (3) cell/array fabrication.

High-purity semiconductor-grade polycrystalline Si now costs about $60 per kg, prepared by a series of processes that are highly developed and using input materials almost unlimited in abundance; Si itself is the second-most abundant of all the elements. Single-crystal ingots of Si, grown by the Czochalski method and with properties adequate for use in fabricating single-crystal wafer-type solar cells of the conventional kind, cost about $0.25 per g for moderate quantities.

GaAs, on the other hand, is prepared almost exclusively as an ultrapure single-crystal semiconductor compound, either in bulk ingot form by Czochralski or Bridgman crystal-growing techniques or in single-crystal layer form by liquid-phase epitaxy (LPE) or chemical vapor deposition (CVD) techniques. Although these processes are now highly developed they are by no means developed on a large production scale. Single-crystal GaAs prepared by the Bridgman technique now costs about $7 per g in bulk ingot form, while ultrahigh purity Ga metal and As metal separately cost about $0.75 and $0.65 per g, respectively, in relatively small quantities. Further, the world supply of Ga (roughly half the weight content of GaAs) is known to be limited, although there appears to be little need for concern about As abundance.*

Caution must be exercised in making input material cost comparisons between Si and GaAs for solar cell use, however. It is semiconductor-grade polycrystalline Si (at ~$60 per kg) that is considered to be the input material for fabrication of Si solar cells, whether such cells are the conventional single-crystal wafer ("space type") configuration, web or ribbon configuration, or other type that requires the use of molten ultrahigh-purity Si for its preparation. In terms of the LSSA Project cost breakdown terminology, this is the Si material cost that is targeted for reduction to less than $10 per kg by 1985, as mentioned earlier. The Si sheet fabrication cost goal (1985) of another ~$17 per m^2 beyond the input Si material cost is the allowance for production of large areas of single-crystal Czochralski-grown wafers of appropriate size and thickness, or of dendritic web or ribbon of feasible dimensions, or of deposited Si layers of appropriate dimensions on a suitable substrate material (and including the cost of the substrate). Another ~$17 per m^2 is allotted as the 1985 cost goal for fabrication of large-area arrays of Si cells from this sheet material (in whatever its form), and includes the actual cell and/or array fabrication processes such as junction or barrier formation, contacting, interconnecting, bonding, encapsulating (as needed), and testing.

*The question of available supplies of Ga is discussed in Section 2.5.3

Because of the variation in the amount (i.e., number of grams) of photovoltaic material required for various types of solar cells of a given solar conversion efficiency, caused by differences in optical properties from material to material or by variations in the amount of the material required (for structural integrity or other reasons) among different physical configurations of a given semiconductor, it is necessary to examine relative materials costs on a unit area basis. For Si solar cells the relationship between Si material cost per m^2 and the thickness of the Si involved in the completed cell structure is shown in Figure 2-36 for both the present cost (~$60 per kg) and the 1985 LSSA Project cost goal (~$10 per kg) for polycrystalline Si input material of semiconductor (or eventually "solar cell") grade.

Thus, the input material cost associated with a 6 μm layer of Si is $0.84 per m^2 in terms of present prices and $0.14 per m^2 in terms of the 1958 cost goals. A 100 μm layer - a more realistic thickness for a Si solar cell - corresponds to a material cost of $13.98 per m^2 at present prices and $2.33 per m^2 at $10 per kg, while the costs for a 200 μm (8 mil) thickness are $27.96 and $4.66 per m^2, respectively. The 1985 goal of $50 per peak kw, which amounts to $50 per m^2 for a 10 percent AM1 (terrestrial) array efficiency, allows up to $16 per m^2 for the input Si material cost, as indicated earlier. The projected Si material cost in thin films, layers, or wafers is clearly less than this and is a small portion of the allowable total array cost of $50 per m^2.

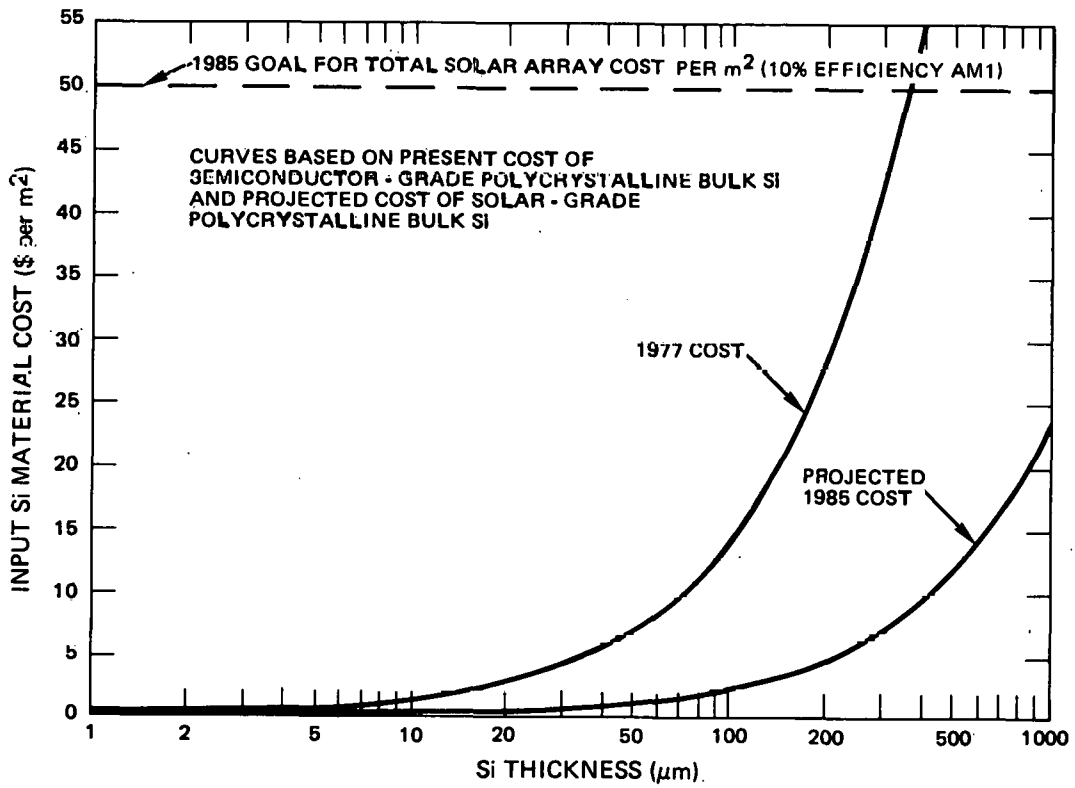

Figure 2-36. Present and Projected Si Material Costs for Si Solar Cells of Various Thicknesses

It is difficult to identify exactly corresponding costs in the same three categories – input material, large-area sheet fabrication, and cell/array fabrication – for GaAs because of significant differences in the input materials and in processing and fabrication techniques. However, it is possible to designate a GaAs input materials cost range, somewhere within which must fit the figure for GaAs that corresponds to the $0.06 per g present cost for semiconductor-grade polycrystalline Si. The upper limit of this range may be taken as the ~$7 per g present cost of high-quality single-crystal GaAs ingot material, and the lower limit may be considered to be the combined cost of 0.48 g of ultrahigh-purity Ga metal and 0.52 g of ultrahigh-purity As metal (the proportion in which they occur in GaAs) at their present separate costs, or ~$0.70 per g – an order of magnitude smaller than the upper limit. Note that this range is from one to two orders of magnitude larger than the present cost per unit weight of semiconductor-grade polycrystalline Si. This difference in cost per unit weight is not surprising in view of the vast differences in technology development, applications history, present market volume, and material abundance in the two cases.

It has evidently been accepted that the projected decrease in Si materials costs by a factor of at least 6 by 1985 (LSSA Project goal) is reasonable. If now it is assumed that the same diligence in technical development and the same large-market motivation that are expected to exist for Si cell material technology will also prevail in GaAs cell material technology in this same time period, then it may also be reasonable to project a similar factor reduction in GaAs cell input materials costs by 1985 – say to a range from $0.10 to $1.00 per g.* The lower end of this suggested range is not greatly different from the present actual cost per gram ($0.06) of semiconductor-grade polycrystalline Si.

The two GaAs input material cost ranges constructed above – one in terms of present costs and one projected (with assumptions) for 1985 – have been converted to cost per m^2 for the same range of semiconductor thicknesses as used for the Si plots in Figure 2-36. The results are shown in Figure 2-37. Because of the density differences (2.33 g/cm^3 for Si and 5.32 g/cm^3 for GaAs), a given thickness of GaAs is ~2.3 times heavier than the same thickness of Si.

As shown in the figure, a 6 μm layer of GaAs has an associated input materials cost of from $22.34 to $223.44 per m^2 in terms of the present price range identified above, and from $3.19 to $31.92 per m^2 in terms of the suggested 1985 cost goals. Similarly, the figures for a 100 μm thickness are $372.40 to $3724 per m^2 for present prices and $53.20 to $532 per m^2 at the projected 1985 level.

When the important allowance is made for the difference in optical absorption properties of Si and GaAs in the region of the solar spectrum some of the apparent materials cost discrepancy between Si and GaAs as represented by Figures 2-36 and 2-37 is greatly reduced. Absorption coefficient data indicate that about 90 percent of the usable solar radiation is absorbed in a ~100 μm layer of Si, but a thickness of only about 2 μm of GaAs is required to absorb the same percentage of the solar radiation usable by a GaAs cell. In other terms, calculation of an idealized short-circuit current for Si and GaAs cells, based on the assumptions of single-pass illumination and transmittance normal to the surface, unity quantum efficiency, and perfect collection efficiency, shows that for AM1 illumination very little additional

*See, however, the discussions in Section 2.5.3, 2.5.4, and 2.5.6.

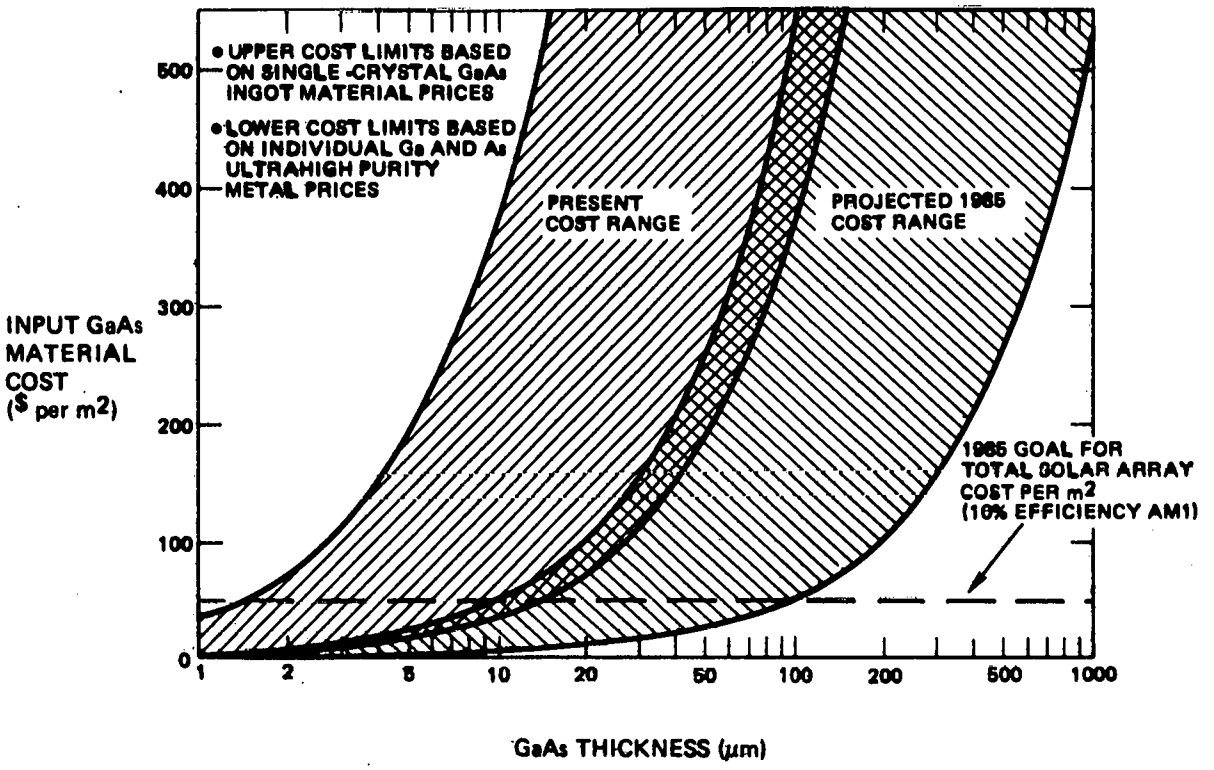

Figure 2-37. Present and Projected Range of Input Material Costs for GaAs Layers of Various Thicknesses

response results for GaAs thicknesses over ~6 μm, while significant additions to the response continue in Si for thicknesses up to 300 μm or more.

The significance of these differences is illustrated in Figure 2-38, which combines the data of the two preceding figures in a full logarithmic plot and shows as shaded areas the approximate thickness regions for Si and GaAs that should be addressed in comparing materials costs. What this figure shows is that for the amount of the semiconductor actually required for the active region of a solar cell of comparable properties in the two cases there is far less than the usually considered material cost difference per unit area of cell, even in terms of current prices. It further shows that if GaAs were subjected to the same kind of input material cost reduction effort as is planned for Si over the next 8 - 10 years then input material costs for the required amount of active semiconductor could actually be quite similar in the two cases.

Clearly there are several assumptions involved in constructing and interpreting Figure 2-38 that are susceptible to serious challenge, but the main purpose in presenting the data in this manner is to emphasize that cost goals for GaAs similar to those already established for Si – and the achievement of those goals – would make GaAs a serious cost competitor in terms of input materials costs alone.

The remaining two cost categories for which 1985 goals have been established for Si solar arrays for terrestrial use – namely, large-area sheet fabrication and cell/array fabrication – can probably be applied with acceptable validity to GaAs solar array fabrication as well. Although details of sheet, cell, and array processing and

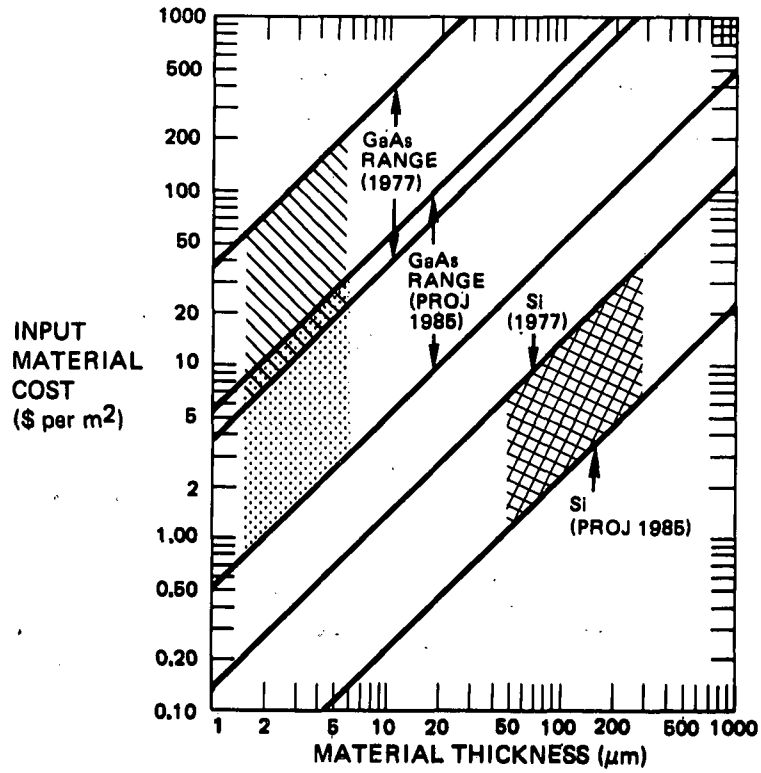

Figure 2-38. Comparison of Present and Projected Input Materials Costs for Si and GaAs Layers of Various Thicknesses

fabrication will surely vary, perhaps extensively, between the two materials, it appears that a cost goal of an additional ~$17 per m^2 value added for each of these two cost categories should also constitute an acceptable target for GaAs solar cell technology for the 1985 time period.

It is obvious that there is no long-established manufacturing process in existence at the present time for GaAs solar cells corresponding to that typical of Si cell production, on which to build a systematic program of automation, process improvement, and cost reduction such as in progress for Si cells. However, as indicated earlier it will be necessary for GaAs cell production to at least approach the same goals as Si cell production is expected to reach if the former is to become competitive in terrestrial array applications. On that basis, the ~$17 per m^2 cost goals are being invoked for GaAs sheet production and for GaAs array fabrication in the considerations of this contract work.

2.5.3 Material Requirements and Available Supplies and Resources

The preceding discussion does not examine the actual amount of GaAs required for solar cells and arrays meeting the 1985 and 2000 production goals of the National Photovoltaic Conversion Program, nor does it make any allowance — in considering input materials costs — for the fact that GaAs cells almost surely will involve GaAℓAs alloys in part of their construction, thus reducing (with respect to GaAs itself) the weight, the cost, and the amount of Ga metal required in a given thickness of material. These questions are addressed briefly in this section, together with a summary of available information on supplies, resources, and reserves of Ga throughout the world.

Figure 2-39a shows the amount of Ga metal involved per m^2 in various thicknesses of GaAs, $Ga_{0.1}A\ell_{0.9}As$, and $Ga_{0.2}A\ell_{0.8}As$. Figure 2-39b shows similar

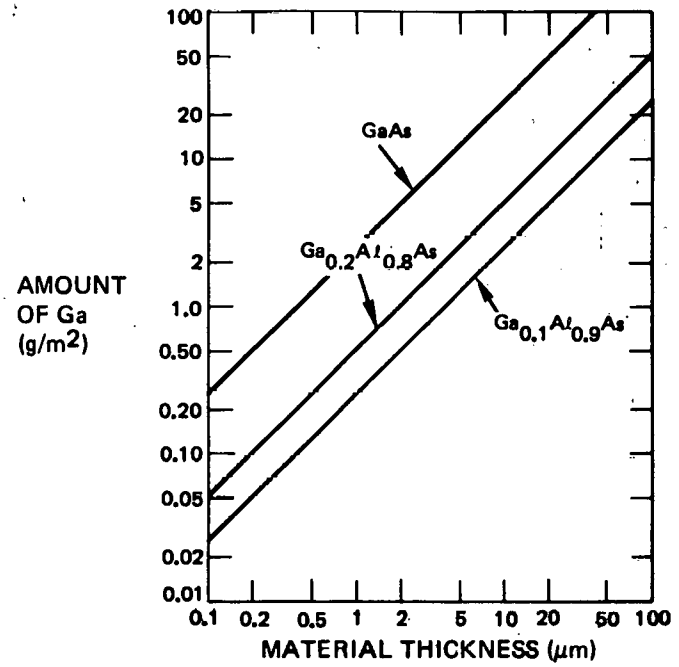

(a)

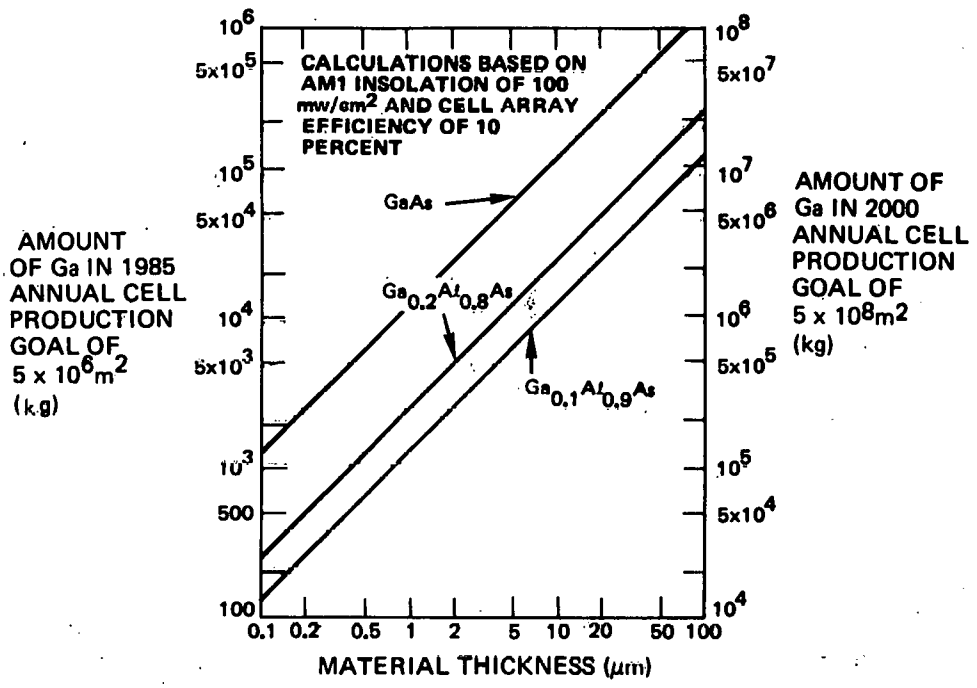

(b)

Figure 2-39. Amount of Ga Metal Involved in Various Thicknesses of GaAs and GaAlAs Alloys. (a) Amount of Ga per m^2; (b) Amount of Ga Required in Annual Production Goals for Years 1985 and 2000

information but for the total amounts of Ga metal involved in the ERDA annual solar cell array production capacity goals for the years 1985 and 2000, based on the assumptions of 10 percent array efficiency and solar insolation of 100 mw/cm^2 (AM1). These figures simply serve to illustrate graphically the amount of Ga metal involved in GaAs and GaAℓAs layers of thicknesses of interest for terrestrial photovoltaic applications. The data given in the figures will be used in subsequent discussion.

2.5.3.1 Material Requirements of GaAℓAs/GaAs Thin-Film Heterostructure Cells

Before the complex question of the availability of Ga metal in national (and world) supplies and resources is addressed, the two conceptual device designs defined in Section 2.5.1 and Figure 2-35 will be examined in terms of their material requirements. Table 2-5 lists the individual component regions of the two cell designs together with the tentatively established thickness of each region and the corresponding amount of each material incorporated in the structure, expressed in g/m^2. Also listed in the table, with its corresponding dimensions and material requirements, is the experimental epitaxial three-layer GaAℓAs/GaAs solar cell (~13 percent AM0, no AR coating) made by MO-CVD and described in Section 2.4.1 and Figure 2-26 of this report. This cell is a special case of design No. 1, with a single-crystal wafer of n-type 0.001 ohm-cm (100)-oriented Si-doped GaAs serving as the substrate and the backside contact being applied on the underside of this substrate rather than at the interface of the n-type GaAs base region and the substrate, as was shown for design No. 1 in Figure 2-35a.

As shown in the table, the two conceptual designs require GaAs total layer thicknesses of 5.5 and 4.5 μm, respectively, and $Ga_{0.1}A\ell_{0.9}As$ window layer thicknesses of 0.5 and 1.5 μm, respectively.* These thicknesses correspond to Ga metal requirements of 14.1 and 11.6 g/m^2, respectively, in the GaAs layers and 0.13 and 0.39 g/m^2, respectively, in the alloy window layers (see Figure 2-39a), or a total Ga metal requirement of 14.2 g/m^2 for design No. 1 and 12.0 g/m^2 for design No. 2. This calculation, of course, is independent of the specific methods used for producing the structures and makes no allowance for various process yields or unavoidable material waste, and simply indicates the amount of Ga actually incorporated in the two composite structures.

The 1985 annual production capacity goal of 5×10^6 m^2 of 10-percent-efficient solar cell arrays thus would require a minimum of 7.1×10^4 kg (71 metric tons) of Ga metal for design No. 1 and 6.0×10^4 kg (60 metric tons) for design No. 2, while the 2000 annual production capacity goal of 5×10^8 m^2 of such cell arrays would require at least 7100 and 6000 metric tons of Ga, respectively, for the two conceptual designs.

The experimental epitaxial three-layer cell, on the other hand, involves not only the two GaAs layers and the alloy ($Ga_{0.2}A\ell_{0.8}As$) layer but also the 375 μm GaAs single-crystal substrate. The total Ga metal requirement for such a structure would thus be ~980 g/m^2. This corresponds to 4.9×10^6 kg (4900 metric tons) of Ga metal required for the 1985 annual production capacity goal and 4.9×10^8 kg (490,000 metric tons) for the 2000 annual production goal.

*A thicker window layer is used in design No. 2 to remove the p-n junction (in the GaAs) farther from the GaAℓAs-substrate interface because of the higher density of defects expected at that interface and to permit use of a thinner contact grid at the interface.

Table 2-5. Materials, Dimensions, and Masses Involved in Two Basic Conceptual Designs and Experimental Epitaxial Thin-film Solar Cell of GaAℓAs/GaAs Window-type Heterostructure

	CONCEPTUAL DESIGN NO. 1† (OPAQUE SUBSTRATE)			EXPERIMENTAL ALL-EPITAXIAL THREE-LAYER GaAℓAs/GaAs CELL*			CONCEPTUAL DESIGN NO. 2† (TRANSPARENT SUBSTRATE)		
COMPONENT/REGION OF CELL	MATERIAL	THICKNESS (μm)	MASS (g/m^2)	MATERIAL	THICKNESS (μm)	MASS (g/m^2)	MATERIAL	THICKNESS (μm)	MASS (g/m^2)
1. Substrate	Glass sheet	375	937.5	GaAs (single-crystal n-type Si-doped wafer)	375	1995.	Glass Sheet	375	937.5
2. Base Region Contact	Mo layer (full coverage)	0.5	5.1	Au-12% Ge alloy layer (full coverage, on underside of substrate wafer)	0.2	2.9	Au-12% Ge alloy layer (full coverage)	0.5	7.4
3. Active Base Region	GaAs film (n-type, Se-doped)	5	26.6	GaAs film (n-type, Se-doped)	5.	26.6	GaAs film (n-type, Se-doped)	4	21.3
4. Front Layer of Cell	GaAs film (p-type, Zn-doped)	0.5	2.7	GaAs film (p-type, Zn-doped)	1.5	8.0	GaAs film (p type, Zn-doped)	0.5	2.7
5. Window Layer	$Ga_{0.1}A\ell_{0.9}As$ film (p-type, Zn-doped)	0.5	1.9	$Ga_{0.2}A\ell_{0.8}As$ film (p-type, Zn-doped)	0.05	0.20	$Ga_{0.1}A\ell_{0.9}As$ film (p-type, Zn-doped)	1.5	5.8
6. Front Contact	Ag-2% Zn alloy square grid (5% area coverage)	1.0 (50μm linewidth)	0.52	Au-Zn-Au square grid (10% area coverage)	~0.4	0.54	Ag-2% Zn alloy square grid (5% area coverage)	0.5 (50μm linewidth)	0.26
7. Antireflection Coating**	-	-	-	-	-	-	-	-	-
TOTALS (Approx)		382.5	974.3		382.2	2033.2		382.0	975.0

†All dimensions (and masses) tentative.
*See Section 2.4.1 and Figure 2-26 for details
**AR coating is omitted from this tabulation

2.5.3.2 Worldwide Ga Production to Present Time

It is instructive to examine these minimum requirements in terms of available Ga supplies and known or projected resources. Ga is more abundant than is widely believed, occurring in the earth's crust in roughly the same concentration as elements such as Pb, As, and Mo – about 10-15 g per metric ton (or ppm). The difficulty is that it does not occur as the free metal or even as the major constituent of minable ores but instead is widely dispersed, in numerous different naturally occurring materials, and is a minor constituent in all cases (at most 0.5-1.0 percent in even the richest ores, and usually orders of magnitude less concentrated). Thus, its recovery has been mainly as a byproduct operation, primarily in the processing of Aℓ and Zn ores. (Ga is always found together with either Zn, or Aℓ, or Ge.) The value of the principal metals (Aℓ and Zn) sought in these ores has been so much greater than that of Ga that more attention has been given to removing Ga as an "impurity" than to improving methods for recovering it. Demand has not been sufficient, to date, to remove it from this status. Production is still determined by the amount that can be sold; that is, supply exceeds demand.

Estimates of annual Ga metal production to the present time, together with an indication of approximate corresponding prices, are given in Table 2-6. These data show a very slow rate of growth of annual Ga production since it was first produced commercially in the first quarter of this century. Estimated worldwide production in 1976 was about 15 metric tons, with a corresponding price of $600-650 per kg, although the estimated worldwide production capacity in that year was 26-35 metric tons (Ref 20).

The richest known Ga-bearing ore is South African germanite, a Ge ore that may contain as much as 1 percent of Ga, but it is so scarce as to provide no impact on potential supplies (Ref 18). Most Zn ores, especially sphalerites, and certain Cu and Pb ores contain Ga in weight concentrations ranging from 0.001 percent to as much as 0.1-0.2 percent in exceptional cases, with the concentration varying greatly with location and type of deposit. Ga is also found in many coals in various parts of the world, in concentrations typically 0.001-0.005 percent, and coal fly ash has been found in some instances (especially England) to bear recoverable concentrations of from 0.001 to as much as 0.1 weight percent Ga. Even some mineral water and sea water has been found with measurable Ga concentrations.

2.5.3.3 Potential Worldwide Ga Supplies from Bauxite and from Aluminum Industry Growth

By far the most significant sources of Ga are the Aℓ-bearing ores, especially bauxite. Typically, bauxite and other Aℓ ores contain Ga in concentrations of 0.002 to perhaps as much as 0.010 percent by weight. Even with this dilute grade, the present huge annual production of Aℓ and the expected continued growth of this industry using bauxite provides the best opportunity for expanded recovery and production of Ga metal.

As pointed out by Weeks (Ref 19), the available data on Ga content in various specific ores mined primarily for other metals are scarce, since most processors have not maintained accurate records for minor constituents over the years. However, the variation in "byproduct" concentrations in ores is not as significant as the details of the processing technologies used in recovering the primary material, since these details determine if the secondary materials, such as Ga, are concentrated or are made even more dilute in the byproduct "waste" in which they reside.

Table 2-6. Estimated Annual Production and Corresponding Approximate Prices for Ga Metal in Past Years*

Year	Estimated Annual Production (kg)		Approximate Price† ($ per g)
	United States	Total World	
1930-1940	–	~50 total prior to 1940[a]	50.00
43	<10	–	–
44	<10	–	–
45	<10	–	–
46	<10	–	–
47	<10	–	–
48	90	–	4.50
49	0	–	–
1950	–	–	4.50
51	90	–	–
52	0	–	3.50
53	–	–	3.25
54	–	–	3.25
55	–	–	3.25 (4.25)[b]
56	–	~50[a]	3.25
57	–	–	3.25
58	–	–	–
59	90	–	–
1960	–	–	3.80[b]
61	–	–	–
62	–	>1000[a]	–
63	–	–	0.95-1.40
64	–	–	–
65	–	~5000 total prior to 1965	2.75[b]
66	–	–	–
67	–	–	–
68	100-300	800-1000	0.60-1.75
69	–	–	–
1970	–	–	0.85[b]
71	–	~1000[b]	0.75
72	–	–	–
73	–	–	0.75[b]
74	–	–	–
75	–	–	–
76	– (10,000-12,000[c])	~15,000[b] (26,000-35,000[c])	0.60-0.65[b]

*Data from Ref 19 unless otherwise specified.

†High purity metal, but not necessarily "electronic grade" except where indicated.

[a]Ref 18.

[b]Ga of six 9's purity (Ref 20).

[c]Estimates of Ga production capacity, not actual Ga production (Ref 20).

For the case of Ga in bauxite, fortunately, the Bayer process that is used in extracting Aℓ from the ore retains the Ga oxide along with the Aℓ oxide, so that selective precipitation, re-solution and electrolysis can extract the Ga metal – typically at ~99.5 percent purity prior to further purification (Ref 20).

An indication of the potential supply of Ga metal can thus be obtained from examination of present and projected supplies of bauxite. Four countries – Australia, Jamaica, Guinea, and Surinam – now produce about 60 percent of the world's supply of bauxite, the production of which (along with Aℓ use) has increased 8-9 percent annually for the past 10-15 years (Ref 20). The total bauxite production in these four countries plus France, Brazil, Guyana, the United States, and the entire world for the past 20 years is shown in Table 2-7. Note the rapid growth of Australia and Guinea as major sources. Jamaica, now the second largest producer, accounts for ~60 percent of the bauxite imported by the United States.

As indicated in the table, the total world production of bauxite in 1974 contained an estimated 3928 metric tons of Ga, of which less than 1 percent was actually recovered and marketed (see Table 2-6). It should be noted that this estimated Ga content in the 1974 worldwide bauxite production is 55 to 65 times the Ga requirements for the 1985 annual production goal for the two conceptual cell designs and 55-65 percent of the Ga requirements for the annual production goal for the year 2000 for these cell designs. It has been estimated (Ref 20) that about 15,920,000 metric tons of bauxite were processed in the United States in 1974, with a total estimated Ga content (not all recovered) of 994 metric tons, or approximately 25 percent of the estimated total Ga content in bauxite produced worldwide that year.

The U. S. Bureau of Mines and the Aluminum Corporation of America have made estimates of bauxite and Ga reserves and resources, based on known ore deposits and typical Ga contents, and these data are given in Table 2-8 (Ref 20) for the same countries that were listed in Table 2-7, along with the estimated world total. The conservatively estimated 1.7×10^{10} metric tons of worldwide bauxite reserves are expected to last for 55-70 years, based on presently projected cumulative demand for about 21 percent of this reserve in the next 25 years – a projection that does not include large-scale use in photovoltaic systems.

The projected future production of bauxite in these same countries, based on Stanford Research Institute estimates (quoted in Ref 20), is also given in Table 2-8 to the year 2000. If the U. S. production is arbitrarily set at 1.5×10^6 metric tons for each of the three years given (U. S. production is actually expected to decrease with respect to its present level over the next 25 years) then the projected totals for the eight countries are 80.5, 123, and 218.5 million metric tons for the years 1980, 1990, and 2000, respectively. These figures are to be compared with 55.7 million metric tons produced in these same countries in 1974 and estimated current worldwide production of 70-80 million metric tons (Table 2-7).

If the same average Ga content is assumed for this projected bauxite production as was used in determining the Ga content associated with bauxite reserves in these countries (Table 2-8) then the projected total associated Ga available in the bauxite to be produced in the eight countries in 1980, 1990, and 2000 would be approximately 3890, 5940, and 10,550 metric tons, respectively. If it is further assumed that the eight countries continue to produce the order of 75 percent of the total world output

Table 2-7. Bauxite Production Totals*
(Thousands of metric tons)†

Country	1955	1960	1965	1970	1974	1975
Australia	7.7	70.5	1186.4	9256.3	20,057.0	-
Jamaica	2687.8	5837.0	8651.0	12,009.7	15,328.4	-
Guinea	493.2	1378.0	1600.0	2490.0	6096.3	-
Surinam	3061.9	3455.0	4360.0	6022.0	5461.1	-
Guyana	2474.4	2510.8	2918.7	4417.2	3048.1	-
France	1493.6	2067.3	2663.8	3050.7	2909.4	-
Brazil	45.1	120.8	188.0	509.8	800.0	-
United States	1817.0	2030.1	1680.5	2115.4	1997.6	1830.8[a]
Total	12,080.7	17,469.5	23,248.4	39,871.1	55,697.9	-
World Total	17,760.4	27,620.1	37,291.5	59,483.8	77,794.7 (3.928)**	72,136[a]

*Ref 20 unless specified otherwise.

†Production totals represent gross weights, without allowance for composition variations.

**Estimated total Ga content in total bauxite produced in 1974; represents possible Ga production - not actual production.

[a]Preliminary estimates from The Statistical Abstract of the United States 1976 Edition (issued December 1976), Bureau of the Census, Department of Commerce, Washington, D.C.

Table 2-8. Estimated Reserves and Resources of Bauxite and Associated Ga* and Projections of Future Bauxite Production
(Thousands of metric tons)

Country	Bauxite		Ga		Projected Bauxite Production†		
	Reserves	Resources (incl. Reserves)	Reserves	Resources (incl. Reserves)	1980	1990	2000
Australia	4.5×10^6	6.0×10^6	270	360	30,000	55,000	80,000
Jamaica	1.0×10^6	1.2×10^6	60	72	20,000	26,000	30,000
Guinea	4.5×10^6	5.0×10^6	135	150	12,000	20,000	80,000
Surinam	0.5×10^6	1.0×10^6	40	80	7000	9000	10,000
Guyana	0.15×10^6	0.30×10^6	4.5	15	5000	5000	5000
France	0.06×10^6	0.25×10^6	2.4	10	3000	2500	2000
Brazil	2.5×10^6	5.0×10^6	125	250	2000	4000	10,000
United States	0.04×10^6	0.35×10^6	2.8	24.5	1500**	1500**	1500**
Total	1.325×10^7	1.910×10^7	639.7	961.5	80,500	123,000	218,500
Other	3.750×10^6	1.040×10^7	145	432.3	-	-	-
World Total	1.700×10^7	2.950×10^7	784.7	1393.8	-	-	-

*Ref 20 unless specified otherwise

†Stanford Research Institute estimates quoted in Ref 20.

**Arbitrary figure; U.S. production is expected to decrease in next 25 years relative to 1975 output.

of bauxite (the percentage ranges from 62 to 72 percent for the years given in Table 2-7) then the projected worldwide production would be ~107, ~164, and ~291 million metric tons in 1980, 1990, and 2000, respectively. This corresponds to about 4940, 7580, and 13,440 metric tons of associated Ga, respectively, that would be potentially available in those years. The situation is summarized in the upper portion of Table 2-9 (lines 1 through 5).

From another point of view, a measure of the possible future growth in Ga production can be obtained from a consideration of the present status and expected growth of the Aℓ industry itself and its dependence upon bauxite ore processing. If a reasonably conservative expansion in Aℓ production (based on past growth and present trends) of about 6 percent per year over the next 25 years is projected, and if the worldwide bauxite production for 1974 (Table 2-7) is used as the reference base for this growth, then a separate projection of Ga available from bauxite in future years can again be made. Using for the relationship between available Ga

Table 2-9. Annual Ga Requirements for Annual Cell Production Capacity Goals* for Years 1985 and 2000 for Two Conceptual Cell Designs and Experimental MO-CVD GaAℓAs/GaAs Cell, and Potential Annual Ga Supplies from Projected Bauxite Production and Aℓ Industry Growth

	Annual Amount of Ga (metric tons)				
	1980	1985	1990	1995	2000
Ga Requirements*					
1. Cell Design No. 1	–	71	–	–	7100
2. Cell Design No. 2	–	60	–	–	6000
3. Experimental MO-CVD Thin-film Cell	–	4900	–	–	490,000
Ga Supplies Available in Bauxite					
Production projections for bauxite ore†					
4. Eight Countries (incl. U.S.)	3890	–	5940	–	10,550
5. World Total	4940	–	7580	–	13,440
Production projections for Aℓ **					
6. World Total	5330	7130	9540	12,780	17,090
Ga Economically Recoverable**					
World Total					
7. Present technology (40%)††	2130	2850	3820	5110	6840
8. Improved technology (80%)††	4260	5700	7630	10,220	13,670

*Based on assumption of 10 percent array efficiency and 100 mw/cm^2 (AM1) solar insolation.
†Based on projected bauxite ore production, as in Table 2-8 and text.
**Based on projected 6 percent annual growth of Aℓ production; see text.
††See text.

and the parent bauxite ore a ratio that is the average of the ratio used in calculating world reserves (Table 2-8) and the ratio for the reference year of 1974 (Table 2-7), the projected data for Ga available annually given in line 6 of Table 2-9 are obtained. Although these projections are somewhat larger in a given year than those based specifically on worldwide bauxite ore production (line 5) the two sets of data are really quite similar.

2.5.3.4 Expected Normal Growth in Ga Demand

The projected demand for Ga metal for the next 20-25 years, without the impact of large-scale photovoltaic applications, is expected to consist primarily of its use in GaAs, GaP, and GaAsP for LED's in digital displays, for other optoelectronic devices, for microwave power transistors, and for garnet magnetic-bubble memory devices. Market growth will probably be the order of ~15 percent per year, increasing the annual Ga demand to 50-100 metric tons per year by about 1985, with essentially no change in the technology of Ga recovery and relatively little change in prices (Ref 20). Thus, in the absence of any new outside stimulus, total Ga production to meet projected non-photovoltaic market demands may just about equal the calculated minimum requirements for Ga metal in either of the two conceptual cell designs for the year 1985 (lines 1 and 2, Table 2-9).

The possibility of expansion of future Ga production beyond this predicted growth is dependent on changes in present technology for Ga extraction and on major changes in worldwide demand. Present technology for Ga recovery from bauxite could extract about 40 percent economically, but an increase to ~80 percent economical recovery is regarded as possible with adequate development and capital investment (Ref 20).

Lines 7 and 8 of Table 2-9 show the projected annual amounts of recoverable Ga for these two levels of technology applied to the projected worldwide totals for Ga available annually as listed in line 6 of the table. It is important to emphasize, however, that growth of Ga production as illustrated in lines 7 and 8 — as distinct from growth of Aℓ production, which is based on established trends and foreseeable demands — is not expected to occur in the absence of an external stimulus. This stimulus would presumably be in the form of outside funding to assure the needed capital investments and technology development (Ref 20).

The question of projected costs of Ga under the conditions of such an expanded market is considered briefly in Section 2.5.6.

2.5.3.5 Conclusions Concerning Ga Availability for Photovoltaic Applications

The data of Table 2-9 lead to the following conclusions:

1. There appears to be more than enough economically recoverable Ga worldwide in bauxite ores to meet the 1985 annual production requirements for GaAs solar cell arrays involving either of the conceptual cell designs (lines 1, 2), using present-day recovery technology (line 7).

2. There is also more than sufficient projected recoverable Ga in bauxite in just the eight countries identified in Tables 2-7 and 2-8 (line 4 of Table 2-9) to meet these same 1985 requirements for Ga in the two conceptual cell designs, again based on present recovery technology.

3. With technology improvements (line 8) there is even enough recoverable Ga worldwide to exceed slightly the Ga metal requirements of the experimental epitaxial cell (line 3) – which involves a single-crystal GaAs substrate wafer – in the quantities specified by the 1985 annual production goal.

4. The annual Ga requirements for the two conceptual cell designs (lines 1, 2) for the year 2000, however, are approximately the same as the projected recoverable Ga amount worldwide for that year based on use of present technology (line 7). If the improved recovery (80 percent) technology is applied (line 8) then the projected recoverable Ga amount exceeds the amount required by the program goal for that year for either cell design by a factor of about 2 — a comfortable margin. (It has been suggested (Ref 20) that a "secure source" of Ga in the range of 8000 metric tons per year appears assured for the 1990-2000 time period.)

5. Not surprisingly, the Ga requirements for the experimental epitaxial cell in quantities corresponding to the production capacity goal for the year 2000 (line 3) far exceed even the projected total annual worldwide supply of available Ga that year (lines 5, 6), no matter what recovery technology is involved. This apparently eliminates such an "all-GaAs" structure from further consideration in the context of the long-range goals of the National Photovoltaic Conversion Program unless concentrator systems are employed.

It must be remembered that all of the above considerations except for the introduction of the Ga recovery efficiency factor (lines 7, 8 of Table 2-9) neglect any matters of process yield, material loss, material reclamation and recycling, and other similar factors. Only the actual amount of Ga involved in the finished cell structures, on the one hand, and the probable maximum amount of Ga projected to be available, on the other hand, have been compared.

Obviously these other factors must be introduced before final conclusions are reached, at least for the case of the annual cell production goals for the year 2000. In that instance, since the projected Ga requirement and the projected Ga supply are similar in magnitude (lines 1, 2, 7, 8 of Table 2-9), any overall change in the ultimate supply of recoverable Ga, any change in the efficiency of utilization of Ga in producing the cell structures, any cell design changes, or any variation in array conversion efficiency with respect to the assumed value (10 percent) will have a significant effect on whether the annual Ga supply is really adequate for both the conventional and the large-scale photovoltaic markets at that time.

However, since there is a factor of from 40 to 95 difference in the Ga requirements and the projected Ga supply for 1985 it does appear that no problem of material availability should arise in that case, even when allowances are made for the important considerations that have been omitted in this preliminary analysis.

The entire subject of reclamation and recycling of unused or "wasted" Ga and Ga compounds has been neglected in this discussion. As the demand for Ga increases, the importance of developing efficient Ga reclamation technologies will also increase. The successful development of such processes will improve considerably the overall efficiency of utilization of future Ga supplies. Such changes can, of course, have a major impact on the problems considered here.

2.5.4 Materials Costs for MO-CVD Thin-film Cells

The materials costs associated with the two conceptual solar cell design structures described in Section 2.5.1 (and shown schematically in Figure 2-35) and also with the experimental epitaxial three-layer GaAlAs/GaAs cell described in Section 2.4.1 are examined in this section from three points of view.

First, the costs of the materials actually incorporated in the cells (i.e., "materials content values") are calculated on the basis of the amounts of materials included in the various regions of the three structures as listed in Table 2-5. Current prices for these materials in the purities required for solar cells are used for these calculations.

Next, the costs of the minimum quantities of the principal reactants required for producing the cell structures by the MO-CVD process are calculated for each of the three cell configurations, again using current market prices. To these are added the costs of the "add-on" materials (specifically contacts) as derived in the first calculations mentioned above, to obtain a second estimate of the total cost of materials.

Finally, the determination of the actual total materials costs involved in producing thin-film cells by the MO-CVD process is addressed briefly, although compilation of a final detailed estimate of such costs has been postponed to a later phase of the program.

Approximate quantities of the various high-purity materials incorporated directly in the structures of the two conceptual designs and the experimental window-type cell were given in Table 2-5, for a cell area of 1 m^2. Approximate costs for these materials at the present time, in the purities required for this application and purchased in moderate quantities, are given in Table 2-10.

In several instances two different costs are given for the same material (columns A and B for each cell structure). The value given in column A is based on the costs of the individual component materials involved, without regard for the particular material combination in use or for the process by which the material is incorporated into the cell structure. The second value (column B) is simply the present market price for that particular composite material, in the appropriate purity and form, if in fact it is available commercially so that such a cost figure can be obtained. The costs given in columns A and B for GaAs (regions 3 and 4) are the costs identified in the general discussion of cost goals in Section 2.5.2.

When these data are applied to the material requirements of Table 2-5 a measure of the total cost of materials incorporated in the three cell structures is obtained. These results are shown in Table 2-11, in columns A and B for each structure. The costs of the functional regions of the three cells are totaled separately from the substrate costs.

The costs given in column A are essentially the same as those given in Table 2-5 of Quarterly Report No. 2 (Ref 9) for the two conceptual designs, except for several changes in the substrate and the base region contact specifications. The data in column B have not been presented before. The totals given in columns A and B serve to define a range of the materials costs per m^2 of cell area, for the experimental cell as well as for the two conceptual designs.

Table 2-10. Approximate Costs per Gram for Materials Incorporated in Structures of Two Basic Conceptual Designs and Experimental Epitaxial Solar Cell of GaAℓAs/GaAs Window-type Heterostructure

	CONCEPTUAL DESIGN NO. 1 (OPAQUE SUBSTRATE)			EXPERIMENTAL ALL-EPITAXIAL THREE-LAYER GaAℓAs/GaAs CELL			CONCEPTUAL DESIGN NO. 2 (TRANSPARENT SUBSTRATE)		
COMPONENT/REGION OF CELL	Material	COST ($ per g)		MATERIAL	COST ($ per g)		MATERIAL	COST ($ per g)	
		A†	B*		A†	B*		A†	B*
1. Substrate	Glass sheet (Corning Code 0317.)		0.015	GaAs (single-crystal n-type Si-doped wafer)	0.70	7.00	Glass sheet (Corning Code 0317)	-	0.015
2. Base Region Contact	Mo layer (full coverage)	0.16	-	Au-12% Ge alloy layer (full coverage, on underside of substrate wafer)	3.62	11.00	Au-12% Ge alloy layer (full coverage)	3.62	12.00
3. Active Base Region	GaAs film (n type, Se-doped)	0.70	7.00††	GaAs film (n type, Se-doped)	0.70	7.00††	GaAs film (n-type Se-doped)	0 70	7.00††
4 Front Layer of Cell	GaAs film (p-type, Zn doped)	0.70	7.00††	GaAs film (p type, Zn-doped)	0.70	7.00††	GaAs film (p-type, Zn-doped)	0.70	7.00††
5 Window Layer	$Ga_{0.1}Al_{0.9}As$ film (p-type, Zn doped)	0.62	-	$Ga_{0.2}Al_{0.8}As$ film (p-type, Zn-doped)	0.63	-	$Ga_{0.1}Al_{0.9}As$ film (p-type, Zn-doped)	0.62	-
6. Front Contact	Ag-2% Zn alloy square grid (5% area coverage)	0.15	6.50	Au-Zn-Au square grid (10% area coverage)	3.31	11.00	Ag-2% Zn alloy square grid (5% area coverage)	0.15	6.50
7. Antireflection Coating**	-	-	-	-	-	-	-	-	-

†Costs in Column A calculated from costs of individual component materials.

*Costs in Column B represent current prices for specific composite materials if commercially available.

††GaAs epitaxial material is not separately priced commercially but it is of quality comparable with that of good single-crystal bulk material, so the price for the latter is used here.

**AR coating omitted from this analysis. (None was used on experimental cell.)

Table 2-11. Approximate Total Costs per m^2 for Materials Incorporated in Structures of Two Basic Conceptual Designs and Experimental Epitaxial Solar Cell of GaAℓAs/GaAs Window-type Heterostructure*

	CONCEPTUAL DESIGN NO. 1 (OPAQUE SUBSTRATE)				EXPERIMENTAL ALL-EPITAXIAL THREE-LAYER GaAℓAs/GaAs CELL				CONCEPTUAL DESIGN NO. 2 (TRANSPARENT SUBSTRATE)			
COMPONENT/REGION OF CELL	MATERIAL	COST ($ per m^2)			MATERIAL	COST ($ per m^2)			MATERIAL	COST ($ per m^2)		
		A†	B†	C††		A†	B†	C††		A†	B†	C††
1. Substrate	Glass sheet (Corning Code 0317)	–	14.06	–	GaAs (single-crystal n-type Si-doped wafer)	1396.50	13,965.00	–	Glass sheet (Corning Code 0317)	–	14.06	–
2. Base Region Contact	Mo layer (full coverage)	0.82	–	–	Au-12% Ge alloy layer (full coverage, on underside of substrate wafer)	10.50	31.90	–	Au-12% Ge alloy layer (full coverage)	26.79	88.80	–
3. Active Base Region	GaAs film (n-type, Se-doped)	18.62	186.20	222.87	GaAs film (n-type, Se-doped)	18.62	186.20	222.87	GaAs film (n-type, Se-doped)	14.91	149.10	178.30
4. Front Layer of Cell	GaAs film (p-type Zn doped)	1.89	18.90	22.29	GaAs film (p-type, Zn doped)	5.60	56.00	66.86	GaAs film (p-type, Zn-doped)	1.89	18.90	22.29
5. Window Layer	$Ga_{0.1}Al_{0.9}As$ film (p-type Zn doped)	1.18	–	15.08	$Ga_{0.2}Al_{0.8}As$ film (p-type, Zn doped)	0.13	–	1.64	$Ga_{0.1}Al_{0.9}As$ film (p-type; Zn doped)	3.60	–	45.24
6. Front Contact	Ag 2% Zn alloy square grid (5% area coverage)	0.08	3.38	–	Au-Zn-Au square grid (10% area coverage)	1.79	5.94	–	Ag 2% Zn alloy square grid (5% area coverage)	0.04	1.69	–
Total** (2 through 6)		22.59	210.48	264.44		36.64	280.17	329.21		47.23	262.09	336.32
Total** (1 through 6)		36.65	224.54	278.50		1433.14	14,245.17	14,294.21		61.29	276.15	350.38

*Based on data of Tables 2-5 and 2-10: excludes AR coating.

**In computing totals for columns A and B, when only one column has an entry for a given region of the structure that entry is used for both columns. Where there is a blank in column C, the larger of the column A and column B entries is used in obtaining the column C tota .

†See Table 2-10 for explanation of cost calculation.

††Costs calculated from cost of reactants TMG, TMAℓ and AsH_3 theoretically required to produce layer.

Another – and partially independent – measure of the materials costs involved in these cell structures can be obtained by consideration of the fundamental chemical reaction that is utilized in the formation of GaAs by the MO-CVD process. The reaction involves the metalorganic compound trimethylgallium (TMG) and the hydride arsine (AsH_3) in a pyrolysis represented by the following expression:

$$(CH_3)_3Ga + AsH_3 \rightarrow GaAs + 3CH_4. \qquad (2\text{-}1)$$

This simplified overall reaction omits the numerous complicated intermediate reaction steps that are known (or believed) to occur. The presence of large concentrations of H_2 or other carrier gas and the role of H_2 in the various intermediate reactions are also not addressed, but the above expression does represent the relationship between initial reactants and final products. The organic byproduct methane (CH_4) is stable at the temperatures normally used for GaAs film deposition by this technique.

A complete (100 percent efficient) reaction of 1 mole (115g) of TMG and 1 mole (77.9g) of AsH_3 would produce 1 mole (145g) of GaAs, according to the expression given. The amount of GaAs required for a layer 1 μm thick is 5.32g per m^2 of layer area. For the moment disregarding the question of how the reaction product (GaAs) would be distributed over such an area by this process, the amount of the two reactants required to produce such a layer would be 4.22g of TMG and 2.86g of AsH_3 per m^2 of GaAs. For a thicker layer the amounts of the reactants required would be proportionately larger.

The GaAlAs alloys are produced by simultaneous pyrolysis of appropriate mixtures of TMG, as indicated above, and of the analogous Al compound trimethylaluminum (TMAl) according to the following simplified reaction:

$$(CH_3)_3Al + AsH_3 \rightarrow AlAs + 3CH_4. \qquad (2\text{-}2)$$

The alloy $Ga_{1-x}Al_xAs$ results from combination of a mole fraction x of AlAs and a mole fraction $y = 1-x$ of GaAs. Just as for GaAs, 1 mole (102g) of AlAs results from the complete reaction of 1 mole (72.0g) of TMAl and 1 mole of AsH_3.

The amount of alloy of composition $Ga_{0.2}Al_{0.8}As$ required for a layer 1 μm thick is 4.06g per m^2, while the amount of $Ga_{0.1}Al_{0.9}As$ required for such a layer is 3.87g per m^2 of layer area. For a completely efficient pyrolysis reaction involving AsH_3 and the appropriate mixture of TMG and TMAl, the formation of the above quantity of $Ga_{0.2}Al_{0.8}As$ would consume 0.844g of TMG, 2.12g of TMAl, and 2.86g of AsH_3, and the formation of the specified quantity of the alloy $Ga_{0.1}Al_{0.9}As$ would require 0.419g of TMG, 2.36g of TMAl, and 2.84g of AsH_3, in each case referred to a layer area of 1 m^2.

It is thus possible to obtain additional estimates of the costs of the semiconductor layers (regions 3, 4, 5) in the three cell structures by determining the minimum amounts of these principal reactants required for producing the specified thicknesses and then applying current market prices for the reactants in these quantities. When this is done, the costs given in column C for each of the structures in Table 2-11 are obtained.

The approximate total materials costs given in Table 2-11 lead to several observations. First, the substrate is the predominant cost-controlling factor in these cell designs. Single-crystal GaAs wafers, such as that used as the substrate for the experimental epitaxial CVD cell (and as the substrate in more conventional GaAlAs/GaAs cells made by the liquid-phase epitaxy method), involve prohibitive costs in terms of present technology for producing such material. Various other substrate materials, however, offer the prospect of eventual low cost per m^2.

For example, high-purity polycrystalline aluminas, such as the ASM805 (as manufactured, not refired) that has been evaluated experimentally in this program, typically cost \$150 – \$775 per m^2 of total area at current prices (for relatively small pieces the order of 25 cm^2 area). Similarly, a high-purity metal such as Mo is expensive in normally fabricated sheet form, although its availability in large areas and its thermal expansion properties make it relatively attractive for the present application. At current prices for sheet 0.05 cm (20 mils) thick, the materials cost for high-purity Mo corresponds to ~ \$350 per m^2. Some low-carbon steels, on the other hand, are available in large-area standard-size sheets in a range of thicknesses down to the thickness being considered here, and the costs for such material are in the range \$1 – \$5 per m^2. The latter materials do not now appear feasible for the application involved here, unfortunately, because of impurity content and thermal expansion behavior.

The glasses still appear to offer the best prospect of achieving substrate costs low enough to permit an overall device design meeting the cost goals as well as the performance requirements for large-area photovoltaic arrays based on thin-film polycrystalline GaAs. There is a wide range of costs represented by the many glasses now being produced commercially, and both the present cost and the eventual cost that might result for a given glass required in large quantity are strongly dependent upon the type of manufacturing process involved, which in turn is in part a consequence of the composition of the particular glass and its desired chemical and physical properties. A typical cost range for some of the commercially available glasses purchased in moderate quantities is \$5 to \$60 per m^2, for standard thicknesses not generally in the range of interest for this application.

Many of the experimental polycrystalline cell structures prepared in this program have involved the use of Corning Code 0317 glass, an alumina soda lime glass with a strain point of 574°C, an annealing point of 622°C, a softening point of 871°C, and an average thermal expansion coefficient (referred to 25°C) of 8.7×10^{-6} per deg C in the range 0-300°C. This glass has been made available for experimental purposes at no charge to the program by the manufacturer (Corning Glass Works). However, for purchase of the glass in experimental quantities the price per m^2 is a strong function of the size of the individual pieces that are supplied; ~ \$45 per m^2 represents an approximate current price for moderate quantities in usable form (with a thickness of 50 – 60 mils). The cost per m^2 given for this glass in column B of Table 2-11 for the two conceptual designs is a proportionately reduced figure, based strictly on the reduced thickness (375 μm) of the substrate in these designs.

It seems a reasonable assumption that the combination of large-scale production methods, such as are used for certain types of glasses in the glass industry (e.g., glass ribbon production and the float-glass process), and large-volume purchases on

a regular basis could result in a drop in the cost per m^2 of this glass by at least one and possibly two orders of magnitude relative to the experimental quantity price given above. A decrease by two orders of magnitude would make such a glass a very practical candidate for use in the low-cost solar cell arrays required for the terrestrial applications of interest here. Such a cost figure for the substrate, the predominant cost-controlling item in the solar cell designs being considered in this program, would make realization of the cost goals of the National Photovoltaic Conversion Program an excellent possibility.

A second observation is that the cost of cell contacts (items 2 and 6 in the table) also covers a wide range, depending upon the contact design and – in particular – upon the materials used. Specifically, contacts involving appreciable amounts of Au are expensive. A reduction in the thickness of a specific contact by a factor of two would reduce the cost significantly, but it would also double the sheet resistance of the contact structure; the effect of this upon the total series resistance of the operating cell would have to be evaluated. A better solution would be to use a contact that does not contain Au. Development of such a contact structure, such as the Mo contact proposed for use in conceptual design No. 1, would produce a major materials cost reduction and should receive careful attention in later work.

Third, it is interesting to note that the approximate materials costs calculated for the functional semiconductor regions of the three cell structures (regions 3, 4, 5) by the "current market price" method of column B and the "minimum required reactants" method of column C are really not greatly different, even though very different approaches were used in the computations. The first method gives a total of approximately \$206, \$242, and \$172 per m^2, respectively, for these regions of the three cell structures in the table, while the latter method gives approximately \$260, \$291, and \$246 per m^2, respectively, for the same regions.

The dominant factor in these costs, of course, is the cost of the GaAs active base region of all three cell structures. It is striking that the approximate costs assigned to this region alone, for all three structures, are quite similar whether computed from present costs of high-quality single-crystal GaAs ingots (as in column B) or from present costs of metalorganic and hydride chemicals (i.e., TMG and AsH_3), products produced by very different processes by very different types of industry. Presumably, the costs of the GaAs (and the GaAlAs) regions of these cell structures bear at least an indirect relationship to the present cost and the present world market for Ga metal. This point will be examined further in later reports.

The total estimated costs of the semiconductors incorporated in the two conceptual designs, as given in Table 2-11, are in the approximate range \$205 — \$260 per m^2 for the conventional configuration involving an opaque substrate and ~ \$170 — \$245 per m^2 for the inverted configuration involving a transparent substrate. These approximate semiconductor costs are from 3 1/2 to 5 times larger than the ERDA total so. array cost goal of ~ \$50 per m^2 for the 1985 time period, and from 11 to 16 times larger than the corresponding materials cost goals for that same time (see Section 2.5.2).

It is clear that major reductions in materials costs are required for the GaAlAs/GaAs thin-film solar cell to meet these cost goals. The materials cost

reductions by a factor of about 7 suggested in Section 2.5.2 as a reasonable goal for 1985 for the input semiconductor materials required for producing GaAs solar cells appear to fall short of the required reductions, based on the estimated present costs in Table 2-11, by an additional factor of perhaps 1 1/2 to 2.

It is very difficult at this time to establish the probability of such cost reductions for the 1985 time period and beyond. However, preliminary consideration of the processes involved in producing these materials and of the probable cost reductions that would be associated with process improvements, mass production, and assured large-quantity purchasing indicates that the proposed heterostructure configuration involving films of GaAℓAs and GaAs deposited by the MO-CVD technique could probably meet the economic (in addition to the technical) goals of the ERDA program provided a satisfactory inexpensive substrate material can be identified and produced in large quantities. This tentative conclusion also assumes that significant reductions in the actual costs of fabricating the solar arrays with these materials can also be realized, in the same time period. This latter question is considered briefly in the next section.

2.5.5 Fabrication and Processing Costs for Experimental Thin-film Cells

It was suggested in Section 2.5.2 that tentative 1985 cost goals for large-area GaAs sheet fabrication and for GaAs cell/array fabrication - the cost categories added to that of the input semiconductor material in establishing the overall 1985 cost goals for the ERDA/JPL Low Cost Silicon Solar Array Project — could reasonably be set at the same level as those adopted for the LSSA Project for that same time period, namely, ~$17 per m^2 for each category. Although various arguments against the validity of that amount can probably be constructed, the fact remains that GaAs solar array production must at least approach the same cost goals as Si array production to become competitive in future terrestrial applications. Thus, $17 per m^2 is being considered a tentative 1985 cost goal for GaAs film production and, separately, for GaAs array fabrication, as proposed earlier.

The sim of $34 per m^2 therefore represents a cost goal for all of the expenditures involved in producing large-area GaAs solar arrays for terrestrial use except for the input semiconductor materials cost. Thus, some of the materials cost estimates included in Table 2-11 (specifically, those of the substrate and the contacts) are more appropriately viewed as debits against this cost goal of $34 per m^2. In any event, preliminary estimates of costs of producing the GaAℓAs/GaAs thin-film multilayer structures and processing them into experimental cells have shown clearly that such costs on the present laboratory scale far exceed the above 1985 production cost goal — a fact not at all surprising. Analysis of the step-by-step fabrication of these experimental devices has been undertaken to provide an accurate indication of the total costs involved, but the study is not complete and will thus be described in later reports.

2.5.6 Future Materials Requirements and Future Costs

The ERDA annual solar array production capacity goals for the years 1985 and 2000, based on the assumption of 10 percent array efficiency and AM1 solar isolation of 100 mw/cm^2, are 5×10^6 m^2 and 5×10^8 m^2, respectively, as indicated earlier (Section 2.5.3). For the two conceptual cell designs of Figure 2-35 and Table 2-5 these area requirements correspond to 146.5 and 14,650 metric tons of GaAs for cell design No. 1, and 120 and 12,000 metric tons of GaAs for cell No. 2. The $Ga_{0.1}Al_{0.9}As$

alloy layer requirements for cell design No. 1 are 9.5 and 950 metric tons, respectively, and for cell design No. 2 they are 29.0 and 2900 metric tons, respectively, for the years 1985 and 2000.

As discussed in Section 2.5.3, the minimum Ga metal content of the 1985 annual production capacity goal is 71 and 60 metric tons for cell designs No. 1 and No. 2, respectively, and for the 2000 annual production goal it is 7100 and 6000 metric tons for designs No. 1 and No. 2, respectively. The significance of these future Ga requirements for solar arrays with respect to the potential future supply of the metal was reviewed earlier.

The principal controlling factor in future costs of the semiconductor materials required for production of these very large quantities of GaAs solar arrays is expected to be the cost of the Ga metal involved, irrespective of the process used or of the exact nature of the physical or chemical form of the Ga-bearing material in question. As is clear from the data of Table 2-6 the market price of Ga has decreased with the passing years as the production volume and the demand have gradually increased.

However, the market price has now appeared to level off. Furthermore, production capacity now appears to exceed the demand, although it is expected that increased demand in applications other than photovoltaic will probably produce a balance in the next several years. However, it does not appear likely that further price reductions will be associated with this gradual growth in the market in the next few years (Ref 20). Whether the drastic reduction in Ga cost that has been referred to earlier (factor of 7 to 10) will come about in the next 5 to 15 years is extremely difficult to predict. The actual occurrence will be a result of many complex factors, such as the degree of certainty of the large-volume markets associated with terrestrial photovoltaic applications, the amount of process development funding and capital investment backing made available to private industry for improving processing yields and reducing processing costs, and the stimulus of competition among various alternative materials for the photovoltaic market. This question will be considered further in subsequent reports.

Finally, the matter of producibility of the very large quantities of GaAs thin-film solar cells required by the future production goals must be considered. One of the advantages of the MO-CVD process that was emphasized in the first quarterly report (Ref 8) is that large-area uniform surface coverage of a substrate can be obtained and that a sequence of layers of various conductivity types and doping levels can be achieved in a single growth sequence, using the same type of commercially available CVD apparatus that is used for epitaxial growth of elemental semiconductors, e.g., Si. This fact distinguishes the MO-CVD process from other methods for growing films of GaAs and related materials.

It also makes it possible to obtain an indication of the extent to which the future annual solar array production goals of the ERDA program can be realized in terms of CVD production equipment available today to the semiconductor device industry. A specially designed CVD reactor system for use in depositing epitaxial Si by the SiH_4 pyrolysis process on 3-in. diameter Si substrates in large numbers has been constructed by a major supplier of production equipment for the semiconductor industry.* This system is designed to accommodate 300 substrate wafers per run,

*The manufacturer is the Tylan Corp., Torrance, CA.

mounted vertically in a vertical cylindrical deposition chamber which is raised and lowered into and out of a 30 kw resistance-heated clamshell furnace. The system has a very fast cycle time (30 min for a 20 μm deposit of Si by SiH_4 pyrolysis in H_2), and is capable of producing 82 m^2 of CVD Si 20 μm thick in a normal five-day 40-hr week.

On the above basis, 400 such reactors could produce 5 x 10^6 m^2 of Si annually operating on a three-shift (24-hr day) five-day-week schedule (with no allowance for down-time and assuming 100 percent yield), while 208 such systems could produce the same amount of CVD Si if operated on a 24-hr-day schedule for 365 days, on the same basis. The cost of such a system (complete) is the order of $250,000. An examination of the possibility of using this type of system for producing CVD Si for the LSSA Project indicated that relatively minor modifications in the deposition chamber and the form and size of the substrates used could reduce the number of such reactor systems required for producing 5 x 10^6 m^2 per year to somewhere in the range 50-75. This is a more encouraging number, but unfortunately this type of system involves batch processing and all of the attendant severe limitations.

Since the MO-CVD process – even one involving deposition of several different layers in sequence – could be applied equally well in such a production system having the required design changes, the above estimates do provide some preliminary indication of the magnitude of the undertaking required to meet the 1985 production goal for GaAlAs/GaAs solar cell arrays. A reduction in cycle time per deposition run, which might be possible because of the thinner layers involved in the GaAs cell structure, could further reduce the number of reactor systems required to meet the production goals, but such an improvement would probably be only slight. The main modification required to achieve the necessary production level and yet keep the associated costs within the established limits is the development of continuous (or semi-continuous) processes for formation of the large-area substrates as well as for deposition of the semiconductor layers. This must be the long-term goal of these and other studies directed toward meeting the future needs of ERDA's photovoltaic conversion program.

THIS PAGE

WAS INTENTIONALLY

LEFT BLANK

3. SUMMARY AND CONCLUSIONS

The first year of work on this contract extended from July 5, 1976 to July 4, 1977. The technical approach of the experimental work in this performance period has involved application of the MO-CVD technique to the formation of films of GaAs and GaAℓAs on both single-crystal and low-cost polycrystalline or amorphous substrate materials, including semiconductors, sapphire, glasses, glass-ceramics, alumina ceramics, and metals.

Ten candidate materials were initially selected for further experimental investigation, on the basis of a set of qualification criteria and initial experimental tests. Those evaluated most extensively include certain glasses, polycrystalline aluminas, and metals, as well as composite substrates of Mo metal films and Ge films on insulating substrates. Some of the glasses were found to be physically and/or chemically unsuited to the growth of GaAs films in H_2, as were the Kovar-like (Co-Ni-Fe alloy) metals. Mo and Ge intermediate layers deposited on Corning Code 0317 glass substrates appear to be compatible with the MO-CVD growth of GaAs. The large-grained alumina and bulk metal substrates are considered too expensive to meet the future cost goals of the ERDA program, but have been used for experimental film growth that provides a comparison with growth on amorphous (or very small-grained) substrates.

A new dedicated reactor system was designed and constructed for use in this program; it was completed in the second quarter of the contract and has been used as one of two MO-CVD reactor systems employed in these investigations. MO-CVD experiments undertaken in these two reactor systems have established that good control and reproducibility of the doping of GaAs:Se, GaAs:Zn, and GaAℓAs:Zn single-crystal films can be achieved. Doping experiments with polycrystalline GaAs films on low-cost insulating substrates have established that a conducting intermediate layer will have to be employed to allow adequate contact to be made to the back surface of a polycrystalline GaAs solar cell grown on such substrates. Such intermediate layers of CVD Ge and sputtered Mo films have been used in the growth of polycrystalline GaAs n/n^+ films for the fabrication of Schottky-barrier solar cells and for the growth of polycrystalline GaAs p-n junction structures.

The single-crystal and polycrystalline films grown in the contract work to date have been evaluated by a variety of characterization techniques. The electrical properties of the polycrystalline GaAs films were analyzed by van der Pauw measurements, and the resistivities were found to be 2-3 orders of magnitude greater than that of single-crystal material of the same input doping level. No difference was observed in the resistivity of n-type and p-type GaAs of comparable doping levels. However, because it is possible to dope p-type GaAs more heavily than n-type material the lowest resistivities have been achieved in p-type GaAs films.

The limits of applicability of C-V measurements for determining impurity concentration have been explored. Only when a back-plane contact to the films is available can these measurements be successfully applied. In addition, films doped higher than 10^{16} cm^{-3} have not been successfully measured, owing to excessive leakage in the Schottky barriers.

The physical and structural properties of polycrystalline GaAs films have been examined by SEM and x-ray diffraction analysis. The films have all shown similar general surface features, with apparent grain sizes of 2-10 μm. The grain size most typically seen for films ~5 μm thick is $\leq$ 5 μm in apparent horizontal dimension. Films grown on refired Vistal alumina substrates have exhibited 1mm-size grains that have grown epitaxially on the large individual $A\ell_2O_3$ grains in the alumina. The preferred orientation of GaAs grown on most of the substrates has been {111}, but the preferred orientation of those grown on glasses has been shown to vary with temperature of deposition.

Techniques for determining the $A\ell$ concentration in $GaA\ell As$ films have been established. Epitaxial films grown on GaAs have been analyzed by electron microprobe x-ray techniques and conventional x-ray lattice constant measurements to establish a working calibration curve for film composition. These data will be used for further studies of $A\ell$ concentration in polycrystalline $GaA\ell As$ films.

Techniques for the determination of grain size in polycrystalline films have been explored in considerable detail, especially during the fourth quarter of the program. EBIC-mode measurements on Schottky barrier devices on polycrystalline films in the SEM demonstrated the presence of localized non-radiative recombination regions that in many cases coincided with apparent grain boundaries in the polycrystalline films.

Both single-crystal and polycrystalline solar cells have been grown by MO-CVD, fabricated, and evaluated. Contact technologies have been explored and suitable ohmic contacts have been developed. Single-crystal $GaA\ell As$/GaAs p-n junction cell structures were prepared with thin (~500Å) $Ga_{1-x}A\ell_xAs$ ($x \approx 0.8$) windows and GaAs:Zn-GaAs:Se junction regions. Efficiencies as high as 12.8 percent under simulated AM0 illumination with no AR coating were obtained, indicating the high quality of the semiconductor layers grown by the MO-CVD technique. Extrapolation of these results to those expected from similar devices with AR coatings indicates that efficiencies as high as those attained by LPE growth methods can be achieved with material made by the MO-CVD process.

Films with grain sizes in the ~5 μm range have been used for fabrication of polycrystalline film solar cells on a variety of substrates. Most attention has been devoted to Schottky-barrier cells. The best results obtained with these devices has been an efficiency of 2.25 percent for AM0 illumination and no AR coating, for n/n^+ GaAs films grown on a composite Mo/glass substrate. Short-circuit current densities of up to 12.5 mA/cm^2 have been achieved in such devices. This particular substrate combination has been found to be a good low-cost baseline reference with which to compare other results. The GaAs-Mo interface was found to be ohmic as long as the donor impurity concentration in the GaAs film exceeds ~10^{18} cm^{-3}.

P-n junctions in polycrystalline GaAs films have also been formed by growing alternate p and n layers by MO-CVD. The electrical properties of these junction structures generally showed excessive leakage currents, resulting in soft and sometimes shorted characteristics for p on n devices and considerably less leaky characteristics for n on p devices. It is thought that diffusion of Zn along grain boundaries is responsible for the leaky device characteristics.

Finally, preliminary analyses of material and processing costs associated with the fabrication of two different conceptual designs of GaAℓAs/GaAs heterostructure solar cells - one involving the conventional configuration on an opaque substrate and one involving an inverted configuration utilizing a transparent substrate - have been prepared. Some consideration has also been given to future material requirements and costs of producing such cells in large quantity. The principal conclusions reached from these anal yses are as follows:

1. A reduction by a factor of 10 to 15 in the cost of the input semiconductor materials relative to present values would probably permit thin-film GaAℓAs/GaAs cells to meet the 1985 ERDA cost goals.

2. The substrate cost remains as the predominant factor in the overall materials costs for thin-film GaAℓAs/GaAs solar cells; glasses still appear as potentially the best substrate material prospect for allowing total array costs to come within the established ERDA goals.

3. Added-value costs of ~ $17 per m^2 for fabrication of large-area films of GaAs and a similar figure for cell and array fabrication, "borrowed" from the ERDA/JPL LSSA Project, appear to be reasonable cost goals for 1985 for GaAs low-cost solar array fabrication, as well.

4. At least in terms of deposited thin-film GaAℓAs/GaAs solar cells on substrates of materials other than single-crystal GaAs, there appears to enough recoverable Ga metal in projected future bauxite ore supplies to meet the ERDA solar array production goals for the years 1985 and 2000, especially if improvements in Ga recovery technology are introduced to increase process efficiencies by relatively modest amounts.

5. The MO-CVD process for fabrication of GaAs cells does appear to be adaptable to continuous or semi-continuous manufacture of large-area thin-film cells in the quantities required for meeting the ERDA 1985 and 2000 production goals, primarily through design of the necessary scaled-up apparatus and through development of companion processes for producing appropriate substrates at sufficiently low cost.

Thus, the CVD technique is still viewed as potentially the best method for achieving large areas of solar cells at sufficiently low cost to meet both the performance goals and the economic goals of ERDA's long-range program. The results of the first year's work have demonstrated that the MO-CVD technique is capable of producing materials of quality sufficient to meet the goals of the photovoltaic conversion program, and that the technique is also a strong candidate for eventual use in fabrication of single-crystal GaAℓAs/GaAs cells for high-efficiency applications, with or without concentrator systems.

Continuation of these studies should emphasize further substrate development as well as improved understanding of the properties and effects of grain boundaries in the polycrystalline films. In addition, additional attention should be devoted to junction formation techniques and techniques which yield larger grain size for equivalent Ga content. Further development of solar cell fabrication technology, including contacts and AR coatings, should also be undertaken.

THIS PAGE

WAS INTENTIONALLY

LEFT BLANK

4. PLANS FOR CONTINUED WORK

It is recommended that the program activities in the first quarter of an extension of this contract work proceed along the following general lines, although subject to change upon review and discussion with ERDA personnel.

Substrate Materials Evaluation

1. Continue attempts to obtain improved substrate materials - especially glasses and glass-ceramics - for use in GaAs and GaAℓAs deposition experiments.

2. Evaluate graphite substrates (from various sources) and composite substrates of Ge/glass and Mo/glass for deposition of polycrystalline GaAs films.

Thin-film Materials Development

1. Continue experimental deposition of polycrystalline GaAs multilayer structures, including p-n junctions, primarily on composite low-cost substrates.

2. Conduct additional grain-size control and enhancement experiments, utilizing in situ annealing, gas-phase etching, CVD parameter variations, and substrate surface texturing.

Evaluation of Film Properties and Study of Grain-boundary Effects

1. Continue routine characterization of structural and electrical properties of polycrystalline films of GaAs and GaAℓAs.

2. Begin detailed studies of recombination, transport, and impurity segregation phenomena at grain boundaries in polycrystalline GaAs.

3. Continue to explore improved techniques for determining grain size and carrier diffusion lengths in polycrystalline GaAs.

Investigation of Barrier Formation Techniques

1. Continue characterization of p-n junction devices in polycrystalline GaAs, with emphasis on question of Zn diffusion through the layers.

2. Continue fabrication and evaluation of Schottky barriers on various polycrystalline film structures.

3. Explore alternative techniques for formation of junctions in polycrystalline GaAs layers.

4. Investigate deposited indium tin oxide (ITO) as component for photovoltaic heterojunction formation with GaAs films.

Development of Photovoltaic Device Designs and Fabrication Techniques

1. Utilize new mask sets for fabrication of experimental thin-film GaAs solar cells (polycrystalline and single-crystal), and characterize photovoltaic properties.

2. Investigate ITO as possible transparent conducting contact material for GaAs cells, and examine other alternative contact materials and contact designs.

Analysis and Projection of Cell Fabrication Costs

1. Prepare updated analysis of step-by-step cell fabrication process (using MO-CVD), and convert results to actual current fabrication costs.

2. Project future requirements for principal materials involved in fabrication of GaAlAs/GaAs thin-film cells by MO-CVD, assuming large-scale production of present designs.

5. REFERENCES

1. J. J. Loferski, J. Appl. Phys. 27, 777 (1956).

2. A. R. Gobat, M. F. Lamorte, and G. W. McIver, IRE Trans. Mil. Electron. MIL-6, 20 (1962). Also see R. D. Gold, H. W. Betram, F. Cohen, E. W. Conley, and M. Dragon, "Manufacturing Methods Program for Gallium Arsenide Solar Cells," Final Report for Contract No. AF33657-8921 (Proj. 7-877), RCA, Somerville, N.J., July 1964 (AD-443496).

3. H. J. Hovel and J. M. Woodall, Conf. Record of the Tenth IEEE Photovoltaic Specialists Conference, Palo Alto, CA., November 1973 (IEEE, New York, 1974), p. 25; J. Electrochem. Soc. 120, 1246 (1973); J. M. Woodall and H. J. Hovel, Appl. Phys. Lett. 21, 379 (1972); H. H. Hovel, J. M. Woodall, and W. E. Howard, in Gallium Arsenide and Related Compounds, Proc. Fourth Int. Symp., Boulder, CO., Sept. 1972 (Inst. of Physics, London, 1973), p. 205.

4. H. M. Manasevit and W. I. Simpson, J. Electrochem. Soc. 116, 1725 (1969).

5. J. M. Woodall and H. J. Hovel, J. Vac. Sci. Technol. 12, 1000 (1975).

6. S. Soclof and P. A. Iles, The Electrochem Soc., Fall Mtng., New York, October 1974, Paper No. 251.

7. H. M. Manasevit and W. I. Simpson, J. Electrochem. Soc. 116, 1725 (1969); H. M. Manasevit, J. Cryst. Growth 13/14, 306 (1972); H. M. Manasevit and A. C. Thorsen, Met. Trans. 1, 623 (1970); H. M. Manasevit, J. Electrochem. Soc. 118, 647 (1971).

8. R. P. Ruth, P. D. Dapkus, R. D. Dupuis, R. E. Johnson, H. M. Masasevit, L. A. Moudy, and J. J. Yang, "Thin Films of Gallium Arsenide on Low-cost Substrates," Quarterly Project Report No. 1, November 1976, Rockwell International, Electronics Research Division, Anaheim, CA 92803. Contract No. E(04-3)-1202, Division of Solar Energy, U. S. Energy Research and Development Administration.

9. R. P. Ruth, P. D. Dapkus, R. D. Dupuis, A. G. Campbell, R. E. Johnson, H. M. Manasevit, L. A. Moudy, and J J. Yang, "Thin Films of Gallium Arsenide on Low-cost Substrates," Quarterly Project Report No. 2, January 1977, Rockwell International, Electronics Research Division, Anaheim, CA 92803. Contract No. E(04-3)-1202, Division of Solar Energy, U. S. Energy Research and Development Administration.

10. R. P. Ruth, P D. Dapkus, R D. Dupuis, A. G. Campbell, R. E. Johnson, H. M. Manasevit, L. A. Moudy, and R. D. Yingling, "Thin Films of Gallium Arsenide on Low-cost Substrates," Quarterly Project Report No. 3, April 1977, Rockwell International, Electronic Devices Division, Anaheim, CA 92803. Contract No. E(04-3)-1202, Division of Solar Energy, U. S. Energy Research and Development Administration.

11. H. J. Hovel, Solar Cells, Vol. 11 of Semiconductors and Semimetals, ed. by R. K. Willardson and A. C. Beer (Academic Press, New York, 1975), p. 107.

12. W. D. Johnston, private communication.

13. Indium preforms 0.010 in. in diameter were alloyed into the sample surface by heating at 400°C for 2 min. in a reducing atmosphere.

14. John Y. W. Seto, J. Appl. Phys. 46, 5247 (1975). Also, R. P. Ruth, H. M. Manasevit, R. E. Johnson, L. A. Moudy, W. I. Simpson, and J. J. Yang, "Chemical Vapor Deposition Growth," Quarterly Report No. 3, 1 January 1977, Rockwell International, Electronics Research Center, Anaheim, CA 92803. JPL Contract No. 954372, performed for the Jet Propulsion Laboratory, California Institute of Technology, under NASA Contract NAS7-100 for the U. S. Energy Research and Development Administration, Division of Solar Energy. See pp. 34-37.

15. J. W. Colby, Bell Laboratories, private communication. MAGIC is acronym for Microprobe Analysis General Intensity Corrections. See "MAGIC - A Computer Program for Quantitative Electron Microprobe Analysis," J. W. Colby, Bell Laboratories, Allentown, PA (1967).

16. E. Estop, A. Izrael, and M. Sauvage, Acta Cryst. A-32, 627 (1976).

17. J. M. Woodall and H. J. Hovel, Appl. Phys. Lett. 21, 379 (1972); also R. Sahai, P. D. Edwall, E. Cory, and J. S. Harris, Late News Paper No. 13.13, 12th IEEE Photovoltaic Specialists Conference, Baton Rouge, LA, November 15-18, 1976.

18. Pierre de la Breteque, Gallium—Propriétés Principales Bibliographie (Institut de Recherches de la Société Francaise pour l'Industrie de l'Aluminium a Marseille, Marseille, 1962) (Library of Congress Catalog Card No. 62-16093).

19. R. A. Weeks, in United States Mineral Resources, ed. by D. A. Brobst and W. P. Pratt, Geological Survey Professional Paper 820, United States Department of the Interior (United States Government Printing Office, Washington, D. C. 1973), pp. 237 - 246.

20. Aluminum Company of America, "Survey of Availability and Economical Extractability of Gallium from Earth Resources," Special Report prepared for Rockwell International, Space Division, Seal Beach, CA, October 1, 1976.

☆U.S. GOVERNMENT PRINTING OFFICE:1979 -640 -014/ 4469 REGION NO. 4